

Guided Wave Principles for Electronics and Optoelectronics

In Chapter 6, we introduced the transmission line and studied propagation and bouncing of waves along a line, applicable to digital electronics. We devoted Chapter 7 to sinusoidal steady-state analysis of waves on transmission lines. We learned that wave propagation along a transmission line is characterized by the waves sliding parallel to its conductors, with electric and magnetic fields entirely transverse to the direction of propagation, and that these waves are known as transverse electromagnetic (TEM) waves.

Another kind of waveguiding mechanism is one in which the waves bounce obliquely between the parallel planes as they progress along the structure, resulting in transverse electric (TE) and transverse magnetic (TM) waves. The arrangement is commonly referred to as a waveguide, although the transmission line is also a waveguide. To continue our study of guided waves for electronics, we introduce in this chapter TE and TM waves supported by plane conductors, as in a parallel-plate transmission line, as well as those supported by a plane dielectric slab, without the conductors. The latter arrangement is particularly applicable to optoelectronics.

We first consider the parallel-plate waveguide, consisting of two parallel plane conductors. To do this, we make use of the superposition of two uniform plane waves propagating at an angle to each other. Hence, we begin the chapter with a discussion of uniform plane wave propagation in an arbitrary direction relative to the coordinate axes.

8.1 UNIFORM PLANE WAVE PROPAGATION IN AN ARBITRARY DIRECTION

In Chapter 3, we introduced the uniform plane wave propagating in the z -direction by considering an infinite plane current sheet lying in the xy -plane. If the current

*Two
dimensions*

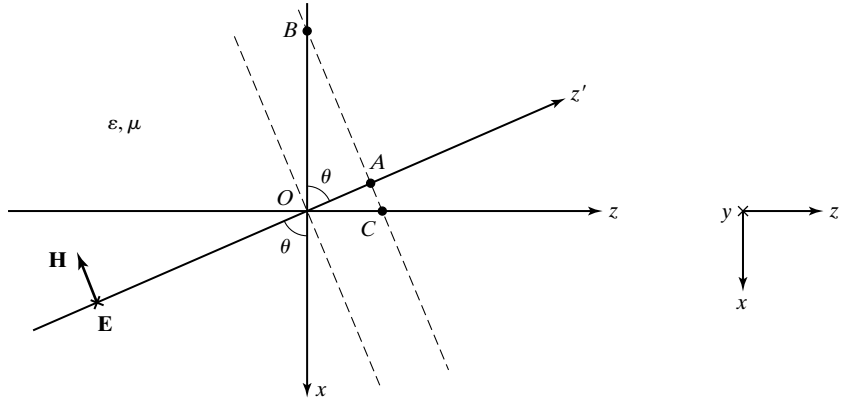


FIGURE 8.1 Uniform plane wave propagating in the z' -direction lying in the xz -plane and making an angle θ with the negative x -axis.

sheet lies in a plane making an angle to the xy -plane, the uniform plane wave would then propagate in a direction different from the z -direction. Thus, let us first consider the two-dimensional case of a uniform plane wave propagating in a perfect dielectric medium in the z' -direction and making an angle θ with the negative x -axis, as shown in Fig. 8.1. Let the electric field of the wave be entirely in the y -direction. The magnetic field would then be directed as shown in the figure so that $\mathbf{E} \times \mathbf{H}$ points in the z' -direction.

We can write the expression for the electric field of the wave as

$$\mathbf{E} = E_0 \cos(\omega t - \beta z') \mathbf{a}_y \tag{8.1}$$

where $\beta = \omega\sqrt{\mu\epsilon}$ is the phase constant, that is, the rate of change of phase with distance along the z' -direction for a fixed value of time. From the construction of Fig. 8.2(a), however, we have

$$z' = -x \cos \theta + z \sin \theta \tag{8.2}$$

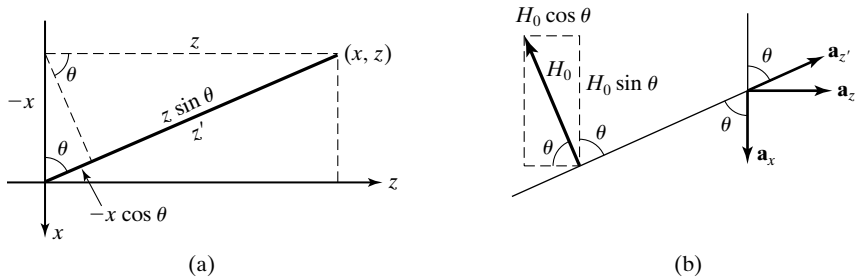


FIGURE 8.2 Constructions pertinent to the formulation of the expressions for the fields of the uniform plane wave of Fig. 8.1.

so that

$$\begin{aligned}
 \mathbf{E} &= E_0 \cos [\omega t - \beta(-x \cos \theta + z \sin \theta)] \mathbf{a}_y \\
 &= E_0 \cos [\omega t - (-\beta \cos \theta)x - (\beta \sin \theta)z] \mathbf{a}_y \\
 &= E_0 \cos (\omega t - \beta_x x - \beta_z z) \mathbf{a}_y
 \end{aligned} \tag{8.3}$$

where $\beta_x = -\beta \cos \theta$ and $\beta_z = \beta \sin \theta$ are the phase constants in the positive x - and positive z -directions, respectively.

We note that $|\beta_x|$ and $|\beta_z|$ are less than β , the phase constant along the direction of propagation of the wave. This can also be seen from Fig. 8.1 in which two constant phase surfaces are shown by dashed lines passing through the points O and A on the z' -axis. Since the distance along the x -direction between the two constant phase surfaces (i.e., the distance OB) is equal to $OA/\cos \theta$, the rate of change of phase with distance along the x -direction is equal to

$$\beta \frac{OA}{OB} = \frac{\beta(OA)}{OA/\cos \theta} = \beta \cos \theta$$

The minus sign for β_x signifies that, insofar as the x -axis is concerned, the wave is progressing in the negative x -direction. Similarly, since the distance along the z -direction between the two constant phase surfaces (i.e., the distance OC) is equal to $OA/\sin \theta$, the rate of change of phase with distance along the z -direction is equal to

$$\beta \frac{OA}{OC} = \frac{\beta(OA)}{OA/\sin \theta} = \beta \sin \theta$$

Since the wave is progressing along the positive z -direction, β_z is positive. We further note that

$$\beta_x^2 + \beta_z^2 = (-\beta \cos \theta)^2 + (\beta \sin \theta)^2 = \beta^2 \tag{8.4}$$

and that

$$-\cos \theta \mathbf{a}_x + \sin \theta \mathbf{a}_z = \mathbf{a}'_z \tag{8.5}$$

where \mathbf{a}'_z is the unit vector directed along the z' -direction, as shown in Fig. 8.2(b). Thus, the vector

$$\boldsymbol{\beta} = (-\beta \cos \theta)\mathbf{a}_x + (\beta \sin \theta)\mathbf{a}_z = \beta_x \mathbf{a}_x + \beta_z \mathbf{a}_z \tag{8.6}$$

defines completely the direction of propagation and the phase constant along the direction of propagation. Hence, the vector $\boldsymbol{\beta}$ is known as the *propagation vector*.

The expression for the magnetic field of the wave can be written as

$$\mathbf{H} = \mathbf{H}_0 \cos (\omega t - \beta z') \tag{8.7}$$

where

$$|\mathbf{H}_0| = \frac{E_0}{\sqrt{\mu/\epsilon}} = \frac{E_0}{\eta} \tag{8.8}$$

since the ratio of the electric field intensity to the magnetic field intensity of a uniform plane wave is equal to the intrinsic impedance of the medium. From the construction in Fig. 8.2(b), we observe that

$$\mathbf{H}_0 = H_0(-\sin \theta \mathbf{a}_x - \cos \theta \mathbf{a}_z) \tag{8.9}$$

Thus, using (8.9) and substituting for z' from (8.2), we obtain

$$\begin{aligned} \mathbf{H} &= H_0(-\sin \theta \mathbf{a}_x - \cos \theta \mathbf{a}_z) \cos [\omega t - \beta(-x \cos \theta + z \sin \theta)] \\ &= -\frac{E_0}{\eta}(\sin \theta \mathbf{a}_x + \cos \theta \mathbf{a}_z) \cos [\omega t - \beta_x x - \beta_z z] \end{aligned} \tag{8.10}$$

Generalization to three dimensions

Generalizing the foregoing treatment to the case of a uniform plane wave propagating in a completely arbitrary direction in three dimensions, as shown in Fig. 8.3, and characterized by phase constants β_x , β_y , and β_z in the x -, y -, and

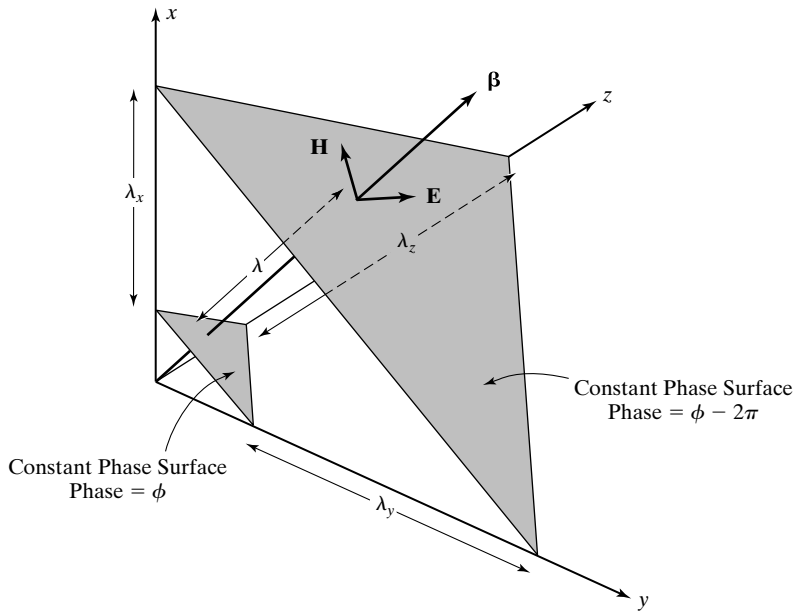


FIGURE 8.3

The various quantities associated with a uniform plane wave propagating in an arbitrary direction.

z -directions, respectively, we can write the expression for the electric field as

$$\begin{aligned}
 \mathbf{E} &= \mathbf{E}_0 \cos(\omega t - \beta_x x - \beta_y y - \beta_z z + \phi_0) \\
 &= \mathbf{E}_0 \cos[\omega t - (\beta_x \mathbf{a}_x + \beta_y \mathbf{a}_y + \beta_z \mathbf{a}_z) \cdot (x \mathbf{a}_x + y \mathbf{a}_y + z \mathbf{a}_z) + \phi_0] \\
 &= \mathbf{E}_0 \cos(\omega t - \boldsymbol{\beta} \cdot \mathbf{r} + \phi_0)
 \end{aligned} \tag{8.11}$$

where

$$\boldsymbol{\beta} = \beta_x \mathbf{a}_x + \beta_y \mathbf{a}_y + \beta_z \mathbf{a}_z \tag{8.12}$$

is the propagation vector,

$$\mathbf{r} = x \mathbf{a}_x + y \mathbf{a}_y + z \mathbf{a}_z \tag{8.13}$$

is the position vector, and ϕ_0 is the phase at the origin at $t = 0$. We recall that the position vector is the vector drawn from the origin to the point (x, y, z) and hence has components x , y , and z along the x -, y -, and z -axes, respectively. The expression for the magnetic field of the wave is then given by

$$\mathbf{H} = \mathbf{H}_0 \cos(\omega t - \boldsymbol{\beta} \cdot \mathbf{r} + \phi_0) \tag{8.14}$$

where

$$|\mathbf{H}_0| = \frac{|\mathbf{E}_0|}{\eta} \tag{8.15}$$

Since \mathbf{E} , \mathbf{H} , and the direction of propagation are mutually perpendicular to each other, it follows that

$$\mathbf{E}_0 \cdot \boldsymbol{\beta} = 0 \tag{8.16a}$$

$$\mathbf{H}_0 \cdot \boldsymbol{\beta} = 0 \tag{8.16b}$$

$$\mathbf{E}_0 \cdot \mathbf{H}_0 = 0 \tag{8.16c}$$

In particular, $\mathbf{E} \times \mathbf{H}$ should be directed along the propagation vector $\boldsymbol{\beta}$, as illustrated in Fig. 8.3, so that $\boldsymbol{\beta} \times \mathbf{E}_0$ is directed along \mathbf{H}_0 . We can therefore combine the facts (8.16) and (8.15) to obtain

$$\begin{aligned}
 \mathbf{H}_0 &= \frac{\mathbf{a}_\beta \times \mathbf{E}_0}{\eta} = \frac{\mathbf{a}_\beta \times \mathbf{E}_0}{\sqrt{\mu/\epsilon}} = \frac{\omega \sqrt{\mu\epsilon} \mathbf{a}_\beta \times \mathbf{E}_0}{\omega\mu} \\
 &= \frac{\boldsymbol{\beta} \mathbf{a}_\beta \times \mathbf{E}_0}{\omega\mu} = \frac{\boldsymbol{\beta} \times \mathbf{E}_0}{\omega\mu}
 \end{aligned} \tag{8.17}$$

where \mathbf{a}_β is the unit vector along $\boldsymbol{\beta}$. Thus,

$$\mathbf{H} = \frac{1}{\omega\mu} \boldsymbol{\beta} \times \mathbf{E} \quad (8.18)$$

*Apparent
wavelengths
and phase
velocities*

Returning to Fig. 8.3, we can define several quantities pertinent to the uniform plane wave propagation in an arbitrary direction. The apparent wavelengths λ_x , λ_y , and λ_z along the coordinate axes x , y , and z , respectively, are the distances measured along those respective axes between two consecutive constant phase surfaces between which the phase difference is 2π , as shown in the figure, at a fixed time. From the interpretations of β_x , β_y , and β_z as being the phase constants along the x -, y -, and z -axes, respectively, we have

$$\lambda_x = \frac{2\pi}{\beta_x} \quad (8.19a)$$

$$\lambda_y = \frac{2\pi}{\beta_y} \quad (8.19b)$$

$$\lambda_z = \frac{2\pi}{\beta_z} \quad (8.19c)$$

We note that the wavelength λ along the direction of propagation is related to λ_x , λ_y , and λ_z in the manner

$$\begin{aligned} \frac{1}{\lambda^2} &= \frac{1}{(2\pi/\beta)^2} = \frac{\beta^2}{4\pi^2} = \frac{\beta_x^2 + \beta_y^2 + \beta_z^2}{4\pi^2} \\ &= \frac{1}{\lambda_x^2} + \frac{1}{\lambda_y^2} + \frac{1}{\lambda_z^2} \end{aligned} \quad (8.20)$$

The apparent phase velocities v_{px} , v_{py} , and v_{pz} along the x -, y -, and z -axes, respectively, are the velocities with which the phase of the wave progresses with time along the respective axes. Thus,

$$v_{px} = \frac{\omega}{\beta_x} \quad (8.21a)$$

$$v_{py} = \frac{\omega}{\beta_y} \quad (8.21b)$$

$$v_{pz} = \frac{\omega}{\beta_z} \quad (8.21c)$$

The phase velocity v_p along the direction of propagation is related to v_{px} , v_{py} , and v_{pz} in the manner

$$\begin{aligned} \frac{1}{v_p^2} &= \frac{1}{(\omega/\beta)^2} = \frac{\beta^2}{\omega^2} = \frac{\beta_x^2 + \beta_y^2 + \beta_z^2}{\omega^2} \\ &= \frac{1}{v_{px}^2} + \frac{1}{v_{py}^2} + \frac{1}{v_{pz}^2} \end{aligned} \quad (8.22)$$

The apparent wavelengths and phase velocities along the coordinate axes are greater than the actual wavelength and phase velocity, respectively, along the direction of propagation of the wave. This fact can be understood physically by considering, for example, water waves in an ocean striking the shore at an angle. The distance along the shoreline between two successive crests is greater than the distance between the same two crests measured along a line normal to the orientation of the crests. Also, to keep pace with a particular crest an observer has to run faster along the shoreline than in a direction normal to the orientation of the crests. We shall now consider an example.

Example 8.1 Verification of properties of uniform plane wave propagating in free space

Let us consider a 30-MHz uniform plane wave propagating in free space and given by the electric field vector

$$\mathbf{E} = 5(\mathbf{a}_x + \sqrt{3}\mathbf{a}_y) \cos [6\pi \times 10^7 t - 0.05\pi(3x - \sqrt{3}y + 2z)] \text{ V/m}$$

We wish to verify the properties and find the magnetic field vector \mathbf{H} and other parameters associated with the wave.

Comparing the given expression for \mathbf{E} with the general expression (8.11), we have

$$\begin{aligned} \mathbf{E}_0 &= 5(\mathbf{a}_x + \sqrt{3}\mathbf{a}_y) \\ \boldsymbol{\beta} \cdot \mathbf{r} &= 0.05\pi(3x - \sqrt{3}y + 2z) \\ &= 0.05\pi(3\mathbf{a}_x - \sqrt{3}\mathbf{a}_y + 2\mathbf{a}_z) \cdot (x\mathbf{a}_x + y\mathbf{a}_y + z\mathbf{a}_z) \\ \boldsymbol{\beta} &= 0.05\pi(3\mathbf{a}_x - \sqrt{3}\mathbf{a}_y + 2\mathbf{a}_z) \\ \boldsymbol{\beta} \cdot \mathbf{E}_0 &= 0.05\pi(3\mathbf{a}_x - \sqrt{3}\mathbf{a}_y + 2\mathbf{a}_z) \cdot 5(\mathbf{a}_x + \sqrt{3}\mathbf{a}_y) \\ &= 0.25\pi(3 - 3) = 0 \end{aligned}$$

Hence, (8.16a) is satisfied; \mathbf{E}_0 is perpendicular to $\boldsymbol{\beta}$.

$$\begin{aligned} \beta &= |\boldsymbol{\beta}| = 0.05\pi|3\mathbf{a}_x - \sqrt{3}\mathbf{a}_y + 2\mathbf{a}_z| = 0.05\pi\sqrt{9 + 3 + 4} = 0.2\pi \\ \lambda &= \frac{2\pi}{\beta} = \frac{2\pi}{0.2\pi} = 10 \text{ m} \end{aligned}$$

This does correspond to a frequency of $(3 \times 10^8)/10$ Hz, or 30 MHz, in free space. The direction of propagation is along the unit vector

$$\mathbf{a}_\beta = \frac{\boldsymbol{\beta}}{|\boldsymbol{\beta}|} = \frac{3\mathbf{a}_x - \sqrt{3}\mathbf{a}_y + 2\mathbf{a}_z}{\sqrt{9 + 3 + 4}} = \frac{3}{4}\mathbf{a}_x - \frac{\sqrt{3}}{4}\mathbf{a}_y + \frac{1}{2}\mathbf{a}_z$$

From (8.17),

$$\begin{aligned} \mathbf{H}_0 &= \frac{1}{\omega\mu_0} \boldsymbol{\beta} \times \mathbf{E}_0 \\ &= \frac{0.05\pi \times 5}{6\pi \times 10^7 \times 4\pi \times 10^{-7}} (3\mathbf{a}_x - \sqrt{3}\mathbf{a}_y + 2\mathbf{a}_z) \times (\mathbf{a}_x + \sqrt{3}\mathbf{a}_y) \\ &= \frac{1}{96\pi} \begin{vmatrix} \mathbf{a}_x & \mathbf{a}_y & \mathbf{a}_z \\ 3 & -\sqrt{3} & 2 \\ 1 & \sqrt{3} & 0 \end{vmatrix} \\ &= \frac{1}{48\pi} (-\sqrt{3}\mathbf{a}_x + \mathbf{a}_y + 2\sqrt{3}\mathbf{a}_z) \end{aligned}$$

Thus,

$$\mathbf{H} = \frac{1}{48\pi} (-\sqrt{3}\mathbf{a}_x + \mathbf{a}_y + 2\sqrt{3}\mathbf{a}_z) \cos [6\pi \times 10^7 t - 0.05\pi(3x - \sqrt{3}y + 2z)] \text{ A/m}$$

To verify the expression for \mathbf{H} just derived, we note that

$$\begin{aligned} \mathbf{H}_0 \cdot \boldsymbol{\beta} &= \left[\frac{1}{48\pi} (-\sqrt{3}\mathbf{a}_x + \mathbf{a}_y + 2\sqrt{3}\mathbf{a}_z) \right] \cdot [0.05\pi(3\mathbf{a}_x - \sqrt{3}\mathbf{a}_y + 2\mathbf{a}_z)] \\ &= \frac{0.05}{48} (-3\sqrt{3} - \sqrt{3} + 4\sqrt{3}) = 0 \end{aligned}$$

$$\begin{aligned} \mathbf{E}_0 \cdot \mathbf{H}_0 &= 5(\mathbf{a}_x + \sqrt{3}\mathbf{a}_y) \cdot \frac{1}{48\pi} (-\sqrt{3}\mathbf{a}_x + \mathbf{a}_y + 2\sqrt{3}\mathbf{a}_z) \\ &= \frac{5}{48\pi} (-\sqrt{3} + \sqrt{3}) = 0 \end{aligned}$$

$$\begin{aligned} \frac{|\mathbf{E}_0|}{|\mathbf{H}_0|} &= \frac{5|\mathbf{a}_x + \sqrt{3}\mathbf{a}_y|}{(1/48\pi)|-\sqrt{3}\mathbf{a}_x + \mathbf{a}_y + 2\sqrt{3}\mathbf{a}_z|} = \frac{5\sqrt{1+3}}{(1/48\pi)\sqrt{3+1+12}} \\ &= \frac{10}{1/12\pi} = 120\pi = \eta_0 \end{aligned}$$

Hence, (8.16b), (8.16c), and (8.15) are satisfied.

Proceeding further, we find that

$$\beta_x = 0.05\pi \times 3 = 0.15\pi$$

$$\beta_y = -0.05\pi \times \sqrt{3} = -0.05\sqrt{3}\pi$$

$$\beta_z = 0.05\pi \times 2 = 0.1\pi$$

We then obtain

$$\lambda_x = \frac{2\pi}{\beta_x} = \frac{2\pi}{0.15\pi} = \frac{40}{3} \text{ m} = 13.333 \text{ m}$$

$$\lambda_y = \frac{2\pi}{|\beta_y|} = \frac{2\pi}{0.05\sqrt{3}\pi} = \frac{40}{\sqrt{3}} \text{ m} = 23.094 \text{ m}$$

$$\lambda_z = \frac{2\pi}{\beta_z} = \frac{2\pi}{0.1\pi} = 20 \text{ m}$$

$$v_{px} = \frac{\omega}{\beta_x} = \frac{6\pi \times 10^7}{0.15\pi} = 4 \times 10^8 \text{ m/s}$$

$$v_{py} = \frac{\omega}{|\beta_y|} = \frac{6\pi \times 10^7}{0.05\sqrt{3}\pi} = 4\sqrt{3} \times 10^8 \text{ m/s} = 6.928 \times 10^8 \text{ m/s}$$

$$v_{pz} = \frac{\omega}{\beta_z} = \frac{6\pi \times 10^7}{0.1\pi} = 6 \times 10^8 \text{ m/s}$$

Finally, to verify (8.20) and (8.22), we note that

$$\begin{aligned} \frac{1}{\lambda_x^2} + \frac{1}{\lambda_y^2} + \frac{1}{\lambda_z^2} &= \frac{1}{(40/3)^2} + \frac{1}{(40/\sqrt{3})^2} + \frac{1}{20^2} \\ &= \frac{9}{1600} + \frac{3}{1600} + \frac{4}{1600} = \frac{1}{100} = \frac{1}{10^2} = \frac{1}{\lambda^2} \end{aligned}$$

and

$$\begin{aligned} \frac{1}{v_{px}^2} + \frac{1}{v_{py}^2} + \frac{1}{v_{pz}^2} &= \frac{1}{(4 \times 10^8)^2} + \frac{1}{(4\sqrt{3} \times 10^8)^2} + \frac{1}{(6 \times 10^8)^2} \\ &= \frac{1}{16 \times 10^{16}} + \frac{1}{48 \times 10^{16}} + \frac{1}{36 \times 10^{16}} \\ &= \frac{1}{9 \times 10^{16}} = \frac{1}{(3 \times 10^8)^2} = \frac{1}{v_p^2} \end{aligned}$$

K8.1. Uniform plane wave; Propagation in an arbitrary direction; Propagation vector; Apparent wavelengths; Apparent phase velocities.

D8.1. For each of the following cases of a uniform plane wave propagating in free space, find the frequency f : **(a)** wavelength along the direction of propagation of the wave is 2 m; **(b)** the propagation vector is $\pi(1.2\mathbf{a}_x + 0.9\mathbf{a}_y)$ rad/m; and **(c)** the apparent wavelengths along three mutually perpendicular directions are 1 m, 1 m, and 2 m.

Ans. **(a)** 150 MHz; **(b)** 225 MHz; **(c)** 450 MHz.

D8.2. For a uniform plane wave of frequency 150 MHz propagating away from the origin into the first octant in a nonmagnetic ($\mu = \mu_0$), perfect dielectric medium of $\epsilon = 2\epsilon_0$, the apparent wavelengths along the x - and y -directions are found to be $2\frac{1}{2}$ m and $3\frac{1}{3}$ m, respectively. Find **(a)** the phase constant along the x -direction; **(b)** the apparent wavelength along the z -direction; **(c)** the apparent

phase velocity along the direction of the unit vector $\frac{1}{13}(3\mathbf{a}_x - 4\mathbf{a}_y + 12\mathbf{a}_z)$; and
(d) the equation of the plane if the source of the wave is an infinite plane sheet of uniform current density passing through the origin.

Ans. **(a)** 0.8π rad/m; **(b)** 2 m; **(c)** 3.25×10^8 m/s; **(d)** $4x + 3y + 5z = 0$.

8.2 TE AND TM WAVES IN A PARALLEL-PLATE WAVEGUIDE

TE waves

In the preceding section, we introduced uniform plane wave propagation in an arbitrary direction. Let us now consider the superposition of two uniform plane waves propagating symmetrically with respect to the z -axis, as shown in Fig. 8.4, and having the electric fields entirely in the y -direction as given by

$$\begin{aligned} \mathbf{E}_1 &= -\frac{E_0}{2} \cos(\omega t - \boldsymbol{\beta}_1 \cdot \mathbf{r}) \mathbf{a}_y \\ &= -\frac{E_0}{2} \cos(\omega t + \beta x \cos \theta - \beta z \sin \theta) \mathbf{a}_y \end{aligned} \quad (8.23a)$$

$$\begin{aligned} \mathbf{E}_2 &= \frac{E_0}{2} \cos(\omega t - \boldsymbol{\beta}_2 \cdot \mathbf{r}) \mathbf{a}_y \\ &= \frac{E_0}{2} \cos(\omega t - \beta x \cos \theta - \beta z \sin \theta) \mathbf{a}_y \end{aligned} \quad (8.23b)$$

where $\beta = \omega\sqrt{\mu\varepsilon}$, with ε and μ being the permittivity and the permeability, respectively, of the medium. The corresponding magnetic fields are given by

$$\mathbf{H}_1 = \frac{E_0}{2\eta} (\sin \theta \mathbf{a}_x + \cos \theta \mathbf{a}_z) \cos(\omega t + \beta x \cos \theta - \beta z \sin \theta) \quad (8.24a)$$

$$\mathbf{H}_2 = \frac{E_0}{2\eta} (-\sin \theta \mathbf{a}_x + \cos \theta \mathbf{a}_z) \cos(\omega t - \beta x \cos \theta - \beta z \sin \theta) \quad (8.24b)$$

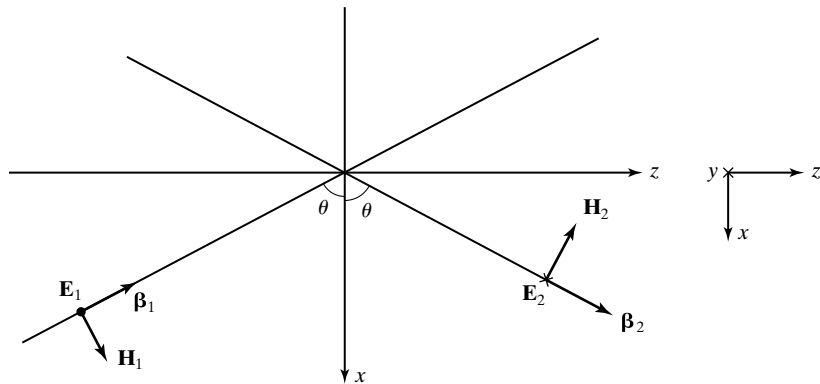


FIGURE 8.4

Superposition of two uniform plane waves propagating symmetrically with respect to the z -axis.

where $\eta = \sqrt{\mu/\epsilon}$. The electric and magnetic fields of the superposition of the two waves are given by

$$\begin{aligned}\mathbf{E} &= \mathbf{E}_1 + \mathbf{E}_2 \\ &= -\frac{E_0}{2} [\cos(\omega t - \beta z \sin \theta + \beta x \cos \theta) \\ &\quad - \cos(\omega t - \beta z \sin \theta - \beta x \cos \theta)] \mathbf{a}_y \\ &= E_0 \sin(\beta x \cos \theta) \sin(\omega t - \beta z \sin \theta) \mathbf{a}_y\end{aligned}\quad (8.25a)$$

$$\begin{aligned}\mathbf{H} &= \mathbf{H}_1 + \mathbf{H}_2 \\ &= \frac{E_0}{2\eta} \sin \theta [\cos(\omega t - \beta z \sin \theta + \beta x \cos \theta) \\ &\quad - \cos(\omega t - \beta z \sin \theta - \beta x \cos \theta)] \mathbf{a}_x \\ &\quad + \frac{E_0}{2\eta} \cos \theta [\cos(\omega t - \beta z \sin \theta + \beta x \cos \theta) \\ &\quad + \cos(\omega t - \beta z \sin \theta - \beta x \cos \theta)] \mathbf{a}_z \\ &= -\frac{E_0}{\eta} \sin \theta \sin(\beta x \cos \theta) \sin(\omega t - \beta z \sin \theta) \mathbf{a}_x \\ &\quad + \frac{E_0}{\eta} \cos \theta \cos(\beta x \cos \theta) \cos(\omega t - \beta z \sin \theta) \mathbf{a}_z\end{aligned}\quad (8.25b)$$

In view of the factors $\sin(\beta x \cos \theta)$ and $\cos(\beta x \cos \theta)$ for the x -dependence and the factors $\sin(\omega t - \beta z \sin \theta)$ and $\cos(\omega t - \beta z \sin \theta)$ for the z -dependence, the composite fields have standing wave character in the x -direction and traveling wave character in the z -direction. Thus, we have standing waves in the x -direction moving bodily in the z -direction, as illustrated in Fig. 8.5, by considering the electric field for two different times. In fact, we find that the Poynting vector is given by

$$\begin{aligned}\mathbf{P} &= \mathbf{E} \times \mathbf{H} = E_y \mathbf{a}_y \times (H_x \mathbf{a}_x + H_z \mathbf{a}_z) \\ &= -E_y H_x \mathbf{a}_z + E_y H_z \mathbf{a}_x \\ &= \frac{E_0^2}{\eta} \sin \theta \sin^2(\beta x \cos \theta) \sin^2(\omega t - \beta z \sin \theta) \mathbf{a}_z \\ &\quad + \frac{E_0^2}{4\eta} \cos \theta \sin(2\beta x \cos \theta) \sin 2(\omega t - \beta z \sin \theta) \mathbf{a}_x\end{aligned}\quad (8.26)$$

The time-average Poynting vector is given by

$$\begin{aligned}\langle \mathbf{P} \rangle &= \frac{E_0^2}{\eta} \sin \theta \sin^2(\beta x \cos \theta) \langle \sin^2(\omega t - \beta z \sin \theta) \rangle \mathbf{a}_z \\ &\quad + \frac{E_0^2}{4\eta} \cos \theta \sin(2\beta x \cos \theta) \langle \sin 2(\omega t - \beta z \sin \theta) \rangle \mathbf{a}_x \\ &= \frac{E_0^2}{2\eta} \sin \theta \sin^2(\beta x \cos \theta) \mathbf{a}_z\end{aligned}\quad (8.27)$$

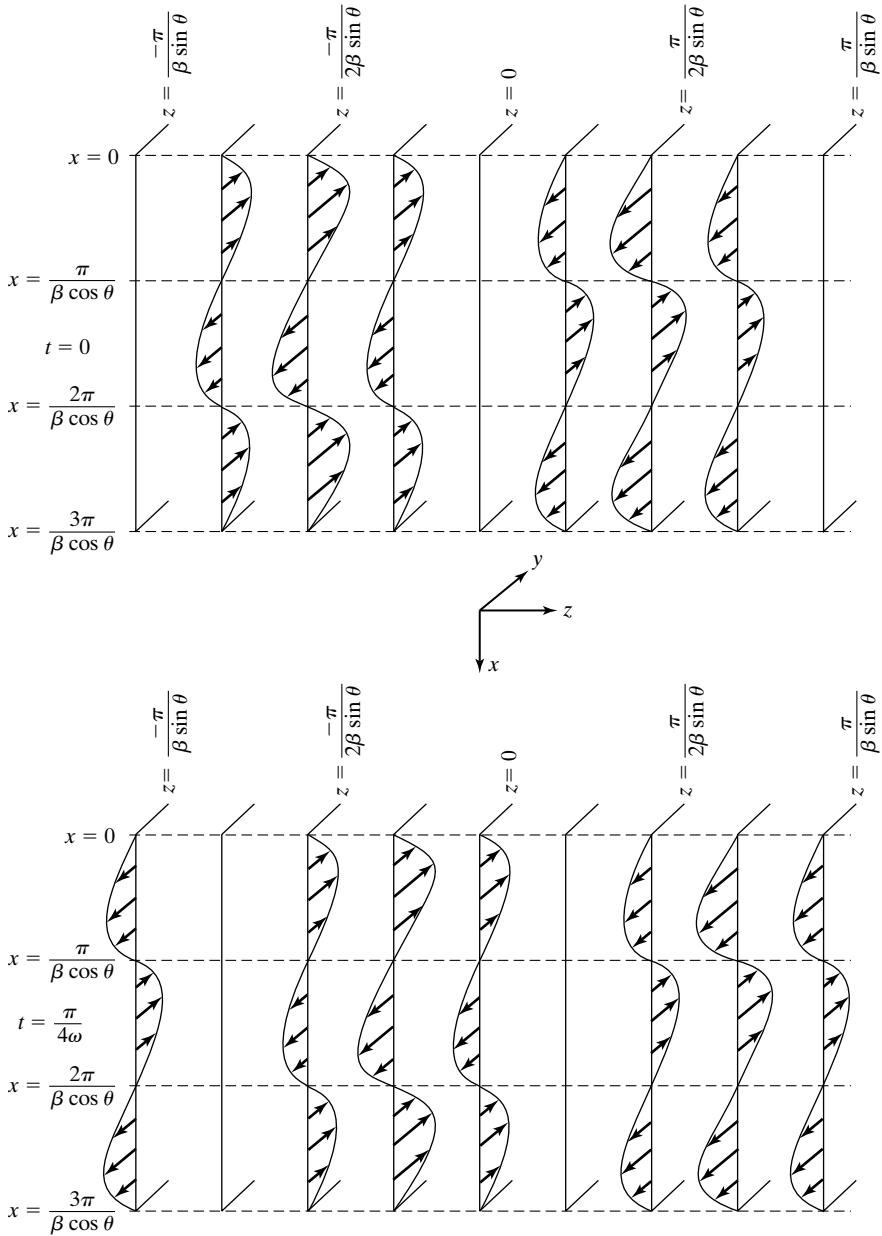


FIGURE 8.5

Standing waves in the x -direction moving bodily in the z -direction.

Thus, the time-average power flow is entirely in the z -direction, thereby verifying our interpretation of the field expressions. Since the composite electric field is directed entirely transverse to the z -direction, that is, the direction of time-average power flow, whereas the composite magnetic field is not, the composite wave is known as the *transverse electric*, or TE, wave.

From the expressions for the fields for the TE wave given by (8.25a) and (8.25b), we note that the electric field is zero for $\sin(\beta x \cos \theta)$ equal to zero, or

$$\begin{aligned} \beta x \cos \theta &= \pm m\pi, \quad m = 0, 1, 2, 3, \dots \\ x &= \pm \frac{m\pi}{\beta \cos \theta} = \pm \frac{m\lambda}{2 \cos \theta}, \quad m = 0, 1, 2, 3, \dots \end{aligned} \quad (8.28)$$

where

$$\lambda = \frac{2\pi}{\beta} = \frac{2\pi}{\omega\sqrt{\mu\epsilon}} = \frac{1}{f\sqrt{\mu\epsilon}}$$

Thus, if we place perfectly conducting sheets in these planes, the waves will propagate undisturbed, as though the sheets were not present, since the boundary condition that the tangential component of the electric field be zero on the surface of a perfect conductor is satisfied in these planes. The boundary condition that the normal component of the magnetic field be zero on the surface of a perfect conductor is also satisfied since H_x is zero in these planes.

If we consider any two adjacent sheets, the situation is actually one of uniform plane waves bouncing obliquely between the sheets, as illustrated in Fig. 8.6 for two sheets in the planes $x = 0$ and $x = \lambda/(2 \cos \theta)$, thereby guiding the wave, and hence the energy, in the z -direction, parallel to the plates. Thus, we have a *parallel-plate metallic waveguide*, as compared to the parallel-plate transmission line in which the uniform plane wave slides parallel to the plates. We note from the constant phase surfaces of the obliquely bouncing wave shown in Fig. 8.6 that $\lambda/(2 \cos \theta)$ is simply one-half of the apparent wavelength of that wave in the x -direction, that is, normal to the plates. Thus, the fields have one-half apparent wavelength in the x -direction. If we place the perfectly conducting sheets in the planes $x = 0$ and $x = m\lambda/(2 \cos \theta)$, the fields will then have m number of one-half apparent wavelengths in the x -direction between the plates. The fields have no variations in the y -direction. Thus, the fields are said to correspond to $TE_{m,0}$ modes, where the subscript m refers to the x -direction, denoting m number of one-half apparent wavelengths in that direction, and the subscript 0 refers to

*Parallel-plate
waveguide*

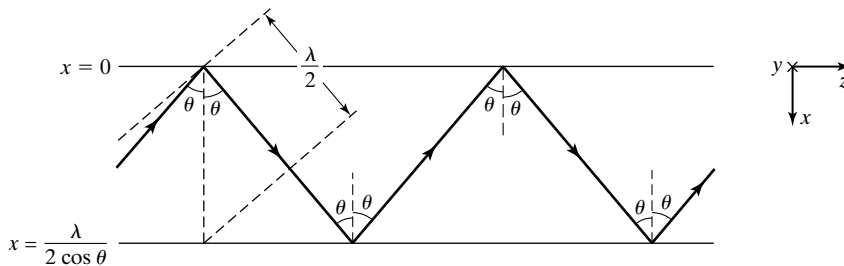


FIGURE 8.6

Uniform plane waves bouncing obliquely between two parallel plane perfectly conducting sheets.

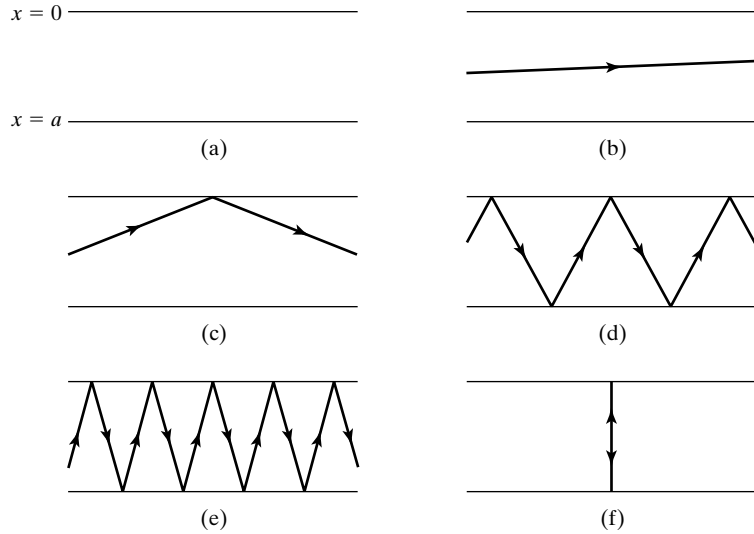


FIGURE 8.7 For illustrating the phenomenon of cutoff in a parallel-plate waveguide.

the y -direction, denoting zero number of one-half apparent wavelengths in that direction.

Cutoff phenomenon

Let us now consider a parallel-plate waveguide with perfectly conducting plates situated in the planes $x = 0$ and $x = a$, that is, having a fixed spacing a between them, as shown in Fig. 8.7(a). Then, for $TE_{m,0}$ waves guided by the plates, we have from (8.28),

$$a = \frac{m\lambda}{2 \cos \theta}$$

or

$$\cos \theta = \frac{m\lambda}{2a} = \frac{m}{2a} \frac{1}{f\sqrt{\mu\epsilon}} \tag{8.29}$$

Thus, waves of different wavelengths (or frequencies) bounce obliquely between the plates at different values of the angle θ . For very small wavelengths (very high frequencies), $m\lambda/2a$ is small, $\cos \theta \approx 0$, $\theta \approx 90^\circ$, and the waves simply slide between the plates as in the case of the transmission line, as shown in Fig. 8.7(b). As λ increases (f decreases), $m\lambda/2a$ increases, θ decreases, and the waves bounce more and more obliquely, as shown in Figs. 8.7(c)–(e). Eventually, λ becomes equal to $2a/m$, for which $\cos \theta = 1$, $\theta = 0^\circ$, and the waves simply bounce back and forth normally to the plates, as shown in Fig. 8.7(f), without any feeling of being guided parallel to the plates. For $\lambda > 2a/m$, $m\lambda/2a > 1$, $\cos \theta > 1$, and θ has no real solution, indicating that propagation does not occur for these wavelengths in the waveguide mode. This condition is known as the *cutoff* condition.

The cutoff wavelength, denoted by the symbol λ_c , is given by

$$\lambda_c = \frac{2a}{m} \quad (8.30)$$

This is simply the wavelength for which the spacing a is equal to m number of one-half wavelengths. Propagation of a particular mode is possible only if λ is less than the value of λ_c for that mode. The cutoff frequency is given by

$$f_c = \frac{m}{2a\sqrt{\mu\varepsilon}} \quad (8.31)$$

Propagation of a particular mode is possible only if f is greater than the value of f_c for that mode. Consequently, waves of a given frequency f can propagate in all modes for which the cutoff wavelengths are greater than the wavelength or the cutoff frequencies are less than the frequency. Note that since the cutoff phenomenon corresponds to the waves bouncing back and forth normal to the plates, that is, transverse to the guide axis, the expressions for the cutoff wavelength and frequency can be obtained directly from considerations of transverse resonance.

Substituting λ_c for $2a/m$ in (8.29), we have

$$\cos \theta = \frac{\lambda}{\lambda_c} = \frac{f_c}{f} \quad (8.32a)$$

$$\sin \theta = \sqrt{1 - \cos^2 \theta} = \sqrt{1 - \left(\frac{\lambda}{\lambda_c}\right)^2} = \sqrt{1 - \left(\frac{f_c}{f}\right)^2} \quad (8.32b)$$

$$\beta \cos \theta = \frac{2\pi}{\lambda} \frac{\lambda}{\lambda_c} = \frac{2\pi}{\lambda_c} = \frac{m\pi}{a} \quad (8.32c)$$

$$\beta \sin \theta = \frac{2\pi}{\lambda} \sqrt{1 - \left(\frac{\lambda}{\lambda_c}\right)^2} \quad (8.32d)$$

We see from (8.32d) that the phase constant along the z -direction, that is, $\beta_z (= \beta \sin \theta)$, is real for $\lambda < \lambda_c$ and imaginary for $\lambda > \lambda_c$. Since

$$\begin{aligned} \cos(\omega t \mp j|\beta_z|z) &= \operatorname{Re} e^{j(\omega t \mp j|\beta_z|z)} \\ &= \operatorname{Re}(e^{\pm|\beta_z|z} e^{j\omega t}) \\ &= e^{\pm|\beta_z|z} \cos \omega t \end{aligned}$$

an imaginary value of the phase constant does not correspond to wave propagation. This once again explains the cutoff phenomenon. We now define the guide wavelength, λ_g , to be the wavelength in the z -direction, that is, along the guide. This is given by

$$\lambda_g = \frac{2\pi}{\beta_z} = \frac{2\pi}{\beta \sin \theta} = \frac{\lambda}{\sqrt{1 - (\lambda/\lambda_c)^2}} = \frac{\lambda}{\sqrt{1 - (f_c/f)^2}} \quad (8.33)$$

This is simply the apparent wavelength, in the z -direction, of the obliquely bouncing uniform plane waves. The phase velocity along the guide axis, which is simply the apparent phase velocity, in the z -direction, of the obliquely bouncing uniform plane waves, is

$$v_{pz} = \frac{\omega}{\beta_z} = \frac{\omega}{\beta \sin \theta} = \frac{v_p}{\sqrt{1 - (\lambda/\lambda_c)^2}} = \frac{v_p}{\sqrt{1 - (f_c/f)^2}} \quad (8.34)$$

Field expressions for TE_{m,0} modes

Finally, substituting (8.32a)–(8.32d) in the field expressions (8.25a) and (8.25b), we obtain

$$\mathbf{E} = E_0 \sin\left(\frac{m\pi x}{a}\right) \sin(\omega t - \beta_z z) \mathbf{a}_y \quad (8.35a)$$

$$\begin{aligned} \mathbf{H} = & -\frac{E_0}{\eta} \frac{\lambda}{\lambda_g} \sin\left(\frac{m\pi x}{a}\right) \sin(\omega t - \beta_z z) \mathbf{a}_x \\ & + \frac{E_0}{\eta} \frac{\lambda}{\lambda_c} \cos\left(\frac{m\pi x}{a}\right) \cos(\omega t - \beta_z z) \mathbf{a}_z \end{aligned} \quad (8.35b)$$

These expressions for the TE_{m,0} mode fields in the parallel-plate waveguide do not contain the angle θ . They clearly indicate the standing-wave character of the fields in the x -direction, having m one-half sinusoidal variations between the plates. We shall now consider an example.

Example 8.2 Finding propagating TE_{m,0} modes in an air–dielectric parallel-plate waveguide

Let us assume the spacing a between the plates of an air–dielectric parallel-plate waveguide to be 5 cm and investigate the propagating TE_{m,0} modes for $f = 10,000$ MHz.

From (8.30), the cutoff wavelengths for TE_{m,0} modes are given by

$$\lambda_c = \frac{2a}{m} = \frac{10}{m} \text{ cm} = \frac{1.0}{m} \text{ m}$$

This result is independent of the dielectric between the plates. Since the medium between the plates is free space, the cutoff frequencies for the TE_{m,0} modes are

$$f_c = \frac{3 \times 10^8}{\lambda_c} = \frac{3 \times 10^8}{0.1/m} = 3m \times 10^9 \text{ Hz}$$

For $f = 10,000$ MHz = 10^{10} Hz, the propagating modes are TE_{1,0} ($f_c = 3 \times 10^9$ Hz), TE_{2,0} ($f_c = 6 \times 10^9$ Hz), and TE_{3,0} ($f_c = 9 \times 10^9$ Hz).

For each propagating mode, we can find θ , λ_g , and v_{pz} by using (8.32a), (8.33), and (8.34), respectively. Values of these quantities are listed in the following:

Mode	λ_c (cm)	f_c (MHz)	θ (deg)	λ_g (cm)	v_{pz} (m/s)
TE _{1,0}	10	3000	72.54	3.145	3.145×10^8
TE _{2,0}	5	6000	53.13	3.75	3.75×10^8
TE _{3,0}	3.33	9000	25.84	6.882	6.882×10^8

We have thus far considered transverse electric or TE waves in a parallel-plate waveguide. In a similar manner, it is possible to have propagation of transverse magnetic or TM waves, so called because the magnetic field is directed entirely transverse to the direction of time-average power flow, whereas the electric field is not. The field expressions for TM waves can be obtained by starting with two uniform plane waves having their magnetic fields entirely in the y -direction, and proceeding in a manner similar to the development of TE waves. However, we shall not pursue that approach. Instead, we shall, by analogy with (8.35a), write the expression for the magnetic field of the TM wave and then derive the electric field by using one of Maxwell's curl equations.

Thus, assuming the guide to be made up of parallel plates in the $x = 0$ and $x = a$ planes, and writing the expression for the magnetic field of the $\text{TM}_{m,0}$ wave and using

$$\nabla \times \mathbf{H} = \frac{\partial \mathbf{D}}{\partial t}$$

we obtain the fields for the TM modes to be

$$\mathbf{H} = H_0 \cos\left(\frac{m\pi x}{a}\right) \sin(\omega t - \beta_z z) \mathbf{a}_y \quad (8.36a)$$

$$\begin{aligned} \mathbf{E} &= \frac{\lambda}{\lambda_g} \eta H_0 \cos\left(\frac{m\pi x}{a}\right) \sin(\omega t - \beta_z z) \mathbf{a}_x \\ &+ \frac{\lambda}{\lambda_c} \eta H_0 \sin\left(\frac{m\pi x}{a}\right) \cos(\omega t - \beta_z z) \mathbf{a}_z \end{aligned} \quad (8.36b)$$

Note that the x -variation of H_y is cosinusoidal, which leads to sinusoidal variation for E_z so that the boundary condition of zero tangential electric field is satisfied on the two plates. The parameters λ_c and λ_g in (8.36a) and (8.36b) and the other parameters f_c and v_{pz} for the TM modes are the same as those for the TE modes, given by (8.30), (8.33), (8.31), and (8.34), respectively.

We have in this section introduced the principle of metallic waveguides by considering the parallel-plate waveguide. In practice, however, metallic waveguides are generally made up of a single conductor having rectangular or circular cross section. We shall defer the consideration of rectangular metallic waveguides to Section 9.1 and discuss in Section 8.4 the important phenomenon of dispersion, characteristic of propagation in parallel-plate as well as rectangular and circular waveguides and leading to the concept of group velocity.

But first we shall conclude this section with a brief description of a naturally occurring waveguide, although of spherical geometry. This is the Earth-ionosphere waveguide. The ionosphere is a region of the upper atmosphere extending from approximately 50 km to more than 1000 km above Earth. In this region, the constituent gases are ionized, mostly because of ultraviolet radiation from the Sun, thereby resulting in the production of positive ions and electrons that are free to move under the influence of the fields of a wave incident on the

TM waves

Field expressions for $\text{TM}_{m,0}$ modes

Earth-ionosphere waveguide

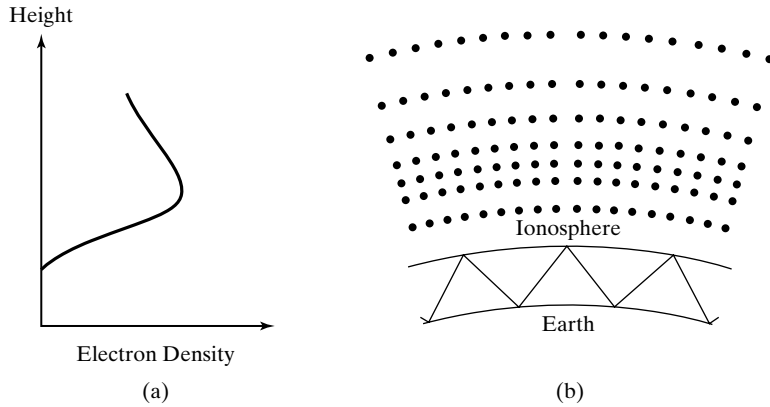


FIGURE 8.8

(a) Variation of electron density with height for a simplified ionosphere. (b) Depiction of waveguide mode of propagation in the Earth-ionosphere waveguide.

medium. The positive ions are, however, heavy compared to the electrons, and hence they are relatively immobile. The electron motion produces a current that influences the wave propagation. The electron density in the ionosphere exists in several layers known as the *D*, *E*, and *F* layers, in which the ionization changes with the hour of the day, the season, and the sunspot cycle. However, for the purpose of our discussion, it is sufficient to assume that the electron density increases continuously from zero at the lower boundary, reaching a peak at some height, typically lying between 250 and 350 km, and then decreases continuously, as shown in Fig. 8.8(a). The wave propagation is influenced by the electrons in such a manner that waves of very low frequencies are reflected at the base. As the frequency is increased, the waves penetrate deeper into the region but still return to Earth after reflection. When their frequency exceeds a certain value, typically between 20 and 40 MHz depending on the angle of incidence, they penetrate through the maximum of the layer and hence do not return to Earth. Thus, for frequencies in the VLF range and lower, the lower boundary of the ionosphere and Earth form a waveguide, thereby permitting a waveguide mode of propagation, as shown in Fig. 8(b).

- K8.2.** Transverse electric wave; Transverse magnetic wave; Parallel-plate waveguide; Cutoff frequency; Cutoff wavelength; Guide wavelength.
- D8.3.** The dimension a of an air-dielectric parallel-plate waveguide is 3 cm. Find the values of θ and λ_g for each of the following cases: (a) $f = 6000$ MHz, $TE_{1,0}$ mode; (b) $f = 15,000$ MHz, $TE_{1,0}$ mode; and (c) $f = 15,000$ MHz, $TE_{2,0}$ mode.
Ans. (a) 33.56° , 9.045 cm; (b) 70.53° , 2.121 cm; (c) 48.19° , 2.683 cm.
- D8.4.** TE waves are excited in an air-dielectric parallel-plate waveguide having the plates in the $x = 0$ and $x = 5$ cm planes by setting up at its input $z = 0$ a field distribution having

$$\mathbf{E} = 40 \sin^3 20\pi x \sin 2 \times 10^{10} \pi t \mathbf{a}_y \text{ V/m}$$

Noting that the electric field of a propagating $TE_{m,0}$ mode is of the form given by (9.35a), find E_0 for each of the following modes: **(a)** $TE_{1,0}$; **(b)** $TE_{2,0}$; and **(c)** $TE_{3,0}$.

Ans. **(a)** 30 V/m; **(b)** 0 V/m; **(c)** -10 V/m.

8.3 TRANSMISSION-LINE EQUIVALENTS

Let us now consider reflection and transmission at a dielectric discontinuity in a parallel-plate guide, as shown in Fig. 8.9. If a TE or TM wave is incident on the junction from section 1, then it will set up a reflected wave into section 1 and a transmitted wave into section 2, provided that mode propagates in that section. The fields corresponding to these incident, reflected, and transmitted waves must satisfy the boundary conditions at the dielectric discontinuity.

Parallel-plate waveguide discontinuity

Considering first TE waves and denoting the incident, reflected, and transmitted wave fields by the subscripts i , r , and t , respectively, we have from the continuity of the tangential component of \mathbf{E} at a dielectric discontinuity,

$$E_{yi} + E_{yr} = E_{yt} \quad \text{at } z = 0 \quad (8.37a)$$

and from the continuity of the tangential component of \mathbf{H} at a dielectric discontinuity,

$$H_{xi} + H_{xr} = H_{xt} \quad \text{at } z = 0 \quad (8.37b)$$

We now define the guide characteristic impedance, η_{g1} , of section 1 as

$$\eta_{g1} = \frac{E_{yi}}{-H_{xi}} \quad (8.38)$$

Recognizing that $\mathbf{a}_y \times (-\mathbf{a}_x) = \mathbf{a}_z$, we note that η_{g1} is simply the ratio of the transverse components of the electric and magnetic fields of the $TE_{m,0}$ wave that give rise to time-average power flow down the guide. From (8.35a) and (8.35b) applied to section 1, we have

$$\eta_{g1} = \eta_1 \frac{\lambda_{g1}}{\lambda_1} = \frac{\eta_1}{\sqrt{1 - (\lambda_1/\lambda_c)^2}} = \frac{\eta_1}{\sqrt{1 - (f_c/f)^2}} \quad (8.39)$$

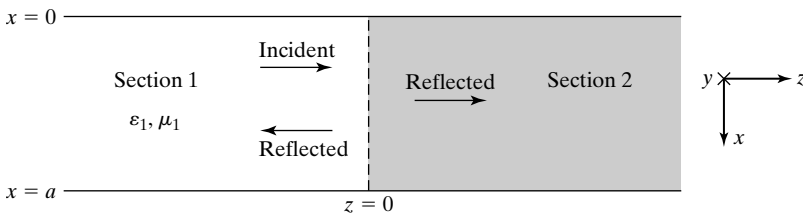


FIGURE 8.9

For consideration of reflection and transmission at a dielectric discontinuity in a parallel-plate waveguide.

The guide characteristic impedance is analogous to the characteristic impedance of a transmission line, if we recognize that E_{yi} and $-H_{xi}$ are analogous to V^+ and I^+ , respectively. In terms of the reflected wave fields, it then follows that

$$\eta_{g1} = -\left(\frac{E_{yr}}{-H_{xr}}\right) = \frac{E_{yr}}{H_{xr}} \quad (8.40)$$

This result can also be seen from the fact that for the reflected wave, the power flow is in the negative z -direction, and since $\mathbf{a}_y \times \mathbf{a}_x = -\mathbf{a}_z$, η_{g1} is equal to E_{yr}/H_{xr} . For the transmitted wave fields, we have

$$\frac{E_{yt}}{-H_{xt}} = \eta_{g2} \quad (8.41)$$

where

$$\eta_{g2} = \eta_2 \frac{\lambda_{g2}}{\lambda_2} = \frac{\eta_2}{\sqrt{1 - (\lambda_2/\lambda_c)^2}} = \frac{\eta_2}{\sqrt{1 - (f_c/f)^2}} \quad (8.42)$$

is the guide characteristic impedance of section 2.

Using (8.38), (8.40), and (8.41), (8.37b) can be written as

$$\frac{E_{yi}}{\eta_{g1}} - \frac{E_{yr}}{\eta_{g1}} = \frac{E_{yt}}{\eta_{g2}} \quad (8.43)$$

Solving (8.37a) and (8.43), we get

$$E_{yi} \left(1 - \frac{\eta_{g2}}{\eta_{g1}}\right) + E_{yr} \left(1 + \frac{\eta_{g2}}{\eta_{g1}}\right) = 0$$

or the reflection coefficient at the junction is given by

$$\Gamma = \frac{E_{yr}}{E_{yi}} = \frac{\eta_{g2} - \eta_{g1}}{\eta_{g2} + \eta_{g1}} \quad (8.44)$$

This expression for the reflection coefficient is the same as that for the voltage reflection coefficient at the load of a lossless transmission line of characteristic impedance η_{g1} terminated by a resistive load η_{g2} . It is also the same as the voltage reflection coefficient at the junction between two transmission lines 1 and 2 having the characteristic impedances η_{g1} and η_{g2} , respectively, as shown in Fig. 8.10, where line 2 is infinitely long and hence its input impedance is equal to η_{g2} . Thus, insofar as reflection and transmission at the discontinuity are concerned, each waveguide section can be replaced by a transmission line

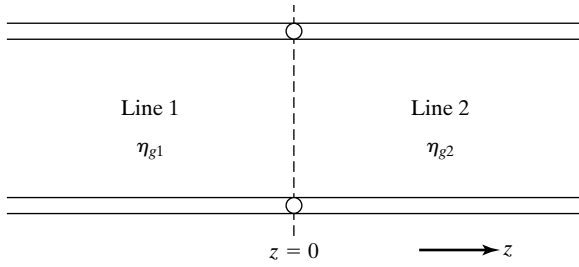


FIGURE 8.10

Transmission-line equivalent of parallel-plate waveguide discontinuity.

of characteristic impedance equal to the guide characteristic impedance given for the TE modes by

$$\boxed{[\eta_g]_{\text{TE}} = \frac{\eta}{\sqrt{1 - (f_c/f)^2}}} \quad (8.45)$$

It should be noted that unlike the characteristic impedance of a lossless line, which is a constant independent of frequency, the guide characteristic impedance of the lossless waveguide is a function of the frequency and the mode of propagation. Before considering TM modes, it should be pointed out that the power reflection coefficient is Γ^2 so that the reflected power is Γ^2 times the incident power and the transmitted power into section 2 is $(1 - \Gamma^2)$ times the incident power.

Turning now to TM waves, we observe from (8.36a) and (8.36b) that the ratio of the transverse electric field component E_x to the transverse magnetic field component H_y , which together are responsible for time-average power flow in the z -direction, is equal to $\eta\lambda/\lambda_g$, and hence the guide characteristic impedance for TM waves is given by

$$\boxed{[\eta_g]_{\text{TM}} = \eta\sqrt{1 - (f_c/f)^2}} \quad (8.46)$$

Thus, the transmission-line equivalent for reflection and transmission of TM waves at the waveguide discontinuity is the same as in Fig. 8.10, except that η_{g1} and η_{g2} follow from (8.46). We shall now consider an example.

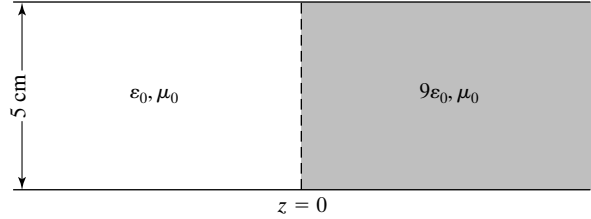
Example 8.3 Parallel-plate waveguide discontinuity

Let us consider the parallel-plate waveguide discontinuity shown in Fig. 8.11. We wish to find the power reflection coefficients for $\text{TE}_{1,0}$ and $\text{TM}_{1,0}$ waves of frequency $f = 5000$ MHz incident on the junction from the free-space side.

For the $\text{TE}_{1,0}$ mode or for the $\text{TM}_{1,0}$ mode, $\lambda_c = 2a = 10$ cm, independent of the dielectric. For $f = 5000$ MHz,

$$\lambda_1 = \text{wavelength on the free space side} = \frac{3 \times 10^8}{5 \times 10^9} = 6 \text{ cm}$$

$$\lambda_2 = \text{wavelength on the dielectric side} = \frac{3 \times 10^8}{\sqrt{9} \times 5 \times 10^9} = \frac{6}{3} = 2 \text{ cm}$$


FIGURE 8.11

For illustrating the computation of reflection and transmission coefficients at a parallel-plate waveguide discontinuity.

Since $\lambda < \lambda_c$ in both sections, $TE_{1,0}$ and $TM_{1,0}$ modes propagate in both sections. Thus, for the $TE_{1,0}$ mode,

$$\begin{aligned}\eta_{g1} &= \frac{\eta_1}{\sqrt{1 - (\lambda_1/\lambda_c)^2}} = \frac{120\pi}{\sqrt{1 - (6/10)^2}} = 471.24 \, \Omega \\ \eta_{g2} &= \frac{\eta_2}{\sqrt{1 - (\lambda_2/\lambda_c)^2}} = \frac{120\pi/\sqrt{9}}{\sqrt{1 - (2/10)^2}} = \frac{40\pi}{\sqrt{1 - 0.04}} = 128.25 \, \Omega \\ \Gamma^2 &= \left(\frac{\eta_{g2} - \eta_{g1}}{\eta_{g2} + \eta_{g1}} \right)^2 = \left(\frac{128.25 - 471.24}{128.25 + 471.24} \right)^2 = (-0.572)^2 = 0.327\end{aligned}$$

For the $TM_{1,0}$ mode,

$$\begin{aligned}\eta_{g1} &= \eta_1 \sqrt{1 - (\lambda_1/\lambda_c)^2} = 301.59 \, \Omega \\ \eta_{g2} &= \eta_2 \sqrt{1 - (\lambda_2/\lambda_c)^2} = 123.12 \, \Omega \\ \Gamma^2 &= \left(\frac{\eta_{g2} - \eta_{g1}}{\eta_{g2} + \eta_{g1}} \right)^2 = \left(\frac{123.12 - 301.59}{123.12 + 301.59} \right)^2 = (-0.42)^2 = 0.176\end{aligned}$$

K8.3. Parallel-plate waveguide discontinuity; Guide characteristic impedance; Transmission-line equivalent.

D8.5. For a parallel-plate waveguide of spacing $a = 3$ cm and filled with a dielectric of $\epsilon = 6.25\epsilon_0$ and $\mu = \mu_0$, find the values of the guide characteristic impedance for each of the following cases: **(a)** $TE_{1,0}$ mode of $f = 3000$ MHz; **(b)** $TM_{1,0}$ mode of $f = 3000$ MHz; and **(c)** $TE_{1,0}$ mode of $f = 6000$ MHz.

Ans. **(a)** 202.3 Ω ; **(b)** 112.4 Ω ; **(c)** 159.94 Ω .

8.4 DISPERSION AND GROUP VELOCITY

In Section 8.2, we learned that for the propagating range of frequencies, the phase velocity and the wavelength along the axis of the parallel-plate waveguide are given by

$$v_{pz} = \frac{v_p}{\sqrt{1 - (f_c/f)^2}} \quad (8.47)$$

and

$$\lambda_g = \frac{\lambda}{\sqrt{1 - (f_c/f)^2}} \quad (8.48)$$

where $v_p = 1/\sqrt{\mu\varepsilon}$, $\lambda = v_p/f = 1/f\sqrt{\mu\varepsilon}$, and f_c is the cutoff frequency. We note that for a particular mode, the phase velocity of propagation along the guide axis varies with the frequency. As a consequence of this characteristic of the guided wave propagation, the field patterns of the different frequency components of a signal comprising a band of frequencies do not maintain the same phase relationships as they propagate down the guide. This phenomenon is known as *dispersion* for its similarity to the phenomenon of dispersion of colors by a prism.

To discuss dispersion, let us consider a simple example of two infinitely long trains A and B traveling in parallel, one below the other, with each train made up of boxcars of identical size and having wavy tops, as shown in Fig. 8.12. Let the spacings between the peaks (centers) of successive boxcars be 50 m and 90 m, and let the speeds of the trains be 20 m/s and 30 m/s, for trains A and B , respectively. Let the peaks of the cars numbered 0 for the two trains be aligned at time $t = 0$, as shown in Fig. 8.12(a). Now, as time progresses, the two peaks get out of alignment as shown, for example, for $t = 1$ s in Fig. 8.12(b), since train B is traveling faster than train A . But at the same time, the gap between the peaks of cars numbered -1 decreases. This continues until at $t = 4$ s, the peak of car -1 of train A having moved by a distance of 80 m aligns with the peak of car -1 of train B , which will have moved by a distance of 120 m, as shown in Fig. 8.12(c). For an observer following the movement of the two trains as a group, the group appears to have moved by a distance of 30 m, although the individual trains will have moved by 80 m and 120 m, respectively. Thus, we can talk of a *group velocity*, that is, the velocity with which the group as a whole is moving. In this case, the group velocity is $(30 \text{ m})/(4 \text{ s})$ or 7.5 m/s.

The situation in the case of the guided wave propagation of two different frequencies in the parallel-plate waveguide is analogous to the two-train example just discussed. The distance between the peaks of two successive cars is analogous to the guide wavelength, and the speed of the train is analogous to the phase velocity along the guide axis. Thus, let us consider the field patterns corresponding to two waves of frequencies f_A and f_B propagating in the same mode, having guide wavelengths λ_{gA} and λ_{gB} , and phase velocities along the guide axis v_{pzA} and v_{pzB} , respectively, as shown, for example, for the electric field of the $\text{TE}_{1,0}$ mode in Fig. 8.13. Let the positive peaks numbered 0 of the two patterns be aligned at $t = 0$, as shown in Fig. 8.13(a). As the individual waves travel with their respective phase velocities along the guide, these two peaks get out of alignment, but some time later, say, Δt , the positive peaks numbered -1 will align at some distance, say, Δz , from the location of the alignment of the 0 peaks, as shown in Fig. 8.13(b). Since the -1 th peak of wave A will have traveled a distance $\lambda_{gA} + \Delta z$ with a phase velocity v_{pzA} and the -1 th peak of

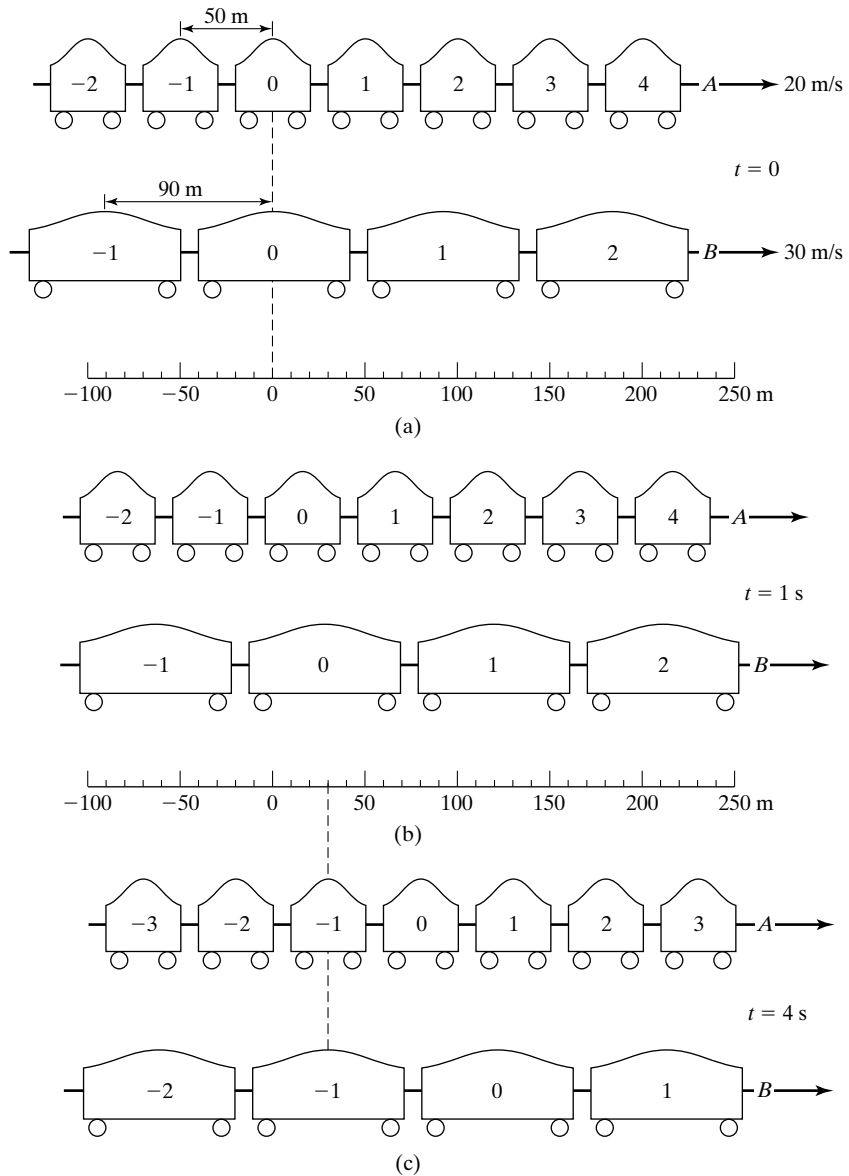


FIGURE 8.12 For illustrating the concept of group velocity.

wave B will have traveled a distance $\lambda_{gB} + \Delta z$ with a phase velocity v_{pzB} in this time Δt , we have

$$\lambda_{gA} + \Delta z = v_{pzA} \Delta t \tag{8.49a}$$

$$\lambda_{gB} + \Delta z = v_{pzB} \Delta t \tag{8.49b}$$

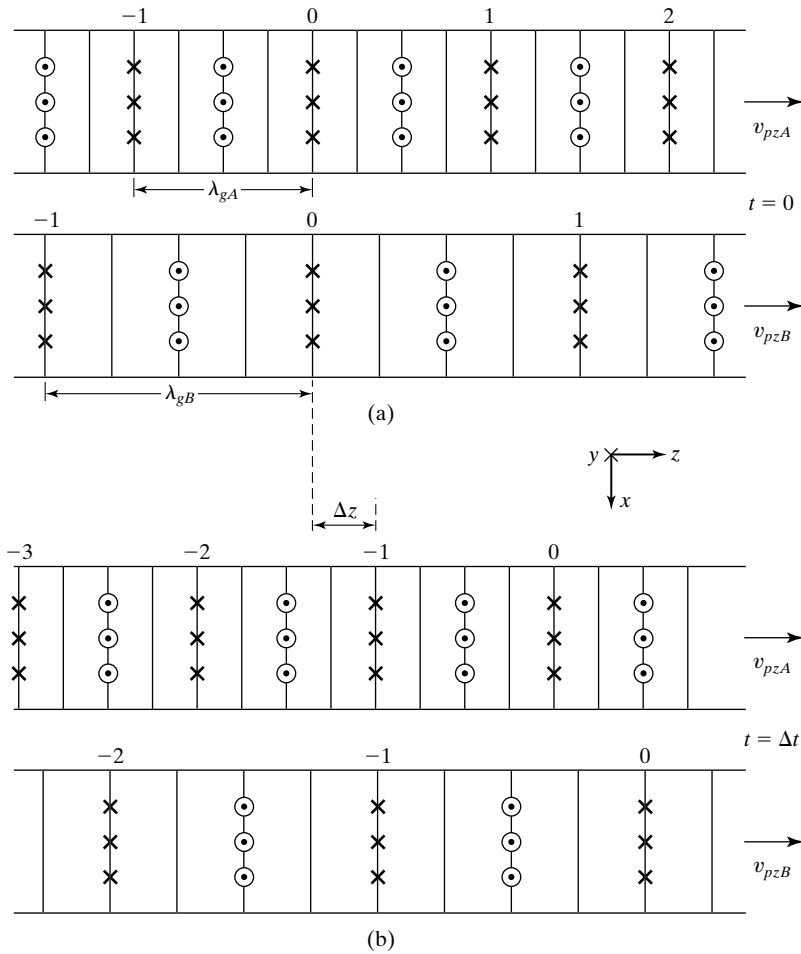


FIGURE 8.13

For illustrating the concept of group velocity for guided wave propagation.

Solving (8.49a) and (8.49b) for Δt and Δz , we obtain

$$\Delta t = \frac{\lambda_{gA} - \lambda_{gB}}{v_{pzA} - v_{pzB}} \quad (8.50a)$$

and

$$\Delta z = \frac{\lambda_{gA}v_{pzB} - \lambda_{gB}v_{pzA}}{v_{pzA} - v_{pzB}} \quad (8.50b)$$

The group velocity, v_g , is then given by

$$\begin{aligned} v_g &= \frac{\Delta z}{\Delta t} = \frac{\lambda_{gA} v_{pzB} - \lambda_{gB} v_{pzA}}{\lambda_{gA} - \lambda_{gB}} = \frac{\lambda_{gA} \lambda_{gB} f_B - \lambda_{gB} \lambda_{gA} f_A}{\lambda_{gA} \lambda_{gB} [(1/\lambda_{gB}) - (1/\lambda_{gA})]} \\ &= \frac{f_B - f_A}{(1/\lambda_{gB}) - (1/\lambda_{gA})} \end{aligned}$$

or

$$\boxed{v_g = \frac{\omega_B - \omega_A}{\beta_{zB} - \beta_{zA}}} \quad (8.51)$$

where β_{zA} and β_{zB} are the phase constants along the guide axis, corresponding to f_A and f_B , respectively. Thus, the group velocity of a signal comprised of two frequencies is the ratio of the difference between the two radian frequencies to the difference between the corresponding phase constants along the guide axis.

*Dispersion
diagram*

If we now have a signal comprised of a number of frequencies, then a value of group velocity can be obtained for each pair of these frequencies in accordance with (8.51). In general, these values of group velocity will all be different. In fact, this is the case for wave propagation in the parallel-plate guide, as can be seen from Fig. 8.14, which is a plot of ω versus β_z corresponding to the parallel-plate guide for which

$$\beta_z = \frac{2\pi}{\lambda_g} = \frac{2\pi}{\lambda} \sqrt{1 - \left(\frac{\lambda}{\lambda_c}\right)^2} = \omega \sqrt{\mu\epsilon} \sqrt{1 - \left(\frac{f_c}{f}\right)^2} \quad (8.52)$$

Such a plot is known as the $\omega - \beta_z$ diagram or *dispersion diagram*. Note that the dispersion diagram begins at $\omega = \omega_c$ on the ω -axis, since for $\omega < \omega_c$, propagation does not occur. The phase velocity along the guide axis given for a particular frequency by

$$\boxed{v_{pz} = \frac{\omega}{\beta_z}} \quad (8.53)$$

is equal to the slope of the line drawn from the origin to the point on the dispersion curve, corresponding to that frequency, as shown in the figure for the three frequencies ω_1 , ω_2 , and ω_3 . The group velocity for a particular pair of frequencies is given by the slope of the line joining the two points on the curve, corresponding to the two frequencies, as shown in the figure for the two pairs ω_1, ω_2 and ω_2, ω_3 . Since the curve is nonlinear, it can be seen that the two group velocities are not equal. We cannot then attribute a particular value of group velocity for the group of the three frequencies ω_1, ω_2 , and ω_3 .

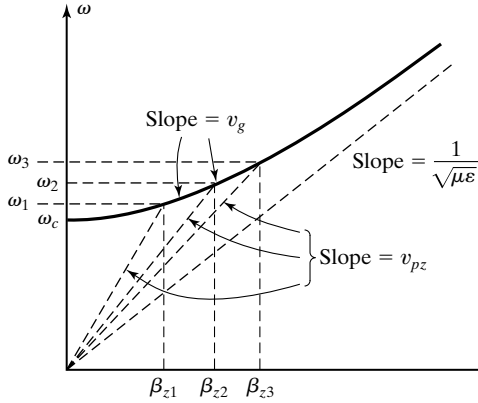


FIGURE 8.14
Dispersion diagram for the parallel-plate
waveguide.

If, however, the three frequencies are very close, as in the case of a narrow-band signal, it is meaningful to assign a group velocity to the entire group having a value equal to the slope of the tangent to the dispersion curve at the center frequency. Thus, the group velocity corresponding to a narrow band of frequencies centered around a predominant frequency ω is given by

$$\boxed{v_g = \frac{d\omega}{d\beta_z}} \quad (8.54)$$

For the parallel-plate waveguide under consideration, we have from (8.52)

$$\begin{aligned} \frac{d\beta_z}{d\omega} &= \sqrt{\mu\epsilon} \sqrt{1 - \left(\frac{f_c}{f}\right)^2} + \omega \sqrt{\mu\epsilon} \cdot \frac{1}{2} \left(1 - \frac{f_c^2}{f^2}\right)^{-1/2} \frac{f_c^2}{\pi f^3} \\ &= \sqrt{\mu\epsilon} \left(1 - \frac{f_c^2}{f^2} + \frac{\omega f_c^2}{2\pi f^3}\right) \left(1 - \frac{f_c^2}{f^2}\right)^{-1/2} \\ &= \sqrt{\mu\epsilon} \left(1 - \frac{f_c^2}{f^2}\right)^{-1/2} \end{aligned}$$

and hence, from (8.54),

$$\boxed{v_g = \frac{d\omega}{d\beta_z} = \frac{1}{\sqrt{\mu\epsilon}} \sqrt{1 - \frac{f_c^2}{f^2}} = v_p \sqrt{1 - \left(\frac{f_c}{f}\right)^2}} \quad (8.55)$$

From (8.47) and (8.55), we note that $v_{pz} > v_p$, $v_g < v_p$, and

$$v_{pz} v_g = v_p^2$$

For a numerical example, let us consider the air-dielectric parallel-plate waveguide of spacing $a = 5$ cm and a narrow-band signal of center frequency $f = 10,000$ MHz propagating in the $TE_{1,0}$ mode. Then from Example 8.2, $f_c = 3000$ MHz, and from (8.55),

$$\begin{aligned} v_g &= 3 \times 10^8 \sqrt{1 - (3/10)^2} \\ &= 2.862 \times 10^8 \text{ m/s} \end{aligned}$$

as compared to $v_{pz} = 3.145 \times 10^8$ m/s found in Example 8.2.

*Amplitude
modulated
signal*

An example of a narrow-band signal is an amplitude-modulated signal, having a carrier frequency ω modulated by a low-frequency $\Delta\omega \ll \omega$ as given by

$$E_x(t) = E_{x0}(1 + m \cos \Delta\omega \cdot t) \cos \omega t \quad (8.56)$$

where m is the percentage modulation. Such a signal is actually equivalent to a superposition of unmodulated signals of three frequencies $\omega - \Delta\omega$, ω , and $\omega + \Delta\omega$, as can be seen by expanding the right side of (8.56). Thus,

$$\begin{aligned} E_x(t) &= E_{x0} \cos \omega t + mE_{x0} \cos \omega t \cos \Delta\omega \cdot t \\ &= E_{x0} \cos \omega t + \frac{mE_{x0}}{2} [\cos (\omega - \Delta\omega)t + \cos (\omega + \Delta\omega)t] \end{aligned} \quad (8.57)$$

The frequencies $\omega - \Delta\omega$ and $\omega + \Delta\omega$ are the side frequencies. When the amplitude-modulated signal propagates in a dispersive channel, such as the parallel-plate waveguide under consideration, the different frequency components undergo phase changes in accordance with their respective phase constants. Thus, if $\beta_z - \Delta\beta_z$, β_z , and $\beta_z + \Delta\beta_z$ are the phase constants corresponding to $\omega - \Delta\omega$, ω , and $\omega + \Delta\omega$, respectively, assuming linearity of the dispersion curve within the narrow band, the amplitude-modulated wave is given by

$$\begin{aligned} E_x(z, t) &= E_{x0} \cos (\omega t - \beta_z z) \\ &\quad + \frac{mE_{x0}}{2} \{ \cos [(\omega - \Delta\omega)t - (\beta_z - \Delta\beta_z)z] \\ &\quad + \cos [(\omega + \Delta\omega)t - (\beta_z + \Delta\beta_z)z] \} \\ &= E_{x0} \cos (\omega t - \beta_z z) \\ &\quad + \frac{mE_{x0}}{2} \{ \cos [(\omega t - \beta_z z) - (\Delta\omega \cdot t - \Delta\beta_z \cdot z)] \\ &\quad + \cos [(\omega t - \beta_z z) + (\Delta\omega \cdot t - \Delta\beta_z \cdot z)] \} \\ &= E_{x0} \cos (\omega t - \beta_z z) + mE_{x0} \cos (\omega t - \beta_z z) \cos (\Delta\omega \cdot t - \Delta\beta_z \cdot z) \\ &= E_{x0} [1 + m \cos (\Delta\omega \cdot t - \Delta\beta_z \cdot z)] \cos (\omega t - \beta_z z) \end{aligned} \quad (8.58)$$

This indicates that although the carrier-frequency phase changes in accordance with the phase constant β_z , the modulation envelope, and hence the information, travels with the group velocity $\Delta\omega/\Delta\beta_z$, as shown in Fig. 8.15. In view of

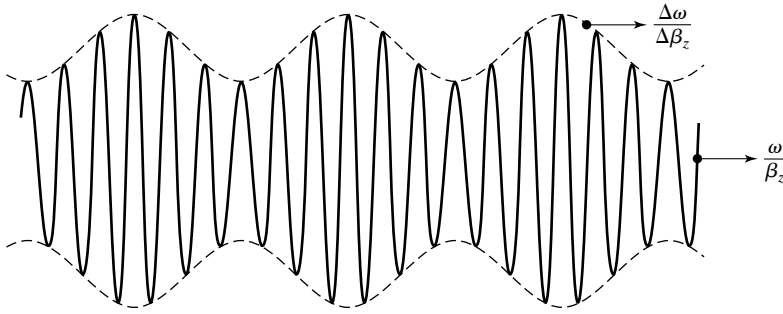


FIGURE 8.15

For illustrating that the modulation envelope travels with the group velocity.

this, and since v_g is less than v_p , the fact that v_{pz} is greater than v_p is not a violation of the theory of relativity. Since it is always necessary to use some modulation technique to convey information from one point to another, the information always takes more time to reach from one point to another in a dispersive channel than in the corresponding nondispersive medium. For further understanding of the concept of group velocity, the reader is advised to view a movie narrated by Van Duzer.¹

K8.4. Dispersion; Group velocity; Dispersion diagram; Narrow-band signal.

D8.6. The ω – β_z curve for a dispersive channel can be approximated by

$$\omega = \omega_0 + k\beta_z^2$$

in the vicinity of $\omega = 1.5\omega_0$, where k is a positive constant. Find **(a)** the phase velocity for a signal of $\omega = 1.4\omega_0$; **(b)** the phase velocity for a signal of $\omega = 1.6\omega_0$; **(c)** the group velocity for a signal composed of two radian frequencies $1.4\omega_0$ and $1.6\omega_0$; and **(d)** the group velocity for a narrow-band signal having the center radian frequency $1.5\omega_0$.

Ans. **(a)** $2.2136\sqrt{k\omega_0}$; **(b)** $2.0656\sqrt{k\omega_0}$; **(c)** $1.4071\sqrt{k\omega_0}$;
(d) $1.4142\sqrt{k\omega_0}$.

8.5 REFLECTION AND REFRACTION OF PLANE WAVES

Let us now consider a uniform plane wave that is incident obliquely on a plane boundary between two different perfect dielectric media at an angle of incidence θ_i to the normal to the boundary, as shown in Fig. 8.16. To satisfy the boundary conditions at the interface between the two media, a reflected wave and a transmitted wave will be set up. Let θ_r be the angle of reflection and θ_t be the angle of transmission. Then without writing the expressions for the fields, we

¹T. Van Duzer, *Wave Velocities, Dispersion and the Omega—Beta Diagram* (Newton, MA: Educational Development Center).

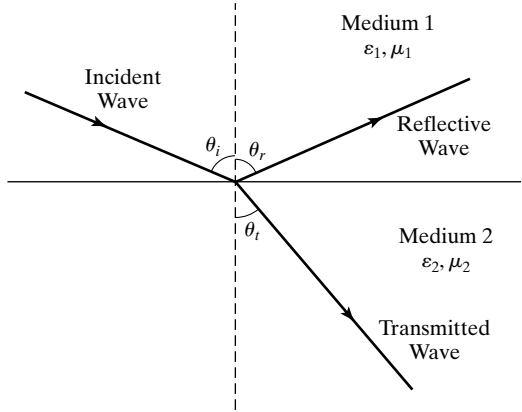


FIGURE 8.16

Reflection and transmission of an obliquely incident uniform plane wave on a plane boundary between two different perfect dielectric media.

can find the relationship among θ_i , θ_r , and θ_t by noting that for the incident, reflected, and transmitted waves to be in step at the boundary, their apparent phase velocities parallel to the boundary must be equal; that is,

$$\frac{v_{p1}}{\sin \theta_i} = \frac{v_{p1}}{\sin \theta_r} = \frac{v_{p2}}{\sin \theta_t} \quad (8.59)$$

where $v_{p1}(= 1/\sqrt{\mu_1\epsilon_1})$ and $v_{p2}(= 1/\sqrt{\mu_2\epsilon_2})$ are the phase velocities along the directions of propagation of the waves in medium 1 and medium 2, respectively.

From (8.59), we have

$$\sin \theta_r = \sin \theta_i \quad (8.60a)$$

$$\sin \theta_t = \frac{v_{p2}}{v_{p1}} \sin \theta_i = \sqrt{\frac{\mu_1\epsilon_1}{\mu_2\epsilon_2}} \sin \theta_i \quad (8.60b)$$

Laws of reflection and refraction

or

$$\theta_r = \theta_i \quad (8.61a)$$

$$\theta_t = \sin^{-1} \left(\sqrt{\frac{\mu_1\epsilon_1}{\mu_2\epsilon_2}} \sin \theta_i \right) \quad (8.61b)$$

Equation (8.61a) is known as the *law of reflection* and (8.61b) is known as the *law of refraction*, or *Snell's law*. Snell's law is commonly cast in terms of the refractive index, denoted by the symbol n and defined as the ratio of the velocity of light in free space to the phase velocity in the medium. Thus, if $n_1(= c/v_{p1})$ and $n_2(= c/v_{p2})$ are the (phase) refractive indices for media 1 and 2, respectively, then

$$\theta_t = \sin^{-1} \left(\frac{n_1}{n_2} \sin \theta_i \right) \quad (8.62)$$

For two dielectrics having $\mu_1 = \mu_2 = \mu_0$, which is usually the case, (8.62) reduces to

$$\theta_t = \sin^{-1} \left(\sqrt{\frac{\epsilon_1}{\epsilon_2}} \sin \theta_i \right) \quad (8.63)$$

We shall now consider the derivation of the expressions for the reflection and transmission coefficients at the boundary. To do this, we distinguish between two cases: (1) the electric field vector of the wave linearly polarized parallel to the interface and (2) the magnetic field vector of the wave linearly polarized parallel to the interface. The law of reflection and Snell's law hold for both cases since they result from the fact that the apparent phase velocities of the incident, reflected, and transmitted waves parallel to the boundary must be equal.

The geometry pertinent to the case of the electric field vector parallel to the interface is shown in Fig. 8.17, in which the interface is assumed to be in the $x = 0$ plane and the subscripts i , r , and t associated with the field symbols denote incident, reflected, and transmitted waves, respectively. The plane of incidence, that is, the plane containing the normal to the interface and the propagation vectors, is assumed to be in the xz -plane, so that the electric field vectors are entirely in the y -direction. The corresponding magnetic field vectors are then as shown in the figure so as to be consistent with the condition that \mathbf{E} , \mathbf{H} , and $\boldsymbol{\beta}$ form a right-handed mutually orthogonal set of vectors. Since the electric field vectors are perpendicular to the plane of incidence, this case is also said to

Perpendicular polarization

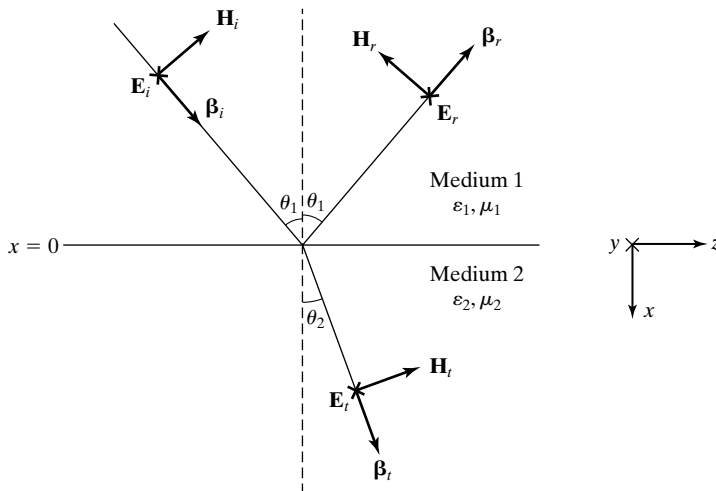


FIGURE 8.17

For obtaining the reflection and transmission coefficients for an obliquely incident uniform plane wave on a dielectric interface with its electric field perpendicular to the plane of incidence.

correspond to perpendicular polarization. The angle of incidence is assumed to be θ_1 . From the law of reflection (8.61a), the angle of reflection is then also θ_1 . The angle of transmission, assumed to be θ_2 , is related to θ_1 by Snell's law, given by (8.61b).

The boundary conditions to be satisfied at the interface $x = 0$ are that (1) the tangential component of the electric field intensity be continuous and (2) the tangential component of the magnetic field intensity be continuous. Thus, we have at the interface $x = 0$

$$E_{yi} + E_{yr} = E_{yt} \quad (8.64a)$$

$$H_{zi} + H_{zr} = H_{zt} \quad (8.64b)$$

Expressing the quantities in (8.64a) and (8.64b) in terms of the total fields, we obtain

$$E_i + E_r = E_t \quad (8.65a)$$

$$H_i \cos \theta_1 - H_r \cos \theta_1 = H_t \cos \theta_2 \quad (8.65b)$$

We also know from one of the properties of uniform plane waves that

$$\frac{E_i}{H_i} = \frac{E_r}{H_r} = \eta_1 = \sqrt{\frac{\mu_1}{\epsilon_1}} \quad (8.66a)$$

$$\frac{E_t}{H_t} = \eta_2 = \sqrt{\frac{\mu_2}{\epsilon_2}} \quad (8.66b)$$

Substituting (8.66a) and (8.66b) into (8.65b) and rearranging, we get

$$E_i - E_r = E_t \frac{\eta_1 \cos \theta_2}{\eta_2 \cos \theta_1} \quad (8.67)$$

Solving (8.65a) and (8.67) for E_i and E_r , we have

$$E_i = \frac{E_t}{2} \left(1 + \frac{\eta_1 \cos \theta_2}{\eta_2 \cos \theta_1} \right) \quad (8.68a)$$

$$E_r = \frac{E_t}{2} \left(1 - \frac{\eta_1 \cos \theta_2}{\eta_2 \cos \theta_1} \right) \quad (8.68b)$$

We now define the reflection coefficient Γ_{\perp} and the transmission coefficient τ_{\perp} as

$$\Gamma_{\perp} = \frac{E_r}{E_i} = \frac{E_{yr}}{E_{yi}} \quad (8.69a)$$

$$\tau_{\perp} = \frac{E_t}{E_i} = \frac{E_{yt}}{E_{yi}} \quad (8.69b)$$

where the subscript \perp refers to perpendicular polarization. From (8.68a) and (8.68b), we then obtain

$$\Gamma_{\perp} = \frac{\eta_2 \cos \theta_1 - \eta_1 \cos \theta_2}{\eta_2 \cos \theta_1 + \eta_1 \cos \theta_2} \quad (8.70a)$$

$$\tau_{\perp} = \frac{2\eta_2 \cos \theta_1}{\eta_2 \cos \theta_1 + \eta_1 \cos \theta_2} \quad (8.70b)$$

Equations (8.70a) and (8.70b) are known as the Fresnel reflection and transmission coefficients, respectively, for perpendicular polarization.

Before we discuss the result given by (8.70a) and (8.70b), we shall derive the corresponding expressions for the case in which the magnetic field of the wave is parallel to the interface. The geometry pertinent to this case is shown in Fig. 8.18. Here again the plane of incidence is chosen to be the xz -plane, so that the magnetic field vectors are entirely in the y -direction. The corresponding electric field vectors are then as shown in the figure so as to be consistent with the condition that \mathbf{E} , \mathbf{H} , and $\boldsymbol{\beta}$ form a right-handed mutually orthogonal set of vectors. Since the electric field vectors are parallel to the plane of incidence, this case is also said to correspond to parallel polarization.

*Parallel
polarization*

Once again the boundary conditions to be satisfied at the interface $x = 0$ are that (1) the tangential component of the electric field intensity be

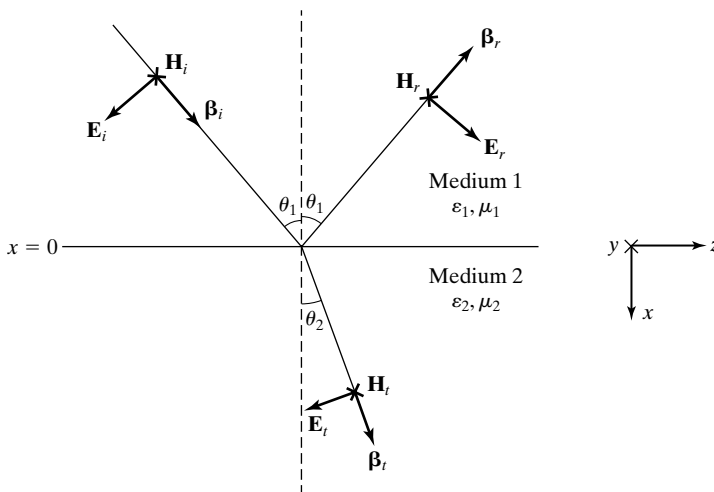


FIGURE 8.18

For obtaining the reflection and transmission coefficients for an obliquely incident uniform plane wave on a dielectric interface with its electric field parallel to the plane of incidence.

continuous and (2) the tangential component of the magnetic field intensity be continuous. Thus, we have at the interface $x = 0$,

$$E_{zi} + E_{zr} = E_{zt} \quad (8.71a)$$

$$H_{yi} + H_{yr} = H_{yt} \quad (8.71b)$$

Expressing the quantities in (8.71a) and (8.71b) in terms of the total fields and also using (8.66a) and (8.66b), we obtain

$$E_i - E_r = E_t \frac{\cos \theta_2}{\cos \theta_1} \quad (8.72a)$$

$$E_i + E_r = E_t \frac{\eta_1}{\eta_2} \quad (8.72b)$$

Solving (8.72a) and (8.72b) for E_i and E_r , we have

$$E_i = \frac{E_t}{2} \left(\frac{\eta_1}{\eta_2} + \frac{\cos \theta_2}{\cos \theta_1} \right) \quad (8.73a)$$

$$E_r = \frac{E_t}{2} \left(\frac{\eta_1}{\eta_2} - \frac{\cos \theta_2}{\cos \theta_1} \right) \quad (8.73b)$$

We now define the reflection coefficient Γ_{\parallel} and the transmission coefficient τ_{\parallel} as

$$\Gamma_{\parallel} = -\frac{E_r}{E_i} \quad (8.74a)$$

$$\tau_{\parallel} = \frac{E_t}{E_i} \quad (8.74b)$$

where the subscript \parallel refers to parallel polarization. From (8.73a) and (8.73b), we then obtain

$$\Gamma_{\parallel} = \frac{\eta_2 \cos \theta_2 - \eta_1 \cos \theta_1}{\eta_2 \cos \theta_2 + \eta_1 \cos \theta_1} \quad (8.75a)$$

$$\tau_{\parallel} = \frac{2\eta_2 \cos \theta_1}{\eta_2 \cos \theta_2 + \eta_1 \cos \theta_1} \quad (8.75b)$$

Note from (8.74a) and (8.74b) that

$$\frac{E_{zr}}{E_{zi}} = \frac{E_r \cos \theta_1}{-E_i \cos \theta_1} = -\frac{E_r}{E_i} = \Gamma_{\parallel} \quad (8.76a)$$

$$\frac{E_{zt}}{E_{zi}} = \frac{-E_t \cos \theta_2}{-E_i \cos \theta_1} = \frac{\cos \theta_2}{\cos \theta_1} \tau_{\parallel} \quad (8.76b)$$

Equations (8.75a) and (8.75b) are known as the Fresnel reflection and transmission coefficients, respectively, for parallel polarization.

We shall now discuss the results given by (8.70a), (8.70b), (8.75a), and (8.75b) for the reflection and transmission coefficients for the two cases:

1. For $\theta_1 = 0$, that is, for the case of normal incidence of the uniform plane wave upon the interface, $\theta_2 = 0$ and

$$\Gamma_{\perp} = \frac{\eta_2 - \eta_1}{\eta_2 + \eta_1}, \quad \Gamma_{\parallel} = \frac{\eta_2 - \eta_1}{\eta_2 + \eta_1}$$

$$\tau_{\perp} = \frac{2\eta_2}{\eta_2 + \eta_1}, \quad \tau_{\parallel} = \frac{2\eta_2}{\eta_2 + \eta_1}$$

Thus, the reflection coefficients as well as the transmission coefficients for the two cases become equal as they should, since for normal incidence there is no difference between the two polarizations except for rotation by 90° parallel to the interface.

2. $\Gamma_{\perp} = 1$ and $\Gamma_{\parallel} = -1$ if $\cos \theta_2 = 0$; that is,

Total internal reflection

$$\sqrt{1 - \sin^2 \theta_2} = \sqrt{1 - \frac{\mu_1 \varepsilon_1}{\mu_2 \varepsilon_2} \sin^2 \theta_1} = 0$$

or

$$\sin \theta_1 = \sqrt{\frac{\mu_2 \varepsilon_2}{\mu_1 \varepsilon_1}} \quad (8.77)$$

where we have used Snell's law given by (8.61b) to express $\sin \theta_2$ in terms of $\sin \theta_1$. If we assume $\mu_2 = \mu_1 = \mu_0$, as is usually the case, (8.77) has real solutions for θ_1 for $\varepsilon_2 < \varepsilon_1$. Thus, for $\varepsilon_2 < \varepsilon_1$, that is, for transmission from a dielectric medium of higher permittivity into a dielectric medium of lower permittivity, there is a critical angle of incidence θ_c given by

$$\theta_c = \sin^{-1} \sqrt{\frac{\varepsilon_2}{\varepsilon_1}} \quad (8.78)$$

for which θ_2 is equal to 90° and $|\Gamma_{\perp}|$ and $|\Gamma_{\parallel}| = 1$. For $\theta_1 > \theta_c$, $\sin \theta_2$ becomes greater than 1, $\cos \theta_2$ becomes imaginary, and Γ_{\perp} and Γ_{\parallel} become complex, but with their magnitudes equal to unity, and *total internal reflection* occurs; that is, the time-average power of incident wave is entirely reflected, the boundary condition being satisfied by an evanescent field in medium 2. To explain the evanescent nature, we note with reference to the geometry of Fig. 8.17 or Fig. 8.18 that

$$\beta_{x2}^2 + \beta_{z2}^2 = \beta_1^2 = \omega^2 \mu_2 \varepsilon_2$$

or

$$\beta_{x2}^2 = \omega^2 \mu_2 \varepsilon_2 - \beta_{z2}^2$$

For $\theta_1 = \theta_c$, $\beta_{z2} = \beta_{z1} = \omega^2 \mu_1 \varepsilon_1 \sin^2 \theta_c = \omega^2 \mu_2 \varepsilon_2$, and $\beta_{x2}^2 = 0$. Therefore, for $\theta_1 > \theta_c$, $\beta_{z2} = \beta_{z1} = \omega^2 \mu_1 \varepsilon_1 \sin^2 \theta_1 > \omega^2 \mu_2 \varepsilon_2$, and $\beta_{x2}^2 < 0$. Thus, β_{x2} should be replaced by $-j\alpha_{x2}$, corresponding to exponential decay of the field in the x -direction without a propagating wave character. The phenomenon of total internal reflection is the fundamental principle of optical waveguides, since if we have a dielectric slab of permittivity ε_1 sandwiched between two dielectric media of permittivity $\varepsilon_2 < \varepsilon_1$, then by launching waves at an angle of incidence greater than the critical angle, it is possible to achieve guided wave propagation within the slab, as we shall learn in the next section.

3. $\Gamma_{\perp} = 0$ for $\eta_2 \cos \theta_1 = \eta_1 \cos \theta_2$; that is, for

$$\eta_2 \sqrt{1 - \sin^2 \theta_1} = \eta_1 \sqrt{1 - \frac{\mu_1 \varepsilon_1}{\mu_2 \varepsilon_2} \sin^2 \theta_1}$$

or

$$\sin^2 \theta_1 = \frac{\eta_2^2 - \eta_1^2}{\eta_2^2 - \eta_1^2 (\mu_1 \varepsilon_1 / \mu_2 \varepsilon_2)} = \mu_2 \frac{\mu_2 - \mu_1 (\varepsilon_2 / \varepsilon_1)}{\mu_2^2 - \mu_1^2} \quad (8.79)$$

For the usual case of transmission between two dielectric materials, that is, for $\mu_2 = \mu_1$ and $\varepsilon_2 \neq \varepsilon_1$, this equation has no real solution for θ_1 , and hence there is no angle of incidence for which the reflection coefficient is zero for the case of perpendicular polarization.

4. $\Gamma_{\parallel} = 0$ for $\eta_2 \cos \theta_2 = \eta_1 \cos \theta_1$; that is, for

$$\eta_2 \sqrt{1 - \frac{\mu_1 \varepsilon_1}{\mu_2 \varepsilon_2} \sin^2 \theta_1} = \eta_1 \sqrt{1 - \sin^2 \theta_1}$$

or

$$\sin^2 \theta_1 = \frac{\eta_2^2 - \eta_1^2}{\eta_2^2 (\mu_1 \varepsilon_1 / \mu_2 \varepsilon_2) - \eta_1^2} = \varepsilon_2 \frac{(\mu_2 / \mu_1) \varepsilon_1 - \varepsilon_2}{\varepsilon_1^2 - \varepsilon_2^2} \quad (8.80)$$

If we assume $\mu_2 = \mu_1$, this equation reduces to

$$\sin^2 \theta_1 = \frac{\varepsilon_2}{\varepsilon_1 + \varepsilon_2}$$

which then gives

$$\cos^2 \theta_1 = 1 - \sin^2 \theta_1 = \frac{\varepsilon_1}{\varepsilon_1 + \varepsilon_2}$$

and

$$\tan \theta_1 = \sqrt{\frac{\varepsilon_2}{\varepsilon_1}}$$

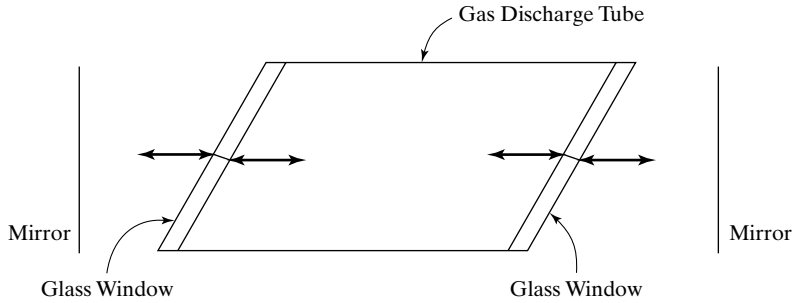


FIGURE 8.19

For illustrating the application of the Brewster angle effect in gas lasers.

Thus, there exists a value of the angle of incidence θ_p , given by

$$\theta_p = \tan^{-1} \sqrt{\frac{\epsilon_2}{\epsilon_1}} \quad (8.81)$$

for which the reflection coefficient is zero, and hence there is complete transmission for the case of parallel polarization.

5. In view of cases 3 and 4, for an elliptically polarized wave incident on the interface at the angle θ_p , the reflected wave will be linearly polarized perpendicular to the plane of incidence. For this reason, the angle θ_p is known as the *polarizing angle*. It is also known as the *Brewster angle*. The phenomenon associated with the Brewster angle has several applications. An example is in gas lasers in which the discharge tube lying between the mirrors of a Fabry–Perot resonator is sealed by glass windows placed at the Brewster angle, as shown in Fig. 8.19, to minimize reflections from the ends of the tube so that the laser behavior is governed by the mirrors external to the tube.

Brewster angle

We shall now consider an example.

Example 8.4 Oblique incidence of uniform plane wave onto a dielectric medium

A uniform plane wave having the electric field

$$\mathbf{E}_i = E_0 \left(\frac{\sqrt{3}}{2} \mathbf{a}_x - \frac{1}{2} \mathbf{a}_z \right) \cos [6\pi \times 10^9 t - 10\pi(x + \sqrt{3}z)]$$

is incident on the interface between free space and a dielectric medium of $\epsilon = 1.5\epsilon_0$ and $\mu = \mu_0$, as shown in Fig. 8.20. We wish to obtain the expressions for the electric fields of the reflected and transmitted waves.

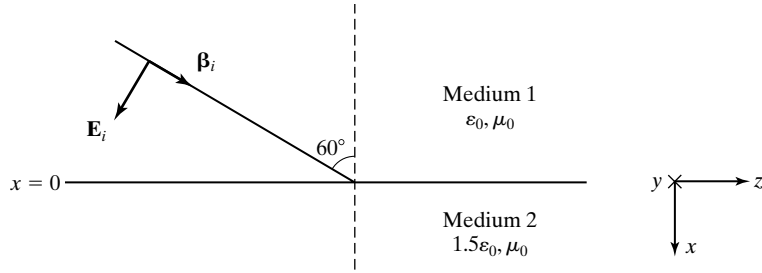


FIGURE 8.20

For Example 8.4.

First, we note from the given \mathbf{E}_i that the propagation vector of the incident wave is given by

$$\boldsymbol{\beta}_i = 10\pi(\mathbf{a}_x + \sqrt{3}\mathbf{a}_z) = 20\pi\left(\frac{1}{2}\mathbf{a}_x + \frac{\sqrt{3}}{2}\mathbf{a}_z\right)$$

the direction of which is consistent with the angle of incidence of 60° . We also note that the electric field vector (which is perpendicular to $\boldsymbol{\beta}_i$) is entirely in the plane of incidence. Thus the situation corresponds to one of parallel polarization, as in Fig. 8.18.

To obtain the required fields, we first find, by using (8.63) and with reference to the notation of Fig. 8.18, that

$$\sin \theta_2 = \sqrt{\frac{\epsilon_0}{1.5\epsilon_0}} \sin 60^\circ = \frac{1}{\sqrt{2}}$$

or $\theta_2 = 45^\circ$. Then from (8.75a)–(8.75b) and (8.76a)–(8.76b), we have

$$\begin{aligned} \Gamma_{\parallel} &= \frac{(\eta_0/\sqrt{1.5}) \cos 45^\circ - \eta_0 \cos 60^\circ}{(\eta_0/\sqrt{1.5}) \cos 45^\circ + \eta_0 \cos 60^\circ} \\ &= \frac{2 - \sqrt{3}}{2 + \sqrt{3}} = 0.072 \end{aligned}$$

$$\begin{aligned} \tau_{\parallel} &= \frac{2(\eta_0/\sqrt{1.5}) \cos 60^\circ}{(\eta_0/\sqrt{1.5}) \cos 45^\circ + \eta_0 \cos 60^\circ} \\ &= \frac{2\sqrt{2}}{2 + \sqrt{3}} = 0.758 \end{aligned}$$

$$\frac{E_r}{E_i} = -0.072$$

$$\frac{E_t}{E_i} = 0.758$$

Finally, noting with the aid of Fig. 8.21 that

$$\boldsymbol{\beta}_r = 20\pi\left(-\frac{1}{2}\mathbf{a}_x + \frac{\sqrt{3}}{2}\mathbf{a}_z\right) = 10\pi(-\mathbf{a}_x + \sqrt{3}\mathbf{a}_z)$$

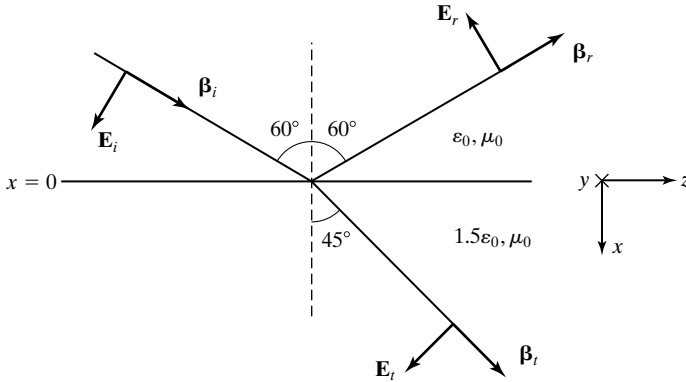


FIGURE 8.21

For writing the expressions for the reflected and transmitted wave electric fields for Example 8.4.

and

$$\boldsymbol{\beta}_t = 20\pi\sqrt{1.5}\left(\frac{1}{\sqrt{2}}\mathbf{a}_x + \frac{1}{\sqrt{2}}\mathbf{a}_z\right) = 10\sqrt{3}\pi(\mathbf{a}_x + \mathbf{a}_z)$$

we write the expressions for the reflected and transmitted wave fields to be

$$\mathbf{E}_r = -0.072E_0\left(\frac{\sqrt{3}}{2}\mathbf{a}_x + \frac{1}{2}\mathbf{a}_z\right)\cos[6\pi \times 10^9t + 10\pi(x - \sqrt{3}z)]$$

and

$$\mathbf{E}_t = 0.758E_0\left(\frac{1}{\sqrt{2}}\mathbf{a}_x - \frac{1}{\sqrt{2}}\mathbf{a}_z\right)\cos[6\pi \times 10^9t - 10\sqrt{3}\pi(x + z)]$$

Note that for $x = 0$, $E_{zi} + E_{zr} = E_{zt}$ and $E_{xi} + E_{xr} = 1.5E_{xt}$, so that the fields do indeed satisfy the boundary conditions.

K8.5. Oblique incidence of uniform plane waves; Plane interface; Law of reflection; Snell's law; Perpendicular and parallel polarizations; Total internal reflection; Brewster angle.

D8.7. Consider a plane boundary between medium 1 ($\epsilon = \epsilon_1, \mu = \mu_0$) and medium 2 ($\epsilon = \epsilon_2, \mu = \mu_0$). Find the value of ϵ_2/ϵ_1 for each of the following cases of uniform plane waves incident on the boundary from medium 1: **(a)** Total internal reflection occurs for $\theta_i \geq 60^\circ$; **(b)** the reflection coefficient for parallel polarization is zero for $\theta_i = 60^\circ$; and **(c)** the critical angle of incidence for total internal reflection is the same as the Brewster angle for incidence from medium 2.

Ans. **(a)** 0.75; **(b)** 3; **(c)** 0.618.

D8.8. In Figs. 8.17 and 8.18, assume that $\epsilon_1 = 3\epsilon_0, \epsilon_2 = 9\epsilon_0, \mu_1 = \mu_2 = \mu_0$, and $\theta_i = 45^\circ$. Find **(a)** E_r/E_i and E_t/E_i for the case of perpendicular polarization (Fig. 8.17) and **(b)** E_r/E_i and E_t/E_i for the case of parallel polarization (Fig. 8.18).

Ans. **(a)** $-0.382, 0.618$; **(b)** $0.146, 0.662$.

8.6 DIELECTRIC SLAB GUIDE

In the preceding section, we learned that for a wave that is incident obliquely from a dielectric medium of permittivity ϵ_1 onto another dielectric medium of permittivity $\epsilon_2 < \epsilon_1$, total internal reflection occurs for angles of incidence θ_i exceeding the critical angle θ_c given by

$$\theta_c = \sin^{-1} \sqrt{\frac{\epsilon_2}{\epsilon_1}} \quad (8.82)$$

where it is assumed that $\mu = \mu_0$ everywhere. In this section, we shall consider the dielectric slab waveguide, which forms the basis for thin-film waveguides, used extensively in integrated optics.

A. Wave-Bounce Approach

Description

The dielectric slab waveguide consists of a dielectric slab of permittivity ϵ_1 , sandwiched between two dielectric media of permittivities less than ϵ_1 . For simplicity, we shall consider the symmetric waveguide, that is, one for which the permittivities of the dielectrics on either side of the slab are the same and equal to ϵ_2 , as shown in Fig. 8.22. Then by launching waves at an angle of incidence $\theta_i > \theta_c$, where θ_c is given by (8.82), it is possible to achieve guided wave propagation within the slab, as shown in the figure. For a given thickness d of the slab and for a given frequency of the waves, there are only discrete values of θ_i for which the guiding can take place. In other words, guiding of a wave of a given frequency is not ensured simply because the condition for total internal reflection is met.

Self-consistency condition for guidance

The allowed values of θ_i are dictated by the self-consistency condition, which can be explained with the aid of the construction in Fig. 8.23, as follows. If we consider a point A on a given wavefront designated 1 and follow that wavefront as it moves to position 1' passing through point B , reflects at the interface $x = d/2$ giving rise to wavefront designated 2, then moves to position 2' passing

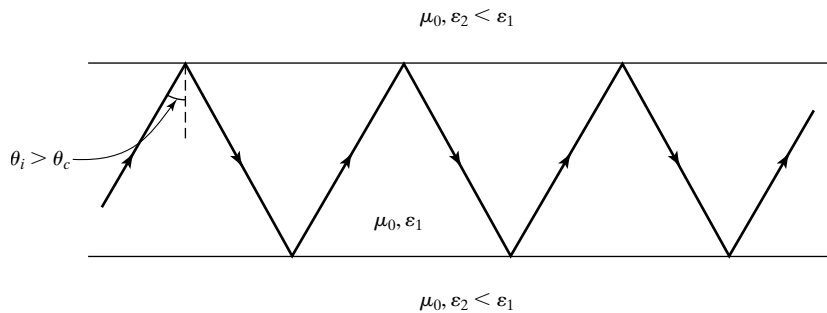


FIGURE 8.22

Total internal reflection in a dielectric slab waveguide.

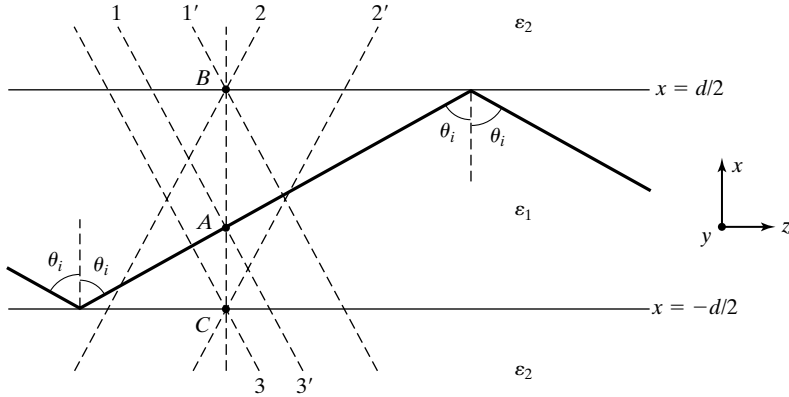


FIGURE 8.23

For explaining the self-consistency condition for waveguiding in a dielectric slab guide.

through point C , reflects at the interface $x = -d/2$ giving rise to wavefront designated 3, and finally moves to position 3' passing through A , then we see that the total phase shift undergone must be equal to an integer multiple of 2π . If λ_0 is the wavelength in free space corresponding to the wave frequency, the self-consistency condition is given by

$$\begin{aligned} \frac{2\pi\sqrt{\epsilon_{r1}}}{\lambda_0}(AB \cos \theta_i) + \angle\bar{\Gamma}_B + \frac{2\pi\sqrt{\epsilon_{r1}}}{\lambda_0}(BC \cos \theta_i) \\ + \angle\bar{\Gamma}_A + \frac{2\pi\sqrt{\epsilon_{r1}}}{\lambda_0}(CA \cos \theta_i) = 2m\pi, \quad m = 0, 1, 2, \dots \end{aligned} \quad (8.83)$$

where $\bar{\Gamma}_A$ and $\bar{\Gamma}_B$ are the reflection coefficients at the interfaces $x = -d/2$ and $x = d/2$, respectively, and $\epsilon_{r1} = \epsilon_1/\epsilon_0$. We recall that under conditions of total internal reflection, the reflection coefficients (8.70a) and (8.75a) become complex with their magnitudes equal to unity. For the symmetric waveguide, $\bar{\Gamma}_A = \bar{\Gamma}_B$. Thus, substituting $\bar{\Gamma}$ for $\bar{\Gamma}_A$ and $\bar{\Gamma}_B$ and $2d$ for $(AB + BC + CA)$, we write (8.83) as

$$\frac{4\pi d\sqrt{\epsilon_{r1}}}{\lambda_0} \cos \theta_i + 2\angle\bar{\Gamma} = 2m\pi, \quad m = 0, 1, 2, \dots$$

or

$$\boxed{\frac{2\pi d\sqrt{\epsilon_{r1}}}{\lambda_0} \cos \theta_i + \angle\bar{\Gamma} = m\pi, \quad m = 0, 1, 2, \dots} \quad (8.84)$$

Characteristic equation for TE modes and solution

To proceed further, we need to distinguish between the cases of perpendicular and parallel polarizations as defined in the preceding section, since the reflection coefficients for the two cases are different. We shall here consider only the case of perpendicular polarization. The situation then corresponds to TE modes, since the electric field has no longitudinal or z -component. Thus, substituting

$$\cos \theta_1 = \cos \theta_i$$

and

$$\begin{aligned} \cos \theta_2 &= \sqrt{1 - \sin^2 \theta_2} \\ &= j\sqrt{\sin^2 \theta_2 - 1} \\ &= j\sqrt{\frac{\epsilon_1}{\epsilon_2} \sin^2 \theta_i - 1} \end{aligned}$$

in (8.70a), we obtain

$$\bar{\Gamma}_{\perp} = \frac{\eta_2 \cos \theta_i - j\eta_1 \sqrt{(\epsilon_1/\epsilon_2) \sin^2 \theta_i - 1}}{\eta_2 \cos \theta_i + j\eta_1 \sqrt{(\epsilon_1/\epsilon_2) \sin^2 \theta_i - 1}} \quad (8.85)$$

so that

$$\begin{aligned} \angle \bar{\Gamma}_{\perp} &= -2 \tan^{-1} \frac{\eta_1 \sqrt{(\epsilon_1/\epsilon_2) \sin^2 \theta_i - 1}}{\eta_2 \cos \theta_i} \\ &= -2 \tan^{-1} \frac{\sqrt{\sin^2 \theta_i - (\epsilon_2/\epsilon_1)}}{\cos \theta_i} \end{aligned} \quad (8.86)$$

Substituting (8.86) into (8.84), we then obtain

$$\frac{2\pi d \sqrt{\epsilon_{r1}}}{\lambda_0} \cos \theta_i - 2 \tan^{-1} \frac{\sqrt{\sin^2 \theta_i - (\epsilon_2/\epsilon_1)}}{\cos \theta_i} = m\pi, \quad m = 0, 1, 2, \dots$$

or

$$\tan \left(\frac{\pi d \sqrt{\epsilon_{r1}}}{\lambda_0} \cos \theta_i - \frac{m\pi}{2} \right) = \frac{\sqrt{\sin^2 \theta_i - (\epsilon_2/\epsilon_1)}}{\cos \theta_i}, \quad m = 0, 1, 2, \dots$$

or

$$\tan [f(\theta_i)] = \begin{cases} g(\theta_i), & m = 0, 2, 4, \dots \\ -\frac{1}{g(\theta_i)}, & m = 1, 3, 5, \dots \end{cases} \quad (8.87)$$

where

$$f(\theta_i) = \frac{\pi d \sqrt{\epsilon_{r1}}}{\lambda_0} \cos \theta_i \quad (8.88a)$$

$$g(\theta_i) = \frac{\sqrt{\sin^2 \theta_i - (\epsilon_2/\epsilon_1)}}{\cos \theta_i} \quad (8.88b)$$

Equation (8.87) is the characteristic equation for the guiding of TE waves in the dielectric slab. For given values of ϵ_1 , ϵ_2 , d , and λ_0 , the solutions for θ_i can be obtained by plotting the two sides of (8.87) versus θ_i and finding the points of intersection. The nature of this construction is shown in Fig. 8.24. Each solution corresponds to one mode. It can be seen from (8.88a) and Fig. 8.24 that for a given set of values of ϵ_1 and ϵ_2 , fewer solutions are obtained for θ_i as the ratio (d/λ_0) becomes smaller, since the number of branches of the plot of $\tan [f(\theta_i)]$ between $\theta_i = \pi/2$ and $\theta_i = \theta_c$ become fewer. It can also be seen that there is always one solution for a given d , even for arbitrarily low values of (d/λ_0) —that is, for large values of λ_0 or low frequencies.

Alternative to the graphical solution, we can use a computer to solve (8.87) for the allowed values of θ_i for specified values of ϵ_{r1} , ϵ_{r2} , d , and λ_0 . Computed values of θ_i for values of $\epsilon_{r1} = 4$, $\epsilon_{r2} = 1$, $d = 10$ mm, and $\lambda_0 = 5$ mm are listed in Table 8.1.

Returning now to Fig. 8.24, we designate the modes associated with the solutions as TE_m modes, where $m = 0, 1, 2, \dots$ correspond to the values of m on the plot. We note from the plot that the solution for a given TE_m mode for

Cutoff frequencies

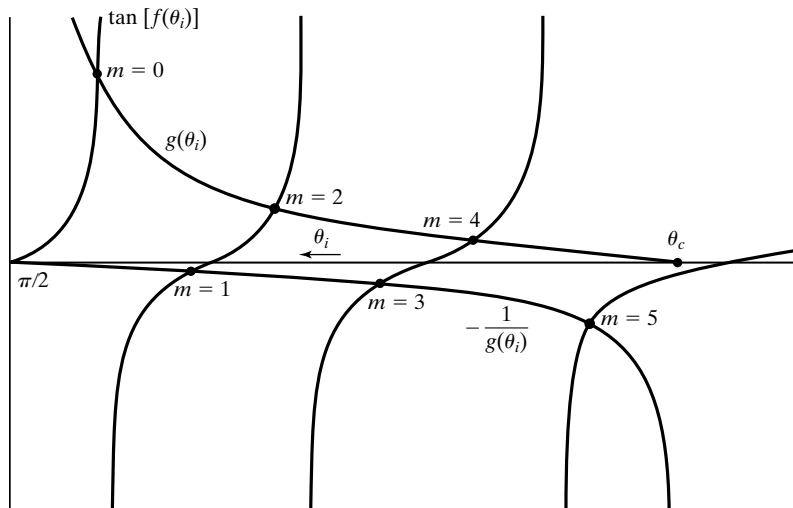


TABLE 8.1 Allowed Values of θ_i for Dielectric Slab Guide Example

m	θ_i (deg)
0	83.42783
1	76.77756
2	69.96263
3	62.87805
4	55.38428
5	47.28283
6	38.30225

$m > 1$ does not exist if $f(\theta_c) < m\pi/2$. Therefore, the cutoff condition is given by

$$\begin{aligned} \frac{\pi d \sqrt{\epsilon_{r1}}}{\lambda_0} \cos \theta_c &< \frac{m\pi}{2} \\ \frac{\pi d \sqrt{\epsilon_{r1}}}{\lambda_0} \sqrt{1 - \frac{\epsilon_2}{\epsilon_1}} &< \frac{m\pi}{2} \\ \lambda_0 &> \frac{2d \sqrt{\epsilon_{r1} - \epsilon_{r2}}}{m} \end{aligned} \tag{8.89}$$

where we have used (8.82). The cutoff frequency is given by

$$f_c = \frac{c}{\lambda_0} = \frac{mc}{2d \sqrt{\epsilon_{r1} - \epsilon_{r2}}}$$

The fundamental mode, TE₀, has no cutoff frequency. Thus,

$$f_c = \frac{mc}{2d \sqrt{\epsilon_{r1} - \epsilon_{r2}}}, \quad m = 0, 1, 2, \dots \tag{8.90}$$

Example 8.5 Finding the number of propagating TE modes in a symmetric dielectric slab waveguide

Finding propagating modes

For the symmetric dielectric slab waveguide of Fig. 8.23, let $\epsilon_1 = 2.56\epsilon_0$, $\epsilon_2 = \epsilon_0$, and $d = 10\lambda_0$. We wish to find the number of TE modes that can propagate by guidance in the slab.

From (8.90),

$$\begin{aligned} f_c &= \frac{mc}{20\lambda_0 \sqrt{2.56 - 1}} \\ &= \frac{mf}{24.98}, \quad m = 0, 1, 2, \dots \end{aligned}$$

Thus, for $m > 24$, $f_c > f$ and the modes are cut off. Therefore, the number of propagating TE modes is 25, corresponding to $m = 0, 1, 2, \dots, 24$.

The entire discussion for guided waves in the dielectric slab guide can be repeated for TM modes by using $\bar{\Gamma}_{\parallel}$ in the place of $\bar{\Gamma}_{\perp}$ in (8.84) to derive the characteristic equation for guidance. We shall include the derivation as Problem 8.27.

TM modes

B. Wave-Field Approach

A formal approach to the investigation of guided modes in the dielectric slab involves the derivation of the field expressions. This is done by recognizing with reference to the geometry in Fig. 8.23 that (a) in the slab the fields have standing wave character in the x -direction and traveling wave character in the z -direction; (b) outside the slab, the fields are evanescent, that is, they decay exponentially away from it in the x -direction and have traveling wave character in the z -direction; and (c) from symmetry considerations, the fields should be even or odd with respect to x .

Field behavior for guided modes

Let us first consider even TE modes—that is, modes with the transverse field components having even symmetry with respect to x . We write the expression for the (only) electric field component \bar{E}_y to be

Field expressions for even TE modes

$$\bar{E}_y = \begin{cases} \bar{A} \cos \beta_{x1} x e^{-j\beta_z z} & \text{for } |x| < d/2 \\ \bar{B} e^{-\alpha_{x2} x} e^{-j\beta_z z} & \text{for } x > d/2 \\ \bar{B} e^{\alpha_{x2} x} e^{-j\beta_z z} & \text{for } x < -d/2 \end{cases} \quad (8.91)$$

where \bar{A} and \bar{B} are constants. Note that subscripts 1 and 2 denote regions of permittivities ϵ_1 and ϵ_2 , respectively, and that the phase constant β_z does not have a subscript 1 or 2, since it must be the same in all three regions, in view of the requirement that the fields be in phase at the boundaries $x = \pm d/2$ for all z . Continuity of \bar{E}_y at $x = \pm d/2$ further requires that

$$\bar{A} \cos \beta_{x1} \frac{d}{2} = \bar{B} e^{-\alpha_{x2} d/2}$$

so that

$$\bar{B} = \bar{A} e^{\alpha_{x2} d/2} \cos \beta_{x1} \frac{d}{2} \quad (8.92)$$

and hence

$$\bar{E}_y = \begin{cases} \bar{A} \cos \beta_{x1} x e^{-j\beta_z z} & \text{for } |x| < d/2 \\ \bar{A} \cos \beta_{x1} \frac{d}{2} e^{-\alpha_{x2}(x-d/2)} e^{-j\beta_z z} & \text{for } x > d/2 \\ \bar{A} \cos \beta_{x1} \frac{d}{2} e^{\alpha_{x2}(x+d/2)} e^{-j\beta_z z} & \text{for } x < -d/2 \end{cases} \quad (8.93)$$

To obtain the corresponding magnetic field components, we use the phasor forms of (3.12a)–(3.12c) with the understanding that $(\partial/\partial t) \rightarrow j\omega$, $(\partial/\partial y) = 0$, $(\partial/\partial z) \rightarrow -j\beta_z$ and $E_x = E_z = 0$:

$$j\beta_z \bar{E}_y = -j\omega \bar{B}_x \quad (8.94a)$$

$$\frac{\partial \bar{E}_y}{\partial x} = -j\omega \bar{B}_z \quad (8.94b)$$

Thus

$$\bar{H}_x = -\frac{\beta_z}{\omega\mu_0} \bar{E}_y \quad (8.95)$$

$$\bar{H}_z = \begin{cases} -\frac{j\beta_{x1}}{\omega\mu_0} \bar{A} \sin \beta_{x1} x e^{-j\beta_z z} & \text{for } |x| < d/2 \\ -\frac{j\alpha_{x2}}{\omega\mu_0} \bar{A} \cos \beta_{x1} \frac{d}{2} e^{-\alpha_{x2}(x-d/2)} e^{-j\beta_z z} & \text{for } x > d/2 \\ \frac{j\alpha_{x2}}{\omega\mu_0} \bar{A} \cos \beta_{x1} \frac{d}{2} e^{\alpha_{x2}(x+d/2)} e^{-j\beta_z z} & \text{for } x < -d/2 \end{cases} \quad (8.96)$$

Now, continuity of \bar{H}_z at $x = \pm d/2$ requires that

$$\tan \beta_{x1} \frac{d}{2} = \frac{\alpha_{x2}}{\beta_{x1}} \quad (8.97)$$

We also know that β_{x1} , β_z , and α_{x2} are not independent, since together the field components must also satisfy the component equations of (3.22) in phasor form with $\mathbf{J} = \mathbf{0}$:

$$-j\beta_z \bar{H}_x - \frac{\partial \bar{H}_z}{\partial x} = \begin{cases} j\omega\epsilon_1 \bar{E}_y & \text{for } |x| < d/2 \\ j\omega\epsilon_2 \bar{E}_y & \text{for } x > d/2 \\ j\omega\epsilon_2 \bar{E}_y & \text{for } x < -d/2 \end{cases} \quad (8.98)$$

Substitution of (8.93), (8.95), and (8.96) gives us

$$\beta_{x1}^2 + \beta_z^2 = \omega^2 \mu_0 \epsilon_1 \quad (8.99a)$$

$$-\alpha_{x2}^2 + \beta_z^2 = \omega^2 \mu_0 \epsilon_2 \quad (8.99b)$$

or

$$\frac{\alpha_{x2}}{\beta_{x1}} = \sqrt{\frac{\omega^2 \mu_0 (\epsilon_1 - \epsilon_2)}{\beta_{x1}^2} - 1} \quad (8.100)$$

Combining (8.97) and (8.100), we obtain the characteristic equation for guidance to be

$$\begin{aligned}\tan\left(\beta_{x1}\frac{d}{2}\right) &= \sqrt{\frac{\omega^2\mu_0(\varepsilon_1 - \varepsilon_2)}{\beta_{x1}^2} - 1} \\ \tan\left(\frac{\beta_1 d}{2}\cos\theta_i\right) &= \sqrt{\frac{\omega^2\mu_0(\varepsilon_1 - \varepsilon_2)}{\omega^2\mu_0\varepsilon_1\cos^2\theta_i} - 1} \\ \tan\left(\frac{\pi d\sqrt{\varepsilon_{r1}}}{\lambda_0}\cos\theta_i\right) &= \frac{\sqrt{\sin^2\theta_i - (\varepsilon_2/\varepsilon_1)}}{\cos\theta_i}\end{aligned}$$

$\tan [f(\theta_i)] = g(\theta_i)$

(8.101)

which is the same as (8.87) for $m = 0, 2, 4, \dots$

Proceeding further, we can interpret the mode number m in terms of the field variations with x in the following manner. For a given value of m , we observe from Fig. 8.24 that $m\pi/2 < \beta_{x1}d/2 [= f(\theta_i)] < (m + 1)\pi/2$. Thus, from $x = 0$ to $x = \pm d/2$, $\cos\beta_{x1}x$ varies from $\cos 0^\circ$ to some value between $\cos m\pi/2$ and $\cos (m + 1)\pi/2$. Near cutoff, $\beta_{x1}d/2 \rightarrow m\pi/2$, $\tan(\beta_{x1}d/2) \rightarrow 0$, and $\alpha_{x2} \rightarrow 0$. The variation of E_y with x is as illustrated in Fig. 8.25(a) for $m = 2$. At high frequencies far from cutoff, $\beta_{x1}d/2 \rightarrow (m + 1)\pi/2$, $\tan\beta_{x1}d/2 \rightarrow \infty$, and $\alpha_{x2} \rightarrow \infty$. The variation of E_y with x is as illustrated in Fig. 8.25(b). Figure 8.25(c) illustrates the situation intermediate to those near cutoff and far from cutoff. Thus, within the thickness of the slab, the behavior of the field components varies from m half-sine variations near cutoff toward $(m + 1)$ half-sine

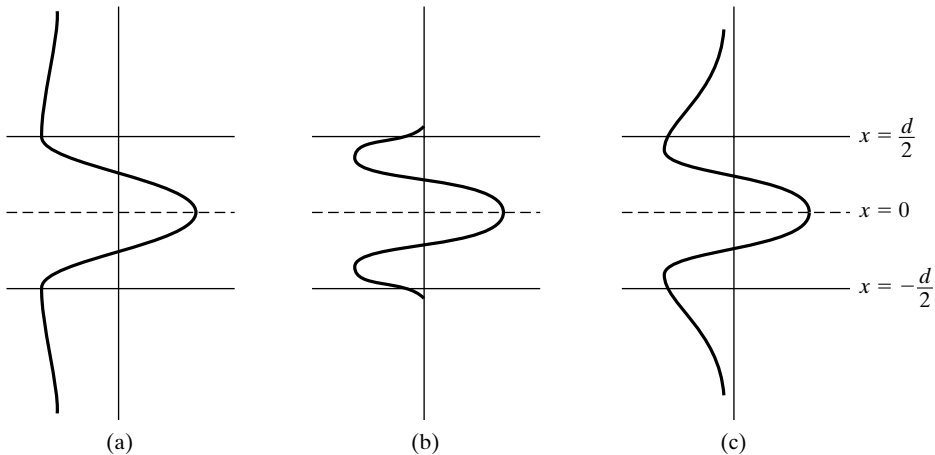


FIGURE 8.25

Variations of E_y with x for the TE_2 mode in the symmetric dielectric slab waveguide for (a) near cutoff; (b) far from cutoff; and (c) intermediate to (a) and (b).

variations far from cutoff, with the evanescence outside the dielectric slab dictated by $\alpha_{x2} \rightarrow 0$ near cutoff toward $\alpha_{x2} \rightarrow \infty$ far from cutoff.

Field expressions for odd TE modes

The field expressions for the odd TE modes, that is, modes with the transverse field components having odd symmetry with respect to x , can be obtained by writing the expression for \bar{E}_y to be

$$\bar{E}_y = \begin{cases} \bar{C} \sin \beta_{x1} x e^{-j\beta_z z} & \text{for } |x| < d/2 \\ \bar{D} e^{-\alpha_{x2} x} e^{-j\beta_z z} & \text{for } x > d/2 \\ -\bar{D} e^{\alpha_{x2} x} e^{-j\beta_z z} & \text{for } x < -d/2 \end{cases} \quad (8.102)$$

where \bar{C} and \bar{D} are constants and proceeding in a manner similar to that for the even modes. We shall omit the details and write down the final results:

$$\bar{E}_y = \begin{cases} \bar{C} \sin \beta_{x1} x e^{-j\beta_z z} & \text{for } |x| < d/2 \\ \bar{C} \sin \beta_{x1} \frac{d}{2} e^{-\alpha_{x2}(x-d/2)} e^{-j\beta_z z} & \text{for } x > d/2 \\ -\bar{C} \sin \beta_{x1} \frac{d}{2} e^{\alpha_{x2}(x+d/2)} e^{-j\beta_z z} & \text{for } x < -d/2 \end{cases} \quad (8.103)$$

$$\bar{H}_x = -\frac{\beta_z}{\omega\mu_0} \bar{E}_y \quad (8.104)$$

$$\bar{H}_z = \begin{cases} \frac{j\beta_{x1}}{\omega\mu_0} \bar{C} \cos \beta_{x1} x e^{-j\beta_z z} & \text{for } |x| < d/2 \\ -\frac{j\alpha_{x2}}{\omega\mu_0} \bar{C} \sin \beta_{x1} \frac{d}{2} e^{-\alpha_{x2}(x-d/2)} e^{-j\beta_z z} & \text{for } x > d/2 \\ -\frac{j\alpha_{x2}}{\omega\mu_0} \bar{C} \sin \beta_{x1} \frac{d}{2} e^{\alpha_{x2}(x+d/2)} e^{-j\beta_z z} & \text{for } x < -d/2 \end{cases} \quad (8.105)$$

Continuity of \bar{H}_z at $x = \pm d/2$ requires that

$$\begin{aligned} \cot \beta_{x1} \frac{d}{2} &= -\frac{\alpha_{x2}}{\beta_{x1}} \\ &= -\sqrt{\frac{\omega^2 \mu_0 (\epsilon_1 - \epsilon_2)}{\beta_{x1}^2} - 1} \end{aligned} \quad (8.106)$$

where we have used (8.100). Thus, the characteristic equation for guidance is

$$\boxed{\tan f(\theta_i) = -\frac{1}{g(\theta_i)}} \quad (8.107)$$

which is the same as (8.87) for $m = 1, 3, 5, \dots$

Proceeding further, we observe from Fig. 8.24 that for a given value of m , $m\pi/2 < \beta_{x1}d/2 [= f(\theta_i)] < (m+1)\pi/2$. Thus, from $x = 0$ to $x = \pm d/2$, $\sin \beta_{x1}x$ varies from $\sin 0^\circ$ to some value between $\sin m\pi/2$ and $\sin (m+1)\pi/2$. Near cutoff, $\beta_{x1}d/2 \rightarrow m\pi/2$, $\cot(\beta_{x1}d/2) \rightarrow 0$, and $\alpha_{x2} \rightarrow 0$. At high frequencies far from cutoff, $\beta_{x1}d/2 \rightarrow (m+1)\pi/2$, $\cot(\beta_{x1}d/2) \rightarrow \infty$, and $\alpha_{x2} \rightarrow \infty$. Thus,

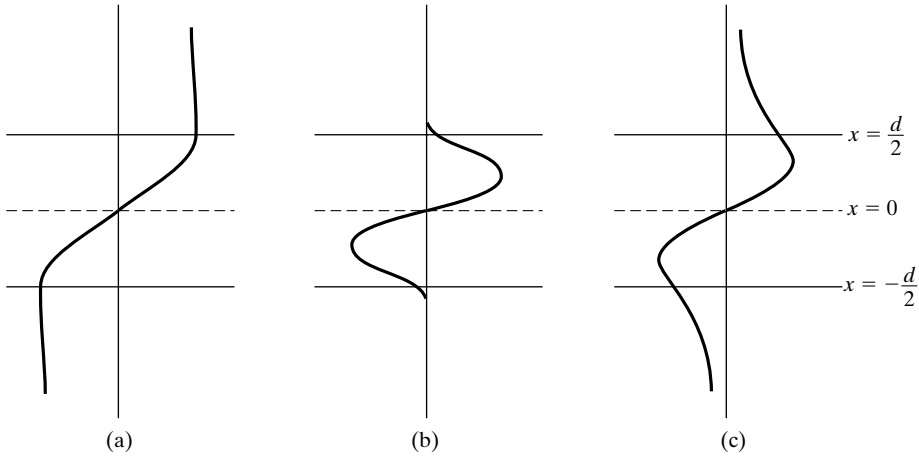


FIGURE 8.26

Variations of E_y with x for TE_1 mode in the symmetric dielectric slab waveguide for (a) near cutoff; (b) far from cutoff; and (c) intermediate to (a) and (b).

the variation of E_y with x for $m = 1$ is illustrated in Fig. 8.26 for three situations: (a) near cutoff, (b) far from cutoff, and (c) intermediate to (a) and (b). As in the case of the even modes, the behavior of the field components varies from m half-sine variations near cutoff toward $(m + 1)$ half-sine variations far from cutoff.

Let us now investigate the time-average power flow down the symmetric slab waveguide for TE modes. First, we write the complex Poynting vector associated with the TE mode fields as given by

Power flow

$$\begin{aligned}\bar{\mathbf{P}} &= \frac{1}{2} \bar{\mathbf{E}} \times \bar{\mathbf{H}}^* \\ &= \frac{1}{2} (\bar{E}_y \bar{H}_z^* \mathbf{a}_x - \bar{E}_y \bar{H}_x^* \mathbf{a}_z)\end{aligned}\quad (8.108)$$

Then, noting from (8.93), (8.95), and (8.96) that $\bar{E}_y \bar{H}_z^*$ is real, whereas $\bar{E}_y \bar{H}_x^*$ is imaginary, we obtain the time-average Poynting vector as given by

$$\begin{aligned}\langle \mathbf{P} \rangle &= \text{Re } \bar{\mathbf{P}} \\ &= \frac{\beta_z}{2\omega\mu_0} |\bar{E}_y|^2 \mathbf{a}_z \\ &= \frac{\beta_z |\bar{A}|^2}{2\omega\mu_0} \begin{cases} \cos^2 \beta_{x1} x \mathbf{a}_z & \text{for } |x| < d/2 \\ \cos^2 \beta_{x1} \frac{d}{2} e^{-2\alpha_{x2}(x-d/2)} \mathbf{a}_z & \text{for } x > d/2 \\ \cos^2 \beta_{x1} \frac{d}{2} e^{2\alpha_{x2}(x+d/2)} \mathbf{a}_z & \text{for } x < -d/2 \end{cases}\end{aligned}\quad (8.109)$$

where we have used the even mode field expression. For the odd modes, the \cos^2 terms will be replaced by \sin^2 terms and the final result will be the same.

The time-average power flow along the guide per unit length in the y -direction (because of the independence of the fields with y) is then given by

$$\begin{aligned}
 \langle P \rangle &= \int_{y=0}^1 \int_{x=-\infty}^{\infty} \langle \mathbf{P} \rangle \cdot dx dy \mathbf{a}_z \\
 &= \frac{\beta_z |\bar{A}|^2}{\omega \mu_0} \left[\int_0^{d/2} \cos^2 \beta_{x1} x dx + \int_{d/2}^{\infty} \cos^2 \beta_{x1} \frac{d}{2} e^{-2\alpha_{x2}(x-d/2)} dx \right] \quad (8.110) \\
 &= \frac{\beta_z |\bar{A}|^2}{\omega \mu_0} \left[\frac{d}{4} + \frac{\sin \beta_{x1} d}{4\beta_{x1}} + \frac{\cos^2 \beta_{x1} d/2}{2\alpha_{x2}} \right]
 \end{aligned}$$

Using (8.97) and substituting

$$\begin{aligned}
 \sin \beta_{x1} d &= 2 \sin \beta_{x1} \frac{d}{2} \cos \beta_{x1} \frac{d}{2} \\
 &= \frac{2\beta_{x1}}{\alpha_{x2}} \sin^2 \beta_{x1} \frac{d}{2}
 \end{aligned}$$

we obtain

$$\begin{aligned}
 \langle P \rangle &= \frac{\beta_z |\bar{A}|^2}{\omega \mu_0} \left(\frac{d}{4} + \frac{1}{2\alpha_{x2}} \right) \\
 &= \frac{\beta_z |\bar{A}|^2}{4\omega \mu_0} \left(d + \frac{2}{\alpha_{x2}} \right) \quad (8.111)
 \end{aligned}$$

Besides giving the expression for the time-average power flow along the guide, (8.111) leads to the definition of fictitious effective boundaries at $x = \pm d_{\text{eff}}/2$, where

$$\boxed{d_{\text{eff}} = d + \frac{2}{\alpha_{x2}}} \quad (8.112)$$

as shown in Fig. 8.27. The physical interpretation of the placement of these effective boundaries relates to the phase shift that the waves experience upon being total internally reflected at the actual boundaries.

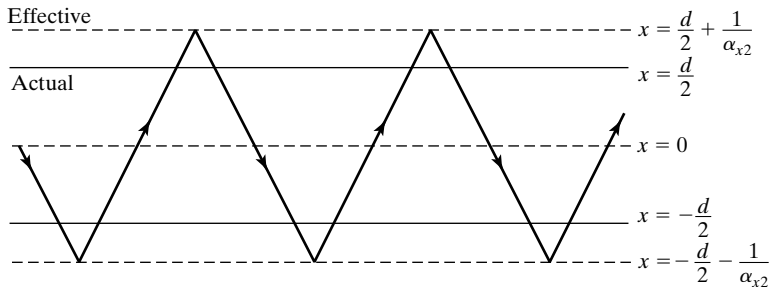


FIGURE 8.27

For illustrating the effective boundaries for waveguiding along the symmetric dielectric slab guide.

Example 8.6 Computation of effective thickness for modes in a symmetric dielectric slab waveguide

For the values of ε_{r1} , ε_{r2} , d , and λ_0 used for Table 8.1, it is desired to find d_{eff} for the first three modes.

From (8.99b),

$$\begin{aligned}\alpha_{x2}^2 &= \beta_z^2 - \omega^2 \mu_0 \varepsilon_2 \\ &= \omega^2 \mu_0 \varepsilon_1 \sin^2 \theta_i - \omega^2 \mu_0 \varepsilon_2 \\ &= \omega^2 \mu_0 \varepsilon_0 (\varepsilon_{r1} \sin^2 \theta_i - \varepsilon_{r2}) \\ \alpha_{x2} &= \frac{2\pi}{\lambda_0} \sqrt{\varepsilon_{r1} \sin^2 \theta_i - \varepsilon_{r2}}\end{aligned}$$

Substituting $\lambda_0 = 5 \text{ mm}$, $\varepsilon_{r1} = 4$, and $\varepsilon_{r2} = 1$, we have

$$\alpha_{x2} = \frac{2\pi}{5 \times 10^{-3}} \sqrt{4 \sin^2 \theta_i - 1}$$

From Table 8.1, we can then compute α_{x2} and hence d_{eff} for the first three modes, as listed in Table 8.2.

Mode	θ_i (deg)	$\alpha_{x2}(\text{m}^{-1})$	$d_{\text{eff}}(\text{mm})$
TE ₀	83.42783	2157.47	10.927
TE ₁	76.77756	2099.27	10.953
TE ₂	69.96263	1998.97	11.001

The entire solution for the field components can be repeated for TM modes by starting with the expression for the (only) magnetic field component \bar{H}_y and proceeding in a manner similar to that used for the TE mode case. We shall not, however, pursue these details here, but we include them as Problems P8.29 and P8.30.

TM modes

We have thus far discussed modes that are guided within the slab. Another type of mode that is possible for the dielectric slab guide is that for which the field variations with x are sinusoidal not only in the slab but also outside it. The situation can be visualized by locating perfectly conducting plates on either side of the slab and parallel to it, as in Fig. 8.28, and displacing the conductors to infinity, thereby obtaining the slab waveguide in the limiting case. Waves that are incident from medium 1 on the interface at angles of incidence less than the critical angle for total internal reflection are transmitted into medium 2 and are reflected at the conductor, giving rise to ray paths such as the one shown. The modes established when the associated self-consistency condition is satisfied are known as the *radiation modes*. These modes are important in the coupling of energy in and out of the dielectric slab.

Radiation modes

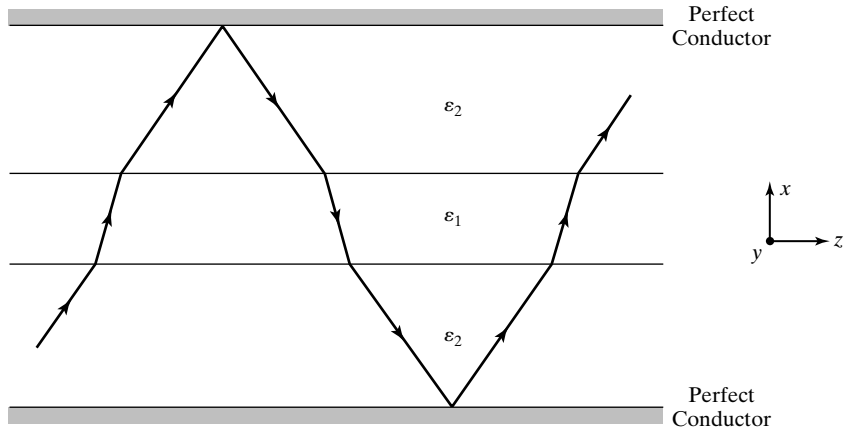


FIGURE 8.28

For explaining the mechanism pertinent to radiation modes in a dielectric slab guide.

- K8.6.** Dielectric slab waveguide; Guiding by total internal reflection; Self-consistency condition; Characteristic equation for guidance; Propagating modes; Derivation of field expressions; Characteristic equation for guidance; Mode behavior; Power flow; Radiation modes.
- D8.9.** For a symmetric dielectric slab waveguide, $\epsilon_1 = 2.25\epsilon_0$ and $\epsilon_2 = \epsilon_0$. Find the following for TE modes: **(a)** the lowest value of d/λ_0 for which an allowed value of θ_i is 60° ; **(b)** the lowest value of d/λ_0 for which an allowed value of θ_i is 75° ; and **(c)** the second lowest value of d/λ_0 for which an allowed value of θ_i is 75° .
Ans. (a) 0.3545; (b) 0.9972; (c) 2.2852.
- D8.10.** For a symmetric dielectric slab waveguide, $\epsilon_{r1} = 4$ and $\epsilon_{r2} = 1$. Find the value of d_{eff}/d for the TE₀ mode for each of the following values of d/λ_0 : **(a)** 2; **(b)** 5; and **(c)** 0.5.
Ans. (a) 1.0927; (b) 1.0368; (c) 1.4047.

8.7 RAY TRACING AND GRADED-INDEX GUIDE

For the dielectric slab waveguide of the preceding section, the permittivity undergoes an abrupt discontinuity from a uniform value of ϵ_1 in the slab to a uniform value of ϵ_2 on either side of the slab. When the permittivity varies within the thickness of the slab, the arrangement is known as a graded-index guide, as compared to the step-index guide of the previous section, where the word “index” refers to the refractive index $n (= c/v_p = \sqrt{\epsilon_r}$ for a nonmagnetic dielectric). To extend our discussion of guided wave propagation to a graded-index slab waveguide, we first introduce the general topic of geometrical optics and ray tracing.

Geometrical optics approximation explained

Geometrical optics is that branch of optics that allows us to study wave phenomena by tracing “rays,” which are paths normal to the wavefronts, from the local application of the laws of reflection and refraction (Snell’s law). Whenever the wavefront extends and is uniform over many wavelengths and when the boundaries are large compared to the wavelength, ray tracing can be usefully employed. Also, as long as the radii of curvature are large in comparison to the wavelength, the boundaries as well as the wavefronts can be nonplanar. In fact, we have already

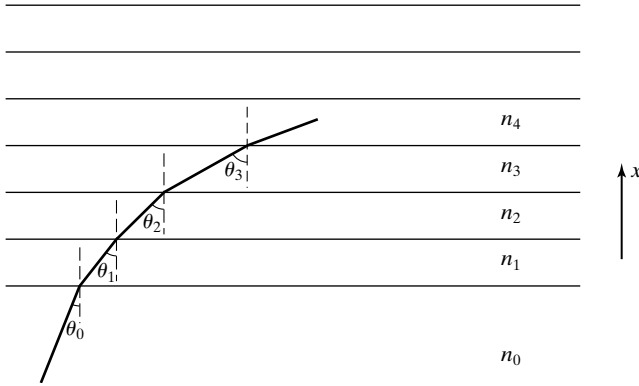


FIGURE 8.29

The bending of ray paths in a series of plane dielectric slabs of uniform refractive indices.

made use of geometrical optics concepts to introduce the cutoff phenomenon in a parallel-plate waveguide in Section 8.2 and to derive the characteristic equation for guidance in the dielectric slab guide in Section 8.6. In all of these cases, the media were uniform and the boundaries were planar and abrupt, so that the ray paths were all straight lines. For nonuniform media, the ray paths become curved.

To formulate the ray tracing procedure, let us consider the arrangement shown in Fig. 8.29, in which a medium of continuously varying refractive index $n(x)$ is approximated by a series of plane slabs of uniform refractive indices n_1, n_2, n_3, \dots . Let a wave be incident from the medium of refractive index n_0 at an angle θ_0 from the vertical. Then assuming $n_0 < n_1 < n_2 < n_3 < \dots$, the ray path bends more and more away from the vertical in accordance with Snell's law applied at the interfaces

*Ray tracing
formulation*

$$\boxed{n_0 \sin \theta_0 = n_1 \sin \theta_1 = n_2 \sin \theta_2 = \dots} \quad (8.113)$$

with the path in each layer being a straight line. In the limit that the thickness of each layer goes to zero, the refractive index varies continuously with x and the ray path becomes curved. To trace the path of the ray, let us consider a differential segment ds along the ray path, having the components dx and dz in the x - and z -directions, respectively, as shown in Fig. 8.30. Then

$$\frac{dz}{dx} = \tan \theta = \frac{\sin \theta}{\sqrt{1 - \sin^2 \theta}} \quad (8.114)$$

From (8.113), $n \sin \theta = n_0 \sin \theta_0$, or $\sin \theta = (n_0/n) \sin \theta_0$. Substituting in (8.114), we obtain

$$\boxed{\frac{dz}{dx} = \frac{n_0 \sin \theta_0}{\sqrt{n^2 - n_0^2 \sin^2 \theta_0}}} \quad (8.115)$$

For a given refractive index profile $n(x)$, the solution of (8.115) gives the ray trajectory in the xz -plane. In general, the solution has to be carried out numerically. For certain functions for $n(x)$, an analytical solution is possible. We shall illustrate by means of an example.

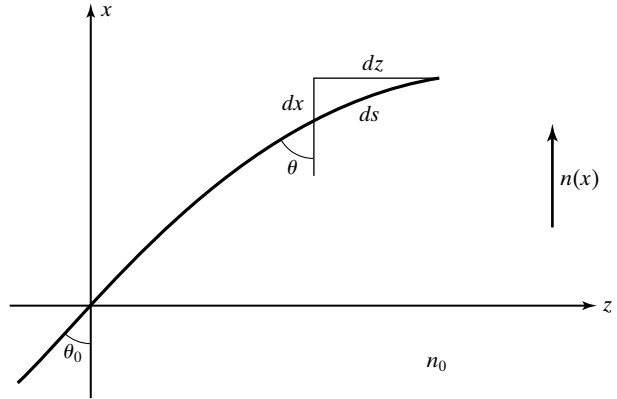


FIGURE 8.30
For the formulation of ray tracing for continuous variation of refractive index.

Example 8.7 Finding the ray trajectory in a dielectric medium with linear profile of permittivity

Let us consider a variation of refractive index as given by

$$n^2 = n_0^2 (1 - \alpha x)$$

where $\alpha > 0$. Note that for a nonmagnetic dielectric medium, this corresponds to a linear profile of permittivity. We wish to find the ray trajectory in the medium in the xz -plane for a wave entering the medium at $x = 0$ and $z = 0$ at an angle θ_0 from the vertical (x -direction).

From (8.115), we have

$$\begin{aligned} \frac{dz}{dx} &= \frac{n_0 \sin \theta_0}{\sqrt{n_0^2 - n_0^2 \alpha x - n_0^2 \sin^2 \theta_0}} \\ &= \frac{\sin \theta_0}{\sqrt{\cos^2 \theta_0 - \alpha x}} \end{aligned}$$

The ray trajectory is given by

$$\begin{aligned} z(x) &= \int_0^x \frac{\sin \theta_0}{\sqrt{\cos^2 \theta_0 - \alpha x}} dx \\ &= -\sin \theta_0 \left[\frac{2}{\alpha} \sqrt{\cos^2 \theta_0 - \alpha x} \right]_0^x \\ &= -\frac{2 \sin \theta_0}{\alpha} [\sqrt{\cos^2 \theta_0 - \alpha x} - \cos \theta_0] \end{aligned}$$

Rearranging, we have

$$\cos^2 \theta_0 - \alpha x = \left(-\frac{\alpha z}{2 \sin \theta_0} + \cos \theta_0 \right)^2$$

or

$$x = \frac{\cos^2 \theta_0}{\alpha} - \left(\frac{\cos \theta_0}{\sqrt{\alpha}} - \frac{\sqrt{\alpha}}{2 \sin \theta_0} z \right)^2$$

Thus, the ray trajectory is parabolic, with the parabola having its apex at $x = (\cos^2 \theta_0)/\alpha$ and $z = (\sin 2\theta_0)/\alpha$. Note that at $x = (\cos^2 \theta_0)/\alpha$, $n^2 = n_0^2(1 - \cos^2 \theta_0)$ or $n = n_0 \sin \theta_0$, and $\theta = 90^\circ$, consistent with the solution obtained.

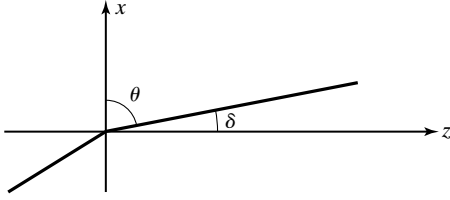


FIGURE 8.31

Geometry pertinent to the paraxial ray approximation.

When the ray trajectories are nearly along the propagation axis, the rays are known as paraxial rays. For paraxial rays, the angle $\delta (= 90^\circ - \theta)$ that the ray makes with the propagation axis, which here is the z -axis as shown in Fig. 8.31, is small such that approximations of $\sin \delta \approx \delta$ and $\cos \delta \approx 1$ can be used.

Paraxial ray approximation

Example 8.8 Paraxial rays in a dielectric medium with parabolic refractive index profile

An important example of a graded refractive index profile is given by

$$n^2 = n_0^2(1 - \alpha^2 x^2) \quad (8.116)$$

Paraxial rays in parabolic index profile

For α sufficiently small that $\alpha x \ll 1$, which is usually the case,

$$n(x) = n_0 \sqrt{1 - \alpha^2 x^2} \approx n_0 \left(1 - \frac{1}{2} \alpha^2 x^2\right) \quad (8.117)$$

corresponds to a parabolic variation. We wish to investigate paraxial rays for this profile.

Let us consider a ray making an angle δ_0 with the z -axis at the point $x = 0$. Then from (8.115),

$$\begin{aligned} \frac{dz}{dx} &= \frac{n_0 \sin \theta_0}{\sqrt{n^2 - n_0^2 \sin^2 \theta_0}} = \frac{n_0 \cos \delta_0}{\sqrt{n^2 - n_0^2 \cos^2 \delta_0}} \\ &= \frac{n_0 \cos \delta_0}{\sqrt{n_0^2(1 - \alpha^2 x^2) - n_0^2 \cos^2 \delta_0}} \\ &= \frac{\cos \delta_0}{\sqrt{\sin^2 \delta_0 - \alpha^2 x^2}} \\ &\approx \frac{1}{\delta_0^2 - \alpha^2 x^2} \\ z &= \int_0^x \frac{dx}{\sqrt{\delta_0^2 - \alpha^2 x^2}} \\ &= \left[\frac{1}{\alpha} \sin^{-1} \left(\frac{\alpha}{\delta_0} x \right) \right]_0^x \\ &= \frac{1}{\alpha} \sin^{-1} \frac{\alpha x}{\delta_0} \end{aligned}$$

or

$$x = \frac{\delta_0}{\alpha} \sin \alpha z \quad (8.118)$$

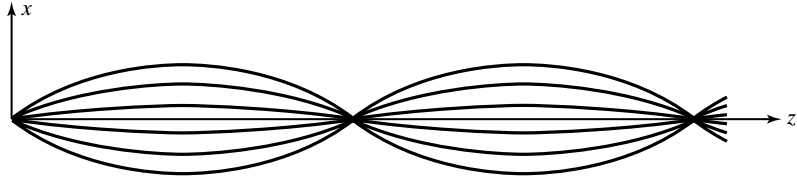


FIGURE 8.32 Paraxial rays in a parabolic index profile.

The ray oscillates about the axis with a period of $2\pi/\alpha$, known as the *pitch*, independent of δ_0 , and a peak amplitude δ_0/α , as shown in Fig. 8.32 for a few values of δ_0 .

Guidance condition for graded-index guide

We may now discuss wave guidance in a graded-index guide. To do this, let us consider, for simplicity, the symmetric refractive index profile of the shape shown in Fig. 8.33(a). Then for those waves that are total internally reflected within $-d/2 < x < d/2$, a sketch of the ray path can be drawn, as in Fig. 8.33(b), with apex points at $x = \pm x_a$, where $x_a < d/2$. From Snell's law, $n(\pm x_a) = n_1(x) \sin \theta(x)$, since $\theta = 90^\circ$ at $x = \pm x_a$. Using the same reasoning as for writing (8.83), we can write the self-consistency condition for guidance to be

$$\int_{x=-x_a}^{x_a} \frac{2\pi}{\lambda_0} \sqrt{\epsilon_{r1}(x)} \cos \theta(x) dx + \angle[\bar{\Gamma}]_{x=x_a} + \int_{x=x_a}^{-x_a} \frac{2\pi}{\lambda_0} \sqrt{\epsilon_{r1}(x)} \cos \theta(x) dx + \angle[\bar{\Gamma}]_{x=-x_a} = 2m\pi, \quad m = 0,1,2,\dots \quad (8.119)$$

In view of symmetry, (8.119) reduces to

$$\frac{4\pi}{\lambda_0} \int_{x=0}^{x_a} \sqrt{\epsilon_{r1}(x)} \cos \theta(x) dx + \angle\bar{\Gamma}_a = m\pi, \quad m = 0,1,2,\dots \quad (8.120)$$

where $\bar{\Gamma}_a = [\bar{\Gamma}]_{x=x_a}$.

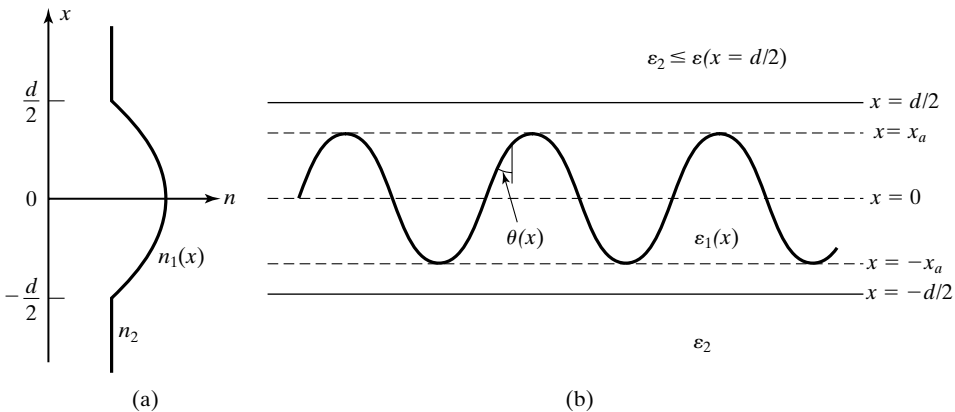


FIGURE 8.33 (a) Refractive index profile for a symmetrical graded-index guide. (b) Ray path within the graded-index region.

To proceed further, we consider the TE case and find $\angle \bar{\Gamma}_a$ by using (8.86). We first write $\bar{\Gamma}_a$ as

$$\begin{aligned}\bar{\Gamma}_a &= \frac{\eta'_2 \cos \theta_i - j\eta'_1 \sqrt{(\varepsilon'_1/\varepsilon'_2) \sin^2 \theta_i - 1}}{\eta'_2 \cos \theta_i + j\eta'_1 \sqrt{(\varepsilon'_1/\varepsilon'_2) \sin^2 \theta_i - 1}} \\ &= \frac{\sqrt{\varepsilon'_1} \cos \theta_i - j\sqrt{\varepsilon'_1 \sin^2 \theta_i - \varepsilon'_2}}{\sqrt{\varepsilon'_1} \cos \theta_i + j\sqrt{\varepsilon'_1 \sin^2 \theta_i - \varepsilon'_2}}\end{aligned}\quad (8.121)$$

where we have inserted primes so as not to confuse with the notation of Fig. 8.33. Now we note that for the situation under consideration,

$$\begin{aligned}\varepsilon'_1 &= [\varepsilon]_{x=x_a-\Delta x} = \varepsilon(x_a-) \\ \varepsilon'_2 &= [\varepsilon]_{x=x_a+\Delta x} = \varepsilon(x_a+) \\ \varepsilon'_1 \sin^2 \theta_i &= [\varepsilon]_{x=x_a} \sin^2 90^\circ = \varepsilon(x_a) \\ \sqrt{\varepsilon'_1} \cos \theta_i &= \sqrt{\varepsilon'_1 - \varepsilon'_1 \sin^2 \theta_i} = \sqrt{\varepsilon(x_a-) - \varepsilon(x_a)}\end{aligned}$$

so that

$$\bar{\Gamma}_a = \frac{\sqrt{\varepsilon(x_a-) - \varepsilon(x_a)} - j\sqrt{\varepsilon(x_a) - \varepsilon(x_a+)}}{\sqrt{\varepsilon(x_a-) - \varepsilon(x_a)} + j\sqrt{\varepsilon(x_a) - \varepsilon(x_a+)}}\quad (8.122)$$

In view of the continuous variation of ε_1 , we now have to take the limit of the right side of (8.122) as x_a- and x_a+ tend to x_a . We note however that this results in a situation of zero divided by zero. To avoid this, we write that in the vicinity of $x = x_a$,

$$\varepsilon(x) \approx \varepsilon(x_a) + (x - x_a) \frac{d\varepsilon}{dx} = \varepsilon(x_a) + \Delta x \frac{d\varepsilon}{dx}$$

Thus,

$$\begin{aligned}\varepsilon(x_a-) - \varepsilon(x_a) &\approx \varepsilon(x_a) - \Delta x \frac{d\varepsilon}{dx} - \varepsilon(x_a) = -\Delta x \frac{d\varepsilon}{dx} \\ \varepsilon(x_a) - \varepsilon(x_a+) &\approx \varepsilon(x_a) - \varepsilon(x_a) - \Delta x \frac{d\varepsilon}{dx} = -\Delta x \frac{d\varepsilon}{dx}\end{aligned}$$

$$\begin{aligned}\bar{\Gamma}_a &= \lim_{\Delta x \rightarrow 0} \frac{\sqrt{-\Delta x \frac{d\varepsilon}{dx}} - j\sqrt{-\Delta x \frac{d\varepsilon}{dx}}}{\sqrt{-\Delta x \frac{d\varepsilon}{dx}} + j\sqrt{-\Delta x \frac{d\varepsilon}{dx}}} \\ &= \frac{1 - j}{1 + j} = 1 \angle -\pi/2\end{aligned}\quad (8.123)$$

so that $\angle \bar{\Gamma}_a = -\pi/2$. The same result can be shown to hold for the TM case, which makes use of Γ_{\parallel} (see Problem P8.35).

Finally, substituting $\angle \bar{\Gamma}_a = -\pi/2$ and also

$$\begin{aligned}\sqrt{\varepsilon_{r1}(x)} \cos \theta &= \sqrt{\varepsilon_{r1}(x) - \varepsilon_{r1}(x) \sin^2 \theta} \\ &= \sqrt{\varepsilon_{r1}(x) - \varepsilon_{r1}(x_a)}\end{aligned}\quad (8.124)$$

into (8.120), we obtain the characteristic equation for guidance to be

$$\frac{4\pi}{\lambda_0} \int_{x=0}^{x_a} \sqrt{\varepsilon_{r1}(x) - \varepsilon_{r1}(x_a)} dx = \left(m + \frac{1}{2}\right)\pi, \quad m = 0, 1, 2, \dots \quad (8.125)$$

or in terms of refractive index

$$\frac{4\pi}{\lambda_0} \int_{x=0}^{x_a} \sqrt{n_1^2(x) - n_1^2(x_a)} dx = \left(m + \frac{1}{2}\right)\pi, \quad m = 0, 1, 2, \dots \quad (8.126)$$

As in the case of the step-index guide, each value of m corresponds to a mode. For a given value of m and for a given profile $n_1(x)$, (8.126) must in general be solved numerically. There are however certain refractive index profiles that permit analytical solution. An example is in order.

Example 8.9 Guided waves in a parabolic index dielectric slab waveguide

Let us consider the refractive index profile of Example 8.8 given by

$$n_1^2(x) = n_0^2[1 - \alpha^2 x^2] \quad (8.127)$$

where α is such that $[n_1]_{x=\pm d/2} \geq n_2$, and investigate guided waves in the slab.

Substituting for $n_1^2(x)$ in (8.126), we have

$$\begin{aligned}\frac{4\pi}{\lambda_0} \int_{x=0}^{x_a} \sqrt{n_0^2(1 - \alpha^2 x^2) - n_0^2(1 - \alpha^2 x_a^2)} dx &= \left(m + \frac{1}{2}\right)\pi, \quad m = 0, 1, 2, \dots \\ \frac{4\pi n_0 \alpha}{\lambda_0} \int_{x=0}^{x_a} \sqrt{x_a^2 - x^2} dx &= \left(m + \frac{1}{2}\right)\pi, \quad m = 0, 1, 2, \dots \\ \frac{2\pi n_0 \alpha}{\lambda_0} \left[x \sqrt{x_a^2 - x^2} + x_a^2 \sin^{-1} \frac{x}{x_a} \right]_{x=0}^{x_a} &= \left(m + \frac{1}{2}\right)\pi, \quad m = 0, 1, 2, \dots\end{aligned}$$

$$x_a^2 = \frac{(2m+1)\lambda_0}{2\pi n_0 \alpha}, \quad m = 0, 1, 2, \dots \quad (8.128)$$

The value of x_a increases with the mode number m , as can also be seen in general from (8.126). Recall that $x_a < d/2$. For paraxial modes, the ray trajectories are given by

$$\begin{aligned} x &= x_a \sin \alpha z \\ &= \sqrt{\frac{(2m+1)\lambda_0}{2\pi n_0 \alpha}} \sin \alpha z \end{aligned} \quad (8.129)$$

In contrast with the modes of the step-index guide in which the ray paths for all modes extend to the boundaries of the slab with varying values of the pitch, for these modes the ray paths possess amplitudes increasing with m but with a fixed pitch.

The numerical solution of (8.126) involves an iterative procedure. For a given refractive index profile and specified values of d and λ_0 , the iterative procedure consists of starting with $m = 0$ and computing x_a that satisfies (8.126). To do this, x_a is set equal to $d/2$ and the integral on the left side is evaluated numerically. If this results in a value of less than $\pi/2$ for the left side of (8.126), then it means that a solution does not exist for any value of m and the computation is terminated. If the value is greater than $\pi/2$, then an interval-bisection procedure is used iteratively, beginning with the interval from 0 to $d/2$, until a value of x_a that satisfies (8.126) to a desired accuracy is found. The value of m is then increased in steps of unity and the computation repeated for each value of m , beginning with the search interval extending from the solution for x_a found for the previous value of m to $d/2$. The entire computation is terminated when a value of m is reached for which the left side of (8.126) yields a value of less than $(m + \frac{1}{2})\pi$.

Returning now to the result of (8.129), we consider its consequence in intermodal dispersion, the type of dispersion resulting from different travel times of rays corresponding to different modes. Because rays of higher modes travel farther but with greater velocities (lower refractive index), the travel times of the different rays are nearly equalized, thereby almost eliminating intermodal dispersion. To discuss in quantitative terms, we note that the phase constant along the guide axis is given by

$$\begin{aligned} \beta_z &= \omega \sqrt{\mu[\epsilon]_{x=x_a}} \\ &= \omega \sqrt{\mu_0 \epsilon_0 [n_1]_{x=x_a}} \\ &= \frac{\omega}{c} n_0 \sqrt{1 - \alpha^2 x_a^2} \\ &\approx \frac{\omega n_0}{c} \left(1 - \frac{1}{2} \alpha^2 x_a^2 \right) \quad \text{for } \alpha^2 x_a^2 \ll 1 \\ &= \frac{\omega n_0}{c} \left[1 - \frac{(2m+1)\lambda_0 \alpha}{4\pi n_0} \right] \\ &= \frac{\omega n_0}{c} - \frac{(2m+1)\alpha}{2} \\ \frac{d\beta_z}{d\omega} &= \frac{n_0}{c} \end{aligned}$$

Intermodal dispersion

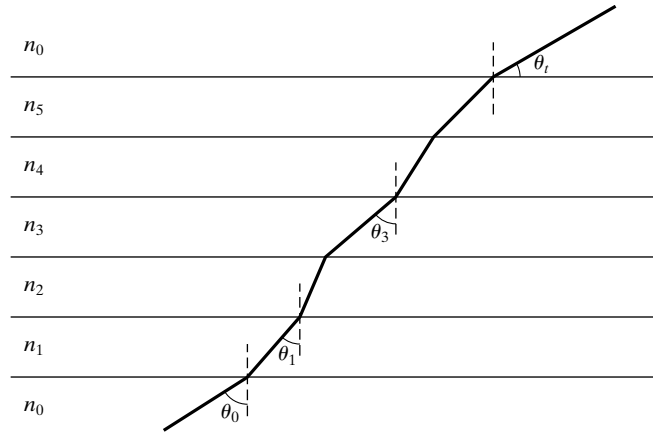


FIGURE 8.34
For Problem D8.11.

Thus, the group velocity along the guide axis is given by

$$v_{gz} = \frac{d\omega}{d\beta_z} = \frac{c}{n_0}$$

independent of m .

- K8.7.** Ray tracing; paraxial rays; parabolic index profile; graded-index guide; intermodal dispersion.
- D8.11.** In Fig. 8.34, a medium of continuously varying refractive index is approximated by a series of plane slabs of uniform refractive indices. If $n_0 = 1$ and $\theta_0 = 60^\circ$, find the following: **(a)** θ_1 if $n_1 = 1.5$; **(b)** n_3 if $\theta_3 = 30^\circ$; and **(c)** θ_t .
Ans. **(a)** 35.26° ; **(b)** $\sqrt{3}$; **(c)** 30° .
- D8.12.** In Example 8.9, let $n_0 = 1.5$, $\alpha = 0.05/\lambda_0$, and $d = 10\lambda_0$. Compute the following: **(a)** x_d for $m = 0$; **(b)** the maximum value of m ; and **(c)** the paraxial angle δ_0 for the value of m computed in (b).
Ans. **(a)** $1.4567\lambda_0$; **(b)** 5; **(c)** 13.88° .

SUMMARY

In this chapter, we studied the principles of waveguides. To introduce the waveguiding phenomenon, we first learned how to write the expressions for the electric and magnetic fields of a uniform plane wave propagating in an arbitrary direction with respect to the coordinate axes. These expressions are given by

$$\begin{aligned}\mathbf{E} &= \mathbf{E}_0 \cos(\omega t - \boldsymbol{\beta} \cdot \mathbf{r} + \phi_0) \\ \mathbf{H} &= \mathbf{H}_0 \cos(\omega t - \boldsymbol{\beta} \cdot \mathbf{r} + \phi_0)\end{aligned}$$

where $\boldsymbol{\beta}$ and \mathbf{r} are the propagation and position vectors given by

$$\begin{aligned}\boldsymbol{\beta} &= \beta_x \mathbf{a}_x + \beta_y \mathbf{a}_y + \beta_z \mathbf{a}_z \\ \mathbf{r} &= x \mathbf{a}_x + y \mathbf{a}_y + z \mathbf{a}_z\end{aligned}$$

and ϕ_0 is the phase of the wave at the origin at $t = 0$. The magnitude of $\boldsymbol{\beta}$ is equal to $\omega\sqrt{\mu\varepsilon}$, the phase constant along the direction of propagation of the wave. The direction of $\boldsymbol{\beta}$ is the direction of propagation of the wave. We learned that

$$\begin{aligned}\mathbf{E}_0 \cdot \boldsymbol{\beta} &= 0 \\ \mathbf{H}_0 \cdot \boldsymbol{\beta} &= 0 \\ \mathbf{E}_0 \cdot \mathbf{H}_0 &= 0\end{aligned}$$

that is, \mathbf{E}_0 , \mathbf{H}_0 , and $\boldsymbol{\beta}$ are mutually perpendicular, and that

$$\frac{|\mathbf{E}_0|}{|\mathbf{H}_0|} = \eta = \sqrt{\frac{\mu}{\varepsilon}}$$

Also, since $\mathbf{E} \times \mathbf{H}$ should be directed along the propagation vector $\boldsymbol{\beta}$, it then follows that

$$\mathbf{H} = \frac{1}{\omega\mu} \boldsymbol{\beta} \times \mathbf{E}$$

The quantities β_x , β_y , and β_z are the phase constants along the x -, y -, and z -axes, respectively. The apparent wavelengths and the apparent phase velocities along the coordinate axes are given, respectively, by

$$\begin{aligned}\lambda_i &= \frac{2\pi}{\beta_i}, & i = x, y, z \\ v_{pi} &= \frac{\omega}{\beta_i}, & i = x, y, z\end{aligned}$$

By considering the superposition of two uniform plane waves having only y -components of electric fields and propagating at an angle to each other and placing perfect conductors in two constant- x planes such that the boundary condition of zero tangential electric field is satisfied, we introduced the parallel-plate waveguide. We learned that the composite wave is a transverse electric, or TE, wave, since the electric field is entirely transverse to the direction of time-average power flow, that is, the guide axis, but the magnetic field is not. In terms of the uniform plane wave propagation, the phenomenon is one of waves bouncing obliquely between the conductors as they progress down the guide. For a fixed spacing a between the conductors of the guide, waves of different frequencies bounce obliquely at different angles such that the spacing a is equal to an integer, say, m number of one-half apparent wavelengths normal to the plates and hence the fields have m number of one-half sinusoidal variations normal to the plates. These are said to correspond to $\text{TE}_{m,0}$ modes, where the subscript 0 implies no variations of the fields in the direction parallel to the plates and transverse to the guide axis. When the frequency is such that the spacing a is equal to m one-half wavelengths, the waves bounce normally to the plates without the feeling of being guided along the

axis, thereby leading to the cutoff condition. Thus, the cutoff wavelengths corresponding to $TE_{m,0}$ modes are given by

$$\lambda_c = \frac{2a}{m}$$

and the cutoff frequencies are given by

$$f_c = \frac{v_p}{\lambda_c} = \frac{m}{2a\sqrt{\mu\epsilon}}$$

A given frequency signal can propagate in all modes for which $\lambda < \lambda_c$ or $f > f_c$. For the propagating range of frequencies, the wavelength along the guide axis, that is, the guide wavelength, and the phase velocity along the guide axis are given, respectively, by

$$\lambda_g = \frac{\lambda}{\sqrt{1 - (\lambda/\lambda_c)^2}} = \frac{\lambda}{\sqrt{1 - (f_c/f)^2}}$$

$$v_{pz} = \frac{v_p}{\sqrt{1 - (\lambda/\lambda_c)^2}} = \frac{v_p}{\sqrt{1 - (f_c/f)^2}}$$

As compared to TE modes, the transverse magnetic, or TM, modes have their magnetic fields entirely transverse to the direction of time-average power flow. They are obtained by considering two uniform plane waves having only y -components of magnetic fields and propagating at an angle to each other and placing two perfect conductors in two constant- x planes. The expressions for the propagation parameters λ_c , f_c , λ_g , and v_{pz} for the TM modes are the same as those for the TE modes.

We discussed the solution of problems involving reflection and transmission at a discontinuity in a waveguide by using the transmission-line analogy. This consists of replacing each section of the waveguide by a transmission line whose characteristic impedance is equal to the guide characteristic impedance, and then computing the reflection and transmission coefficients as in the transmission-line case. The guide characteristic impedance, η_g , is the ratio of a transverse electric-field component to the corresponding transverse magnetic-field component, which together with the electric-field component gives rise to time-average power flow down the guide. It is given for TE modes by

$$[\eta_g]_{TE} = \frac{\eta}{\sqrt{1 - (\lambda/\lambda_c)^2}} = \frac{\eta}{\sqrt{1 - (f_c/f)^2}}$$

and for TM modes by

$$[\eta_g]_{TM} = \eta \sqrt{1 - \left(\frac{\lambda}{\lambda_c}\right)^2} = \eta \sqrt{1 - \left(\frac{f_c}{f}\right)^2}$$

We then discussed the phenomenon of dispersion arising from the frequency dependence of the phase velocity along the guide axis, and we introduced the concept of group velocity. Group velocity is the velocity with which the envelope of a narrow-band modulated signal travels in the dispersive channel, and hence it is the velocity with which the information is transmitted. It is given by

$$v_g = \frac{d\omega}{d\beta_z}$$

where β_z is the phase constant along the guide axis. On the dispersion diagram or the ω - β_z diagram, the group velocity is equal to the slope of the tangent to the dispersion curve at the center frequency of the narrow-band signal. For the parallel-plate waveguide, it is given by

$$v_g = v_p \sqrt{1 - \left(\frac{f_c}{f}\right)^2}$$

To extend the discussion of waveguides to integrated optics, we then considered oblique incidence of a uniform plane wave on the boundary between two perfect dielectric media. We derived the *laws of reflection and refraction*, given, respectively, by

$$\begin{aligned}\theta_r &= \theta_i \\ \theta_t &= \sin^{-1} \left(\sqrt{\frac{\mu_1 \varepsilon_1}{\mu_2 \varepsilon_2}} \sin \theta_i \right)\end{aligned}$$

where θ_i , θ_r , and θ_t are the angles of incidence, reflection, and transmission, respectively, of a uniform plane wave incident from medium 1 (ε_1, μ_1) onto medium 2 (ε_2, μ_2). The law of refraction is also known as *Snell's law*. We then derived the expressions for the reflection and transmission coefficients for the cases of perpendicular and parallel polarizations. An examination of these expressions revealed the following, under the assumption of $\mu_1 = \mu_2$: (1) for incidence from a medium of higher permittivity onto one of lower permittivity, there is a critical angle of incidence given by

$$\theta_c = \sin^{-1} \sqrt{\frac{\varepsilon_2}{\varepsilon_1}}$$

beyond which total internal reflection occurs, and (2) for the case of parallel polarization, there is an angle of incidence, known as the Brewster angle and given by

$$\theta_p = \tan^{-1} \sqrt{\frac{\varepsilon_2}{\varepsilon_1}}$$

for which the reflection coefficient is zero.

Next, we introduced the dielectric slab waveguide, consisting of a dielectric slab of permittivity ϵ_1 sandwiched between two dielectric media of permittivities $\epsilon_2 < \epsilon_1$. We learned that by launching waves at an angle of incidence θ_i greater than the critical angle for total internal reflection, it is possible to achieve guided wave propagation within the slab. For a given frequency, several modes are possible corresponding to values of θ_i that satisfy the self-consistency condition associated with the bouncing waves. We derived the characteristic equation for computing these values of θ_i for the TE case and discussed its solution. The modes are designated TE_m modes and their cutoff frequencies are given by

$$f_c = \frac{mc}{2d\sqrt{\epsilon_{r1} - \epsilon_{r2}}}, \quad m = 0, 1, 2, \dots$$

where d is the thickness of the slab. The fundamental mode, TE_0 , has no cutoff frequency. We also discussed the guided modes by using the approach of deriving the field expressions, based on the behavior that (a) in the transverse (x -) direction, the fields have standing wave character inside the slab and are evanescent outside the slab, and (b) in the longitudinal (z -) direction, the fields have traveling wave character both inside and outside the slab. Dividing the modes into even and odd modes with respect to x from symmetry considerations, we derived the field expressions for the TE modes and (a) obtained the associated characteristic equation for guidance to be the same as that obtained from the wave-bounce approach, (b) discussed the field behavior from near cutoff to far from cutoff, and (c) investigated power flow down the guide.

To extend the treatment of dielectric waveguide to one of graded-index guide, that is, one in which the refractive index varies within the thickness of the slab, we first introduced the topic of ray tracing, making use of the geometrical optics concept. The ray tracing procedure involves the application of Snell's law in conjunction with the geometry associated with the problem. Although in general the solution has to be carried out numerically, for certain functions for the refractive index variation, analytical solutions are possible, as illustrated by considering (a) a linear profile of permittivity, and (b) paraxial rays, that is, rays that make small angles to the propagation axis, in a parabolic index profile. For the latter case, we found that the ray oscillates about the axis with a pitch independent of the angle of takeoff from the axis at the starting point. We then considered the graded-index guide having a symmetric refractive index profile and derived the condition for guidance. Applying the guidance condition to investigate modes in a parabolic index guide, we showed that, for paraxial rays in the parabolic index guide, intermodal dispersion is nearly eliminated.

REVIEW QUESTIONS

- Q8.1.** What is the propagation vector? Interpret the significance of its magnitude and direction.
- Q8.2.** Discuss how the phase constants along the coordinate axes are less than the phase constant along the direction of propagation of a uniform plane wave propagating in an arbitrary direction.

- Q8.3.** Write the expressions for the electric and magnetic fields of a uniform plane wave propagating in an arbitrary direction, and list all the conditions to be satisfied by the electric field, magnetic field, and propagation vectors.
- Q8.4.** What are apparent wavelengths? Why are they longer than the wavelength along the direction of propagation?
- Q8.5.** What are apparent phase velocities? Why are they greater than the phase velocity along the direction of propagation?
- Q8.6.** Discuss how the superposition of two uniform plane waves propagating at an angle to each other gives rise to a composite wave consisting of standing waves traveling bodily transverse to the standing waves.
- Q8.7.** What is a transverse electric wave? Discuss the reasoning behind the nomenclature $TE_{m,0}$ modes.
- Q8.8.** Compare the phenomenon of guiding of uniform plane waves in a parallel-plate waveguide with that in a parallel-plate transmission line.
- Q8.9.** Discuss how the cutoff condition arises in a parallel-plate waveguide. Explain the relationship between the cutoff wavelength and the spacing between the plates of a parallel-plate waveguide based on the phenomenon at cutoff.
- Q8.10.** Is the cutoff wavelength dependent on the dielectric in the waveguide? Is the cutoff frequency dependent on the dielectric in the waveguide?
- Q8.11.** What is guide wavelength?
- Q8.12.** Provide a physical explanation for the frequency dependence of the phase velocity along the guide axis.
- Q8.13.** What is a transverse magnetic wave? Compare and contrast TE and TM waves in a parallel-plate waveguide.
- Q8.14.** Discuss the phenomenon of guiding of waves in the Earth-ionosphere waveguide.
- Q8.15.** How is guide characteristic impedance defined? Discuss guide characteristic impedance for both TE and TM modes.
- Q8.16.** Discuss the use of the transmission-line analogy for solving problems involving reflection and transmission at a waveguide discontinuity.
- Q8.17.** Why are the reflection and transmission coefficients for a given mode at a lossless waveguide discontinuity dependent on frequency, whereas the reflection and transmission coefficients at the junction of two lossless lines are independent of frequency?
- Q8.18.** Discuss the phenomenon of dispersion.
- Q8.19.** Discuss the concept of group velocity with the aid of an example.
- Q8.20.** What is a dispersion diagram? Explain how the phase and group velocities can be determined from a dispersion diagram.
- Q8.21.** When is it meaningful to attribute a group velocity to a signal comprised of more than two frequencies? Why?
- Q8.22.** Discuss the propagation of a narrow-band amplitude-modulated signal in a dispersive channel.
- Q8.23.** Discuss the condition required to be satisfied by the incident, reflected, and transmitted waves at the interface between two dielectric media.
- Q8.24.** What is Snell's law?
- Q8.25.** What is meant by the plane of incidence? Distinguish between the two different linear polarizations pertinent to the derivation of the reflection and transmission coefficients for oblique incidence on a dielectric interface.

- Q8.26.** Briefly discuss the determination of the Fresnel reflection and transmission coefficients for an obliquely incident wave on a dielectric interface.
- Q8.27.** What is total internal reflection? Discuss the nature of the reflection coefficient and the manner in which the boundary condition is satisfied for an angle of incidence greater than the critical angle for total internal reflection.
- Q8.28.** What is the Brewster angle? What is the polarization of the reflected wave for an elliptically polarized wave incident on a dielectric interface at the Brewster angle? Discuss an application of the Brewster angle effect.
- Q8.29.** Discuss the principle of optical waveguides by considering the dielectric slab waveguide.
- Q8.30.** Explain the self-consistency condition for waveguiding in a dielectric slab waveguide.
- Q8.31.** Discuss the dependence of the number of propagating modes in a dielectric slab waveguide on the ratio of the thickness d of the dielectric slab to the wavelength λ_0 .
- Q8.32.** Considering TE modes in a dielectric slab guide, specify the fundamental mode and discuss the associated cutoff condition.
- Q8.33.** Outline the considerations that come into play in deriving the field expressions for the modes in a dielectric slab guide.
- Q8.34.** Discuss the mode designation for a dielectric slab guide with reference to the field variations in the guide. Further discuss the behavior of the even and odd modes as the situation changes from near cutoff to far from cutoff.
- Q8.35.** Discuss the concept of effective boundary for waveguiding along a dielectric slab guide.
- Q8.36.** Explain radiation modes with reference to a dielectric slab guide.
- Q8.37.** What is geometrical optics approximation? Under what conditions is it valid?
- Q8.38.** Outline the formulation of the procedure for ray tracing in a plane-stratified medium of continuously varying refractive index.
- Q8.39.** What is paraxial ray approximation? Discuss paraxial rays in a medium of parabolic index profile.
- Q8.40.** Outline the derivation of the self-consistency condition for wave guidance in a graded-index dielectric slab guide.
- Q8.41.** Compare and contrast the ray trajectories associated with modes in a graded-index guide with those associated with modes in a step-index guide.
- Q8.42.** What is intermodal dispersion? Why is it minimized for the case of paraxial rays in a parabolic index guide?

PROBLEMS

Section 8.1

- P8.1. Finding the parameters for a uniform plane wave from a specified electric field.** The electric field of a uniform plane wave propagating in a perfect dielectric medium having $\epsilon = 9\epsilon_0$ and $\mu = \mu_0$ is given by

$$\mathbf{E} = 10(2\mathbf{a}_x + \mathbf{a}_y - 2\mathbf{a}_z) \cos [3\pi \times 10^7 t - 0.1\pi(2x - 2y + z)]$$

Find: **(a)** the frequency; **(b)** the direction of propagation; **(c)** the wavelength along the direction of propagation; **(d)** the apparent wavelengths along the x -, y -, and z -axes; and **(e)** the apparent phase velocities along the x -, y -, and z -axes.

- P8.2. Finding whether a given \mathbf{E} represents that of a uniform plane wave in free space.** Given

$$\mathbf{E} = 10(4\mathbf{a}_x + 5\mathbf{a}_y - 3\mathbf{a}_z) \cos [3\pi \times 10^7 t - 0.02\pi(3x + 4z)]$$

(a) Determine if the given \mathbf{E} represents the electric field of a uniform plane wave propagating in free space. **(b)** If the answer is “yes,” find the corresponding magnetic-field vector \mathbf{H} .

- P8.3. Finding whether a given \mathbf{E} - \mathbf{H} pair represents that of a uniform plane wave in a dielectric.** Given

$$\begin{aligned}\mathbf{E} &= (\mathbf{a}_x + 2\mathbf{a}_y + \sqrt{3}\mathbf{a}_z) \cos [15\pi \times 10^6 t - 0.05\pi(\sqrt{3}x - z)] \\ \mathbf{H} &= \frac{1}{60\pi}(\mathbf{a}_x - 2\mathbf{a}_y + \sqrt{3}\mathbf{a}_z) \cos [15\pi \times 10^6 t - 0.05\pi(\sqrt{3}x - z)]\end{aligned}$$

(a) Perform all necessary tests and determine if these fields represent a uniform plane wave propagating in a perfect dielectric medium. **(b)** If the answer is “yes,” find the permittivity and the permeability of the medium.

- P8.4. Properties of a uniform plane wave from specified apparent phase velocities.**

The apparent phase velocities of a uniform plane wave propagating in a perfect dielectric medium are measured in three directions as follows: 4×10^8 m/s along the x -direction, 2×10^8 m/s along the direction of the unit vector $\frac{1}{5}(4\mathbf{a}_x + 3\mathbf{a}_y)$, and 12×10^8 m/s along the direction of the unit vector $\frac{1}{3}(\mathbf{a}_x - 2\mathbf{a}_y + 2\mathbf{a}_z)$. Find the direction of propagation of the wave and the phase velocity along the direction of the unit vector $\frac{1}{3}(2\mathbf{a}_x + 2\mathbf{a}_y - \mathbf{a}_z)$.

- P8.5. Finding the parameters for a uniform plane wave from specified phasor electric field.** The electric field of a uniform plane wave propagating in free space is given in phasor form by

$$\bar{\mathbf{E}} = 10(\mathbf{a}_x + j0.4\mathbf{a}_y + j0.3\mathbf{a}_z)e^{j(0.6y - 0.8z)}$$

(a) Determine the frequency of the wave. **(b)** What is the direction of propagation? **(c)** Obtain the associated magnetic field in phasor form. **(d)** Discuss the polarization of the wave. **(e)** Find the time-average power flow per unit area normal to the direction of propagation.

Section 8.2

- P8.6. Finding the spacing for the plates of a parallel-plate waveguide for a given condition.** Find the spacing a for a parallel-plate waveguide having a dielectric of $\epsilon = 9\epsilon_0$ and $\mu = \mu_0$ such that 6000 MHz is 20 percent above the cutoff frequency of the dominant mode, that is, the mode with the lowest cutoff frequency.

- P8.7. Finding propagating modes and their characteristics in a parallel-plate waveguide.** The dimension a of a parallel-plate waveguide with a dielectric of $\epsilon = 4\epsilon_0$ and $\mu = \mu_0$ is 3 cm. Determine the propagating modes for a wave of frequency 6000 MHz. For each propagating mode, find λ_c , f_c , θ , λ_g , and v_{pz} .
- P8.8. Finding propagating modes in a parallel-plate waveguide for a given excitation.** Transverse electric modes are excited in an air dielectric parallel-plate waveguide of dimension $a = 5$ cm by setting up at its mouth a field distribution having

$$\mathbf{E} = 10(\sin 20\pi x + 0.5 \sin 60\pi x) \sin 10^{10}\pi t \mathbf{a}_y$$

Determine the propagating mode(s) and obtain the expression for the electric field of the propagating wave.

- P8.9. Finding E for the propagating wave in a parallel-plate waveguide for a given excitation.** TE modes are excited in an air-dielectric parallel-plate waveguide having the plates in the $x = 0$ and $x = 5$ cm planes by setting up at its input $z = 0$ a field distribution such that

$$\mathbf{E} = E_0 \sin^3 20\pi x \cos 5\pi \times 10^9 t \cos 15\pi \times 10^9 t \mathbf{a}_y$$

Find the expression for the electric field of the propagating wave.

- P8.10. Finding fields for the propagating wave in a parallel-plate waveguide from the excitation.** TM mode is excited in a parallel-plate waveguide filled with a dielectric of $\epsilon = 4\epsilon_0$ and $\mu = \mu_0$ and having the plates in the $x = 0$ and $x = 5$ cm planes by setting up at its input $z = 0$ the magnetic field distribution

$$\mathbf{H} = H_0 \cos 40\pi x \sin 8\pi \times 10^9 t \mathbf{a}_y$$

Find the expressions for the electric and magnetic fields of the propagating wave.

Section 8.3

- P8.11. Power reflection coefficient at a parallel-plate waveguide discontinuity for several cases.** For the parallel-plate waveguide discontinuity of Example 8.3, find the power reflection coefficient for $f = 7500$ MHz for each of the following cases: (a) TEM mode; (b) $TE_{1,0}$ mode; and (c) $TM_{1,0}$ mode.
- P8.12. Power reflection coefficient at a parallel-plate waveguide discontinuity for several cases.** The left half (section 1) of a parallel-plate waveguide of dimensions $a = 5$ cm is filled with a dielectric of $\epsilon = 9\epsilon_0$ and $\mu = \mu_0$. The right half (section 2) is filled with a dielectric of $\epsilon = 16\epsilon_0$ and $\mu = \mu_0$. For waves of frequency 2500 MHz incident on the discontinuity from the left, find the power reflection coefficient for each of the following cases: (a) $TE_{1,0}$ mode; (b) $TE_{2,0}$ mode; (c) $TM_{1,0}$ mode; and (d) $TM_{2,0}$ mode.
- P8.13. Finding the dielectric permittivity at an air-dielectric interface in a parallel-plate guide.** Assume that the permittivity of the dielectric to the right side of the parallel-plate waveguide discontinuity of Fig. 8.11 is unknown. If the reflection coefficient for $TE_{1,0}$ waves of frequency 5000 MHz incident on the junction from the free space side is -0.2643 , find the permittivity of the dielectric.

Section 8.4

- P8.14. Finding the group velocity for a group of two trains.** For the two-train example of Fig. 8.12, find the group velocity if the speed of train *B* is (a) 36 m/s and (b) 40 m/s, instead of 30 m/s. Discuss your results with the aid of sketches.
- P8.15. Finding phase and group velocities from a dispersion curve.** The ω - β curve for a dispersive channel can be approximated by

$$\frac{1}{\omega^2} = \frac{1}{\omega_0^2} + \frac{k^2}{\beta^2}$$

in the vicinity of $\omega = 0.5\omega_0$, where k is a constant. Find the following: **(a)** the phase velocity for a signal of $\omega = 0.5\omega_0$; **(b)** the group velocity for a signal composed of two frequencies $0.4\omega_0$ and $0.6\omega_0$; and **(c)** the group velocity for a narrow-band signal having the center frequency $0.5\omega_0$.

- P8.16. Finding group velocities of signals propagating in a parallel-plate waveguide.** For a parallel-plate waveguide of dimension $a = 2.5$ cm and having a perfect dielectric of $\epsilon = 9\epsilon_0$ and $\mu = \mu_0$, find the group velocity for: **(a)** a signal composed of the two frequencies $f_1 = 2500$ MHz and $f_2 = 3000$ MHz; and **(b)** a narrow-band signal having the center frequency 2500 MHz.
- P8.17. Finding group velocities of signals propagating in a parallel-plate waveguide.** Find the group velocity of propagation of a TE wave in a parallel-plate waveguide filled with a perfect dielectric of $\epsilon = 2.25\epsilon_0$ and $\mu = \mu_0$ and having the plates in the $x = 0$ and $x = 10$ cm planes for each of the following cases of electric field distribution at its input $z = 0$:

- (a)** $E_0 \sin 10\pi x \cos 10^9\pi t \cos 4 \times 10^9\pi t \mathbf{a}_y$
(b) $E_0 \sin 10\pi x(1 + 0.5 \cos 10^4\pi t) \cos 4 \times 10^9\pi t \mathbf{a}_y$

- P8.18. A geometric interpretation of the group velocity in a parallel-plate waveguide.** By considering the parallel-plate waveguide, show that a point on the obliquely bouncing wavefront, traveling with the phase velocity along the oblique direction, progresses parallel to the guide axis with the group velocity.

Section 8.5

- P8.19. Fresnel coefficients for the case of interface between two perfect dielectric media.** For the case of two nonmagnetic ($\mu = \mu_0$), perfect dielectric media, show that the Fresnel coefficients for perpendicular polarization (8.70a) and (8.70b) reduce to

$$\Gamma_{\perp} = \frac{\sin(\theta_2 - \theta_1)}{\sin(\theta_2 + \theta_1)} \quad \text{and} \quad \tau_{\perp} = \frac{2 \cos \theta_1 \sin \theta_2}{\sin(\theta_2 + \theta_1)}$$

respectively, and the Fresnel coefficients for parallel polarization (8.75a) and (8.75b) reduce to

$$\Gamma_{\parallel} = \frac{\tan(\theta_2 - \theta_1)}{\tan(\theta_2 + \theta_1)} \quad \text{and} \quad \tau_{\parallel} = \frac{2 \cos \theta_1 \sin \theta_2}{\sin(\theta_1 + \theta_2) \cos(\theta_1 - \theta_2)}$$

respectively.

- P8.20. Oblique incidence of uniform plane wave onto a dielectric medium.** In Example 8.4, assume that

$$E_i = E_0(\mathbf{a}_x - \mathbf{a}_z) \cos [6\pi \times 10^8 t - \sqrt{2}\pi(x + z)]$$

and the angle of incidence is 45° . Obtain the expressions for the electric fields of the reflected and transmitted waves.

- P8.21. Oblique incidence of uniform plane wave onto a dielectric medium.** Repeat Problem P8.20 for

$$\mathbf{E}_i = E_0 \mathbf{a}_y \cos [6\pi \times 10^8 t - \sqrt{2}\pi(x + z)]$$

- P8.22. Oblique incidence of uniform plane wave onto a dielectric medium at Brewster angle.** In Example 8.4, assume that the permittivity ϵ_2 of medium 2 is unknown and that

$$\begin{aligned} \mathbf{E}_i = E_0 \left(\frac{\sqrt{3}}{2} \mathbf{a}_x - \frac{1}{2} \mathbf{a}_z \right) \cos [6\pi \times 10^9 t - 10\pi(x + \sqrt{3}z)] \\ + E_0 \mathbf{a}_y \sin [6\pi \times 10^9 t - 10\pi(x + \sqrt{3}z)] \end{aligned}$$

- (a) Find the value of ϵ_2 for which the reflected wave is linearly polarized.
 (b) For the value of ϵ_2 found in (a), find the expressions for the reflected and transmitted wave electric fields.

- P8.23. Consistency of Fresnel coefficients with power flow normal to the interface.** For oblique incidence of a uniform plane wave on a dielectric interface, show that the Fresnel reflection and transmission coefficients are consistent with the condition that for power flow normal to the interface, the sum of the reflected power and the transmitted power be equal to the incident power, for each of the two cases: (a) perpendicular polarization and (b) parallel polarization.

Section 8.6

- P8.24. Minimum bouncing angle for total internal reflection in a thin-film waveguide.** A thin-film waveguide employed in integrated optics consists of a substrate on which a thin film of refractive index (c/v_p) greater than that of the substrate is deposited. The medium above the film is air. For relative permittivities of the substrate and the film equal to 2.25 and 2.4, respectively, find the minimum bouncing angle of total internally reflected waves in the film. Assume $\mu = \mu_0$ for both substrate and film.
- P8.25. TE modes in a symmetric dielectric slab waveguide.** For a symmetric dielectric slab waveguide, $\epsilon_1 = 2.25\epsilon_0$ and $\epsilon_2 = \epsilon_0$. (a) Find the number of propagating TE modes for $d/\lambda_0 = 10$. (b) Find the maximum value of d/λ_0 for which the waveguide supports only one TE mode.
- P8.26. Design of a symmetric dielectric slab waveguide.** Design a symmetric dielectric slab waveguide, with $\epsilon_{r1} = 2.25$ and $\epsilon_{r2} = 2.13$, by finding the value of d/λ_0 such that the TE_1 mode operates at 20% above its cutoff frequency.

P8.27. Guiding of waves in a symmetric dielectric slab waveguide for parallel polarization. Consider the derivation of the characteristic equation for guiding of waves in the symmetric dielectric slab waveguide for the case of parallel polarization, which corresponds to TM modes. Noting that in Fig. 8.18, $H_r/H_i = E_r/E_i = -\Gamma_{\parallel}$, where Γ_{\parallel} is given by (8.75a), show that the characteristic equation is given by

$$\tan [f(\theta_i)] = \begin{cases} g(\theta_i), & m = 0, 2, 4, \dots \\ -\frac{1}{g(\theta_i)}, & m = 1, 3, 5, \dots \end{cases}$$

where

$$f(\theta_i) = \frac{\pi d \sqrt{\epsilon_{r1}}}{\lambda_0} \cos \theta_i$$

$$g(\theta_i) = \frac{\sqrt{\sin^2 \theta_i - (\epsilon_2/\epsilon_1)}}{(\epsilon_2/\epsilon_1) \cos \theta_i}$$

- P8.28. Power confinement factor for dielectric slab waveguide.** The ratio of the power associated with the region of the slab ($|x| < d/2$) to the total power ($-\infty < x < \infty$) is known as the *power confinement factor*. Show that for a given frequency, the power confinement factor is the highest for the dominant mode. Find the power confinement factors for the three modes in Example 8.6.
- P8.29. Even TM modes in a symmetric dielectric slab waveguide.** Beginning with an expression for \bar{H}_y , analogous to that of \bar{E}_y , for even TE modes given by (8.91), derive the field expressions for even TM modes for the symmetric dielectric slab waveguide and obtain the characteristic equation for guidance.
- P8.30. Odd TM modes in a symmetric dielectric slab waveguide.** Repeat Problem P8.29 for odd TM modes, beginning with an expression for \bar{H}_y , analogous to that of \bar{E}_y , for odd TE modes given by (8.102).
- P8.31. Dispersion relation for the TE_m mode in a symmetric dielectric slab waveguide.** For the symmetric dielectric slab guide, show that the ω versus β_z , or the dispersion relation for the TE_m mode, is given by

$$\tan^2 \left(\frac{d}{2} \sqrt{\omega^2 \mu_0 \epsilon_1 - \beta_z^2} - \frac{m\pi}{2} \right) = \frac{\beta_z^2 - \omega^2 \mu_0 \epsilon_2}{\omega^2 \mu_0 \epsilon_1 - \beta_z^2}$$

Then find the value of d/λ_0 for which the phase velocity along the guide axis v_{pz} is equal to $\sqrt{v_{p1}v_{p2}}$, where $v_{p1} = 1/\sqrt{\mu_0\epsilon_1}$ and $v_{p2} = 1/\sqrt{\mu_0\epsilon_2}$, for the fundamental mode, if $\epsilon_{r1} = 4.0$ and $\epsilon_{r2} = 2.25$. Note that since \tan^2 is always positive, $\omega^2\mu_0\epsilon_2 < \beta_z^2 < \omega^2\mu_0\epsilon_1$, or $v_{p2} > v_{pz} > v_{p1}$, as it should be.

Section 8.7

- P8.32. Derivation of the laws of geometrical optics from Fermat's principle.** The laws of geometrical optics can be derived from Fermat's principle, which states that the optical path length $\int_A^B n ds$ of a ray of light from point A to point B is an

extremum, so that the variation in the optical path length, $\delta \int_A^B n ds$, is equal to zero. Derive from this property the laws of reflection and refraction for oblique incidence on a plane boundary between two different perfect dielectric media.

- P8.33. Ray tracing in spherical geometry.** Consider ray tracing in spherical geometry, as shown in Fig. 8.35, in which n is a function of r , the radial distance from the center of a spherical interface (radius r_0). A ray is incident on the interface at an angle θ_0 from a medium of uniform refractive index n_0 . Show that the ray path for $r > r_0$ is governed by a modified form of Snell's law given by

$$nr \sin \theta = \text{constant} = n_0 r_0 \sin \theta_0$$

and hence by the solution of the differential equation

$$\frac{d\theta}{dr} = \frac{n_0 r_0 \sin \theta}{r \sqrt{n^2 r^2 - n_0^2 r_0^2 \sin^2 \theta}}$$

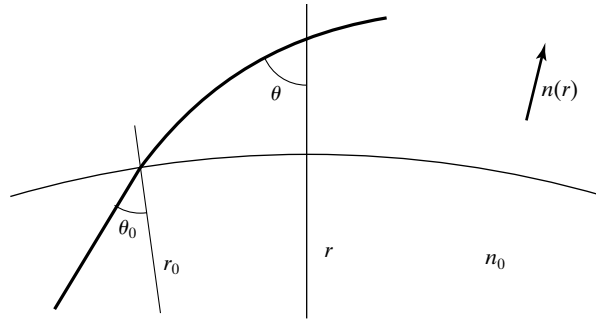


FIGURE 8.35
For Problem P8.33.

- P8.34. Paraxial rays in a dielectric medium with linear refractive index profile.** In Example 8.8, assume

$$n(x) = n_0(1 - \alpha|x|)$$

Obtain the solution for $z(x)$ for paraxial rays and find the approximate peak amplitude and the approximate pitch in terms of δ_0 .

- P8.35. Guidance condition for the graded-index guide for the TM case.** Show that the guidance condition for the graded-index guide for the TM case is the same as that given by (8.125) or (8.126) for the TE case by showing that $\bar{\Gamma}_a$ for the TM case is $1/\sqrt{-\pi/2}$. Note that $\bar{\Gamma}$ to be used for the TM case is $-\Gamma_{\parallel}$ (see Problem P8.27), where Γ_{\parallel} is given by (8.75a).

- P8.36. Graded-index guide with linear profile of dielectric permittivity.** In Example 8.9, assume

$$n_1^2(x) = n_0^2(1 - \alpha|x|)$$

Obtain the expression for x_a for the m th mode.

REVIEW PROBLEMS

- R8.1. Application of information on apparent phase velocities of a uniform plane wave.** The apparent phase velocities of a uniform plane wave of frequency 10^9 Hz propagating in a nonmagnetic ($\mu = \mu_0$), perfect dielectric medium are given for three directions as follows: 2.25×10^8 m/s along the direction of the unit vector $\frac{1}{3}(2\mathbf{a}_x + \mathbf{a}_y + 2\mathbf{a}_z)$; 4.5×10^8 m/s along the direction of the unit vector $\frac{1}{3}(2\mathbf{a}_x - 2\mathbf{a}_y + \mathbf{a}_z)$; and 18×10^8 m/s along the direction of the unit vector $\frac{1}{3}(2\mathbf{a}_x + \mathbf{a}_y - 2\mathbf{a}_z)$. Find **(a)** the permittivity of the medium and **(b)** the apparent wavelength along the direction of the unit vector $\frac{1}{3}(2\mathbf{a}_x + 2\mathbf{a}_y - \mathbf{a}_z)$.
- R8.2. TM wave reflection and transmission at a parallel-plate waveguide discontinuity.** The left half ($z < 0$) of a parallel-plate waveguide having the plates in the $x = 0$ and $x = 2.5$ cm planes is filled with a dielectric of $\epsilon = 4\epsilon_0$ and $\mu = \mu_0$, whereas the right half ($z > 0$) is filled with a dielectric of $\epsilon = 2.25\epsilon_0$ and $\mu = \mu_0$. A TM wave having the magnetic field at $z = 0$ given by

$$\mathbf{H}_i = H_0 \cos^3 40\pi x \cos 3\pi \times 10^{10}t \mathbf{a}_y$$

is incident on the discontinuity $z = 0$ from the left. Find the expressions for the electric and magnetic fields as functions of z and t for the incident and reflected waves for $z < 0$ and the transmitted wave for $z > 0$.

- R8.3. Finding the ratio of group velocity to phase velocity for an interval on a dispersion curve.** The ω - β curve for a certain dispersive channel is such that at a frequency $\omega = \omega_0$, the group and phase velocities are equal, and the group velocity is proportional to ω in a certain frequency interval around $\omega = \omega_0$. Find the ratio v_g/v_p in that frequency interval.
- R8.4. Oblique incidence of uniform plane wave onto a dielectric medium at Brewster angle.** Region 1 ($x < 0$) is free space, whereas region 2 ($x > 0$) is a perfect dielectric of $\epsilon = 16\epsilon_0$ and $\mu = \mu_0$. For an elliptically polarized uniform plane wave incident from free space onto the boundary $x = 0$, it is found that the reflected wave is linearly polarized with electric-field amplitude E_1 and the transmitted wave is circularly polarized with electric-field magnitude E_2 . **(a)** Find E_2/E_1 . **(b)** Find the axial ratio of the polarization ellipse for the incident wave.
- R8.5. Design of a symmetric dielectric slab waveguide.** Design a symmetric dielectric slab waveguide with $\epsilon_{r1} = 2.25$ and $\epsilon_{r2} = 1.00$ by finding the value of d/λ_0 such that θ_i for the TM_0 mode is 88° . Then find the value of θ_i for the TE_0 mode and the number of remaining propagating TE and TM modes.
- R8.6. Paraxial rays in a graded-index guide with linear profile of dielectric permittivity.** For a graded-index guide with the refractive index profile given by

$$n_1^2(x) = n_0^2(1 - \alpha|x|)$$

obtain the solution for $z(x)$ for paraxial rays and find the approximate amplitude and approximate pitch in terms of δ_0 . Then find the approximate value of δ_0 in terms of mode number.